

**Hydrophobically Modified Water-soluble Polymers:
Synthesis, Characterization & Rheology**

Thesis submitted to,

University of Pune

For the degree of

Doctor of Philosophy

in

Chemistry

by

A S Shedge

***Polymer Science and Engineering Division
National Chemical Laboratory***

PUNE

(2011-2012)

Certificate

Certified that the work presented in the thesis entitled “**Hydrophobically Modified Water-soluble Polymers: Synthesis, Characterization & Rheology**” submitted by Ms. A. S. Shedge was carried out by the candidate under my supervision. Material obtained from other sources has been duly acknowledged in the thesis.

Place: Pune

Date: 30/12/2011

Dr. M. V. Badiger

(Research Guide)

Declaration by the Candidate

The research work reported in this thesis entitled “**Hydrophobically Modified Water-soluble Polymers: Synthesis, Characterization & Rheology**” has been carried out at National Chemical Laboratory, Pune. This work is original and has not been submitted to any other institute or university for any other degree.

(A. S. Shedge)

(Research student)

Acknowledgement

This is an opportunity to express my gratitude towards people who were very helpful for the completion of Ph D. It was a *novel* and *unforgettable* experience.

I am thankful to research guide Dr. Badiger for his guidance and thesis. I am thankful to Dr. Lele, Dr. Wadgaonkar, Dr. Bhat and Prof. Christophe Chassenieux for their guidance.

I am grateful to the Director National Chemical Laboratory for allowing me to work for Ph. D in National Chemical Laboratory and appreciation. I am grateful to Council of Scientific and Industrial Research for awarding me senior research fellowship. I am also grateful to EGIDE sandwich thesis fellowship. I am also grateful to Dr. B. D. Kulkarni and Dr. Ranade for allowing me to work in NCL.

I am grateful to Dr. K. N. Ganesh, Dr. Maybhate, Dr. Likhite and Dr. Deshpande for their guidance during M Sc project which was a first introduction to research.

I would like to thank Anitha, Deepti and Pooja (project students). I would like to thank my friends Gauri, Ajay, Lalita and Sakshi. I thank my M Sc classmates, Harshada, Unmani, Rashmi, Poorva and Shubhada.

I would like to thank Harshada, Rakesh, Hameed, Pujari, Swapnajali, Snehlata, Anjana, Madhuri, Aditya, Srinivas, Samruddhi, Divya, Venugopal E., Girish, Vivek, Rajeshwari, Mohan, Sony, Chandrashekhar, Kanitkar, Grace, Rasika, Harsha, Amit, Ramesh, Hemant, Pallavi, Hari and Sarika.

I would like to thank my M Sc teachers, Kaulgud, Mahamulkar, Bhatawdekar, Mane, Kondedeshmukh, Pol, Pardeshi and the library staff Mrs. Deshpande, Mr. Gade. I would like to specifically mention Gadre (B. Sc.), Mahamulkar, Bhatawdekar, Kondedeshmukh and Mane sir. I would like to thank entire staff of stores, purchase, glass blowing, engineering section, library, administration, accounts, IP group, CMC, central NMR facility, medical centre. I am thankful to Dr. Ponrathnam, Dr. Rajan, Dr. Rajmohanan, Dr. Ajith, Dr. Ravikumar. Dr. Chavan, Dr. Jog, Dr. Kharul, Dr. Guruswamy, Dr. Varma, Kokane, Sangeeta Hambir, Neelima Bulakh, Mr. Thakar. I am thankful to Mr.

Radhakrishnan, Mr. P D. Sidhshwar for their help. I would like to thank Mr. U. V. Dhavale, Mr. Bharatiji, Mr. Yadav.

The word thank you is not enough to express my emotions towards my family for their colossal support throughout my Ph D. I thank them for teaching me to be ground to earth during the success and perseverance during failure. I am indebted to my sister Gauri as a source of inspiration and support during the tough time on work front. I would like to thank Mr. U. J. Mahurkar and Mr. J. G. Mahurkar for their help and support. My family has taught me to be independent personally and my lab mates have taught me to be independent professionally so I thank both for making me the way I am today.

CONTENTS

*	Index	i
*	List of Tables	ii
*	List of Schemes	iii
*	List of Figures	iv
*	Abstract	v

INDEX

<i>Chapter</i>	<i>Title</i>	<i>P No.</i>
Chapter:1	<i>Hydrophobically Modified Polymers [HMPs]: A Literature Review</i>	1
1.1	<i>Introduction</i>	2
1.2	<i>Synthesis of HMPs</i>	3
	1.2.1 <i>Copolymerization</i>	4
	1.2.2 <i>Post-polymerization functionalization</i>	5
1.3	<i>Types of HMPs</i>	5
	1.3.1 <i>Hydrophobically modified alkali swellable/soluble emulsion</i>	5
	1.3.2 <i>Telechelic polymers</i>	7
	1.3.3 <i>Amphiphilic block copolymers</i>	8
	1.3.4 <i>Hydrophobically modified cellulose</i>	9
	1.3.5 <i>Hydrophobically modified poly(acryl amide)</i>	10
1.4	<i>Rheological behavior of HMPs</i>	11
	1.4.1 <i>Dilute solution viscosity</i>	13
	1.4.2 <i>Shear thickening and shear thinning behavior of HMPs</i>	15
	1.4.3 <i>Viscoelasticity in HMPs</i>	15
1.5	<i>Applications of HMPs</i>	19
	1.5.1 <i>Personal care and cosmetics</i>	19
	1.5.2 <i>Paints and coatings</i>	20

	1.5.3	<i>Enhanced oil recovery</i>	21
1.6		<i>Techniques used in the characterization of HMPs reported in this thesis</i>	22
	1.6.1	<i>Rheology</i>	22
	1.6.2	<i>Rheometer</i>	22
	1.6.3	<i>Geometry</i>	23
	1.6.4	<i>Creep</i>	23
	1.6.5	<i>Oscillatory Measurements</i>	24
	1.6.6	<i>Light scattering</i>	25
	1.6.7	<i>Confocal microscopy</i>	29
1.7		<i>Summary</i>	29
		<i>References</i>	30
Chapter:2		<i>Scope and Objectives</i>	38
2.1		<i>Specific objectives</i>	41
		<i>References</i>	42
Chapter:3		<i>Synthesis of Hydrophobic Compounds Derived from Natural Resource Materials</i>	44
3.1		<i>Introduction</i>	45
	3.1.1	<i>Cashew nut-shell liquid [CNSL]</i>	47
	3.1.2	<i>Gallic acid</i>	48
3.2		<i>Experimental</i>	50
	3.2.1	<i>Materials</i>	50
3.3		<i>IR and NMR spectroscopy</i>	50
3.4		<i>Synthesis of 3-PDCA</i>	50
	3.4.1	<i>Preparation of 3-pentadecyl cyclohexanol</i>	51
	3.4.2	<i>Preparation of 3-pentadecyl cyclohexanone</i>	51
	3.4.3	<i>Preparation of 3-pentadecyl cyclohexane oxime</i>	51
	3.4.4	<i>Preparation of 3-pentadecyl cyclohexyl amine</i>	52

3.5		<i>Synthesis of 3-PDCAL</i>	52
	3.5.1	<i>Preparation of (E/Z)-1-(methoxy methylene) -3-pentadecyl cyclohexane</i>	52
	3.5.2	<i>Preparation of 3-pentadecyl cyclohexane carbaldehyde</i>	53
3.6		<i>Preparation of hydrophobic compounds from gallic acid</i>	53
	3.6.1	<i>Synthesis of methyl 3, 4, 5-tris octyloxy benzoate [MGC₈]</i>	53
	3.6.1.1	<i>Preparation of methyl 3, 4, 5-trihydroxybenzoate (methyl gallate)</i>	54
	3.6.1.2	<i>Preparation of methyl 3, 4, 5-tris (n-octyloxy) benzoate (MGC₈)</i>	54
	3.6.1.3	<i>Synthesis of methyl 3, 4, 5-tris (dodecyloxy) benzoate [MGC₁₂]</i>	54
3.7		<i>Results and Discussion</i>	55
	3.7.1	<i>Preparation of 3-Pentadecyl cyclohexyl amine [3-PDCA]</i>	55
		<i>FT-IR spectrum of 3-PDCA</i>	55
		<i>¹H NMR of 3-PDCA</i>	56
		<i>¹³C NMR of 3-PDCA</i>	57
	3.7.2	<i>Preparation of 3-pentadecyl cyclohexane carbaldehyde (3-PDCAL)</i>	58
		<i>FT-IR spectrum of 3-PDCAL</i>	58
		<i>¹H NMR of 3-PDCAL</i>	59
		<i>¹³C NMR of 3-PDCAL</i>	60
	3.7.3	<i>Synthesis of hydrophobic compounds from gallic acid: [MGC₈, MGC₁₂]</i>	61
		<i>FT-IR spectrum of MGC₈</i>	62
		<i>¹H NMR spectrum of MGC₈</i>	62
		<i>¹³C NMR of MGC₈</i>	63
	3.7.4	<i>Methyl 3, 4, 5 tris-octyloxy benzoate [MGC₁₂]</i>	64
		<i>FT-IR spectrum of 3-PDCAL</i>	65
		<i>¹H NMR of 3-PDCAL</i>	65
		<i>¹³C NMR of 3-PDCAL</i>	66

3.8		<i>Conclusion</i>	67
		<i>References</i>	68
Chapter:4		<i>Hydrophobically modified poly(vinyl alcohol):Synthesis, Characterization and Solution properties</i>	70
4.1		<i>Introduction</i>	71
4.2		<i>Experimental</i>	72
	4.2.1	<i>Materials</i>	72
	4.2.2	<i>Hydrophobic modification of PVA with MGC₈</i>	72
	4.2.3	<i>Characterization</i>	73
	4.2.4	<i>Gel permeation chromatography (GPC) and light scattering (LS)</i>	73
	4.2.5	<i>NMR spectroscopy</i>	73
	4.2.6	<i>Sample preparation</i>	73
	4.2.7	<i>Rheology</i>	74
4.3		<i>Results and Discussion</i>	74
	4.3.1	<i>Synthesis of hydrophobically modified PVA using MGC₈</i>	74
	4.3.2	<i>¹H NMR spectra of PVA, PVAS-10, HMPVAs</i>	77
4.4		<i>Rheology</i>	79
	4.4.1	<i>Specific viscosity as a function of polymer concentration</i>	79
	4.4.2	<i>Steady shear data</i>	80
	4.4.3	<i>Time temperature superposition-Master curve</i>	81
	4.4.4	<i>Oscillatory Measurements</i>	82
	4.4.5	<i>Activation Energy (E_a)</i>	85
	4.4.6	<i>Strain-Rate Frequency Superposition: [SRFS]</i>	86
4.5		<i>Conclusions</i>	90
		<i>References</i>	91
Chapter:5		<i>Hydrophobically Modified Poly(N, N'-dimethyl acryl amide-co-acrylic acid): Synthesis, Characterization and Rheology</i>	92

5.1		<i>Introduction</i>	93
5.2		<i>Experimental</i>	96
	5.2.1	<i>Materials</i>	96
	5.2.2	<i>Synthesis</i>	96
	5.2.2.1	<i>Preparation of poly(N, N'-dimethyl acrylamide-co-acrylic acid) and its hydrophobic modification using 3-PDCA</i>	96
	5.2.2.2	<i>Synthesis of poly(N, N'-dimethyl acrylamide-co-acrylic acid) [(70 mol % DMA/30 mol % AA)]</i>	96
	5.2.2.3	<i>Hydrophobic modification of poly(N, N'-dimethyl acrylamide-co-acrylic acid) using 3-PDCA</i>	97
5.3		<i>Gel permeation Chromatography</i>	97
5.4		<i>¹H and ¹³C NMR Spectroscopy</i>	98
5.5		<i>Sample Preparation</i>	98
5.6		<i>Rheology</i>	98
5.7		<i>Results and Discussion</i>	99
	5.7.1	<i>Synthesis of poly(N, N'-dimethyl acrylamide-co-acrylic acid) [(70 mol % DMA/30 mol % AA)]</i>	99
	5.7.2	<i>Hydrophobic modification of poly(N, N'-dimethyl acrylamide-co-acrylic acid) using 3-PDCA</i>	100
	5.7.3	<i>NMR spectroscopy</i>	101
	5.7.4	<i>Rheology</i>	103
	5.7.4.1	<i>Concentration dependence of zero shear viscosity</i>	103
	5.7.4.2	<i>Steady shear experiment</i>	105
	5.7.4.3	<i>Stress ramp experiment</i>	107
	5.7.4.4	<i>Creep experiments at different stresses</i>	109
	5.7.4.5	<i>Gelation time & the applied stress</i>	110
	5.7.4.6	<i>Stability of shear induced gels</i>	111
	5.7.4.7	<i>Elastically active chains</i>	116
5.8		<i>Conclusions</i>	119
		<i>References</i>	121

Chapter-6		<i>Hydrophobically Modified Chitosan: Synthesis, Characterization and Rheology</i>	123
6.1		<i>Introduction</i>	124
6.2		<i>Experimental</i>	125
	6.2.1	<i>Materials</i>	125
	6.2.2	<i>Synthesis of hydrophobically modified chitosans (HMCs) using 3-pentadecyl cyclohexane carbaldehyde (3-PDCAL)</i>	125
	6.3.3	<i>Determination of degree of deacetylation using ¹H NMR spectroscopy</i>	126
	6.2.4	<i>Sample preparation</i>	127
	6.2.5	<i>NMR spectroscopy</i>	127
	6.2.6	<i>Rheology</i>	127
	6.2.7	<i>Light scattering</i>	127
6.3		<i>Results and Discussion</i>	128
	6.3.1	<i>Synthesis of Hydrophobically Modified Chitosan</i>	128
	6.3.2	<i>¹H NMR spectroscopy</i>	129
	6.3.3	<i>Rheology data</i>	130
		6.3.3.1	<i>Specific viscosity (η_{sp}) vs polymer concentration (C_p)</i>
		6.3.3.2	<i>Dynamic frequency sweep</i>
			6.3.3.2.1
			<i>Oscillatory data as a function of hydrophobic modification</i>
			6.3.3.2.2
			<i>Oscillatory data as a function of polymer concentration</i>
	6.3.4		<i>Light scattering</i>
		6.3.4.1	<i>Static light scattering (SLS)</i>
		6.3.4.2	<i>Dynamic light scattering (DLS)</i>
6.5			<i>Conclusions</i>
			<i>References</i>
Chapter-7		<i>Summary and Conclusions</i>	138
		<i>Future perspectives</i>	141

	<i>Synopsis</i>	143
	<i>List of publications</i>	148

List of Tables

3.1	<i>Different hydrophobic compounds used for the modification of water-soluble polymers along with references</i>	45
4.1	<i>Stoichiometry of the reaction between PVA, 1, 3-propane sultone and MGC₈</i>	76
4.2	<i>GPC data obtained for PVA and PVAS-10</i>	77
4.3	<i>Comparison of activation energy calculated from steady-shear and oscillatory shear data</i>	85
5.1	<i>Stoichiometry for the hydrophobic modification of poly(N, N'-dimethyl acrylamide-co- acrylic acid)</i>	100
5.2	<i>Values of stress, gel modulus, relaxation time and retardation time calculated from creep recovery data</i>	112
5.3	<i>Fraction of Elastically Active Chains in Shear-Induced Gels</i>	117
6.1	<i>Stoichiometry of the reaction between chitosan, sodium cyanoborohydride and 3-pentadecyl cyclohexane carbaldehyde (3-PDCAL)</i>	126
6.2	<i>Data obtained from static and dynamic light scattering analysis</i>	134
6.3	<i>Data obtained from dynamic light scattering using autocorrelation function</i>	135

List of Schemes

3.1	<i>Synthesis of 3-pentadecyl cyclohexylamine</i>	55
3.2	<i>Synthesis of 3-pentadecyl cyclohexane carbaldehyde</i>	58
3.3	<i>Preparation of methyl 3, 4, 5-tris octyloxy benzoate</i>	62
3.4	<i>Preparation of methyl 3, 4, 5-tris dodecyloxy benzoate</i>	64
4.1	<i>Reaction mechanism for the preparation of HMPVA</i>	75
5.1	<i>Reaction pathway for the preparation of poly (N, N'-dimethyl acryl amide - co-Acrylic acid)</i>	99
5.2	<i>Reaction pathway for the preparation of hydrophobically modified poly(N, N'-dimethyl acryl amide -co-Acrylic acid)</i>	100
5.3	<i>Coupling reaction for the preparation of hydrophobically modified poly(N, N'-dimethyl acrylamide-co-acrylic acid)</i>	101
6.1	<i>Reaction pathway for the hydrophobic modification of chitosan using 3-PDCAL</i>	128

List of Figures

1.1	<i>Functional groups which impart water solubility to polymer</i>	2
1.2	<i>Hydrophobically modified poly (acryl amide)</i>	4
1.3	<i>Chemical structure of HASE polymer</i>	6
1.4a	<i>Hydrophobically end-capped poly (ethylene glycol)</i>	7
1.4b	<i>Hydrophobically end-capped poly(ethylene glycol)</i>	7
1.5	<i>Schematic representation of di, tri and graft copolymers</i>	9
1.6	<i>Chemical structure of HM-EHEC</i>	10
1.7	<i>Hydrophobically modified poly(acryl amide)</i>	11
1.8	<i>Viscosity as a function of concentration [Dilute, semi-dilute (unentangled and entangled) and concentrated regime]</i>	12
1.9	<i>Storage modulus (G') and loss modulus (G'') as a function of frequency (ω)</i>	16
1.10	<i>Loops, bridges and dangling chains present in Flower-like micelles off telechelic polymers</i>	18
1.11	<i>Types of geometries used for rheology measurements</i>	23
1.12	<i>Creep measurements</i>	24
1.13	<i>Oscillatory test response of viscoelastic material at a range of frequencies</i>	25
1.14	<i>Autocorrelation function as a function of particle size</i>	28
3.1	<i>Source of CNSL</i>	47
3.2	<i>Constituents of cashew nut-shell liquid. (CNSL)</i>	48
3.3	<i>Source of gallic acid</i>	49
3.4	<i>Structure of gallotannins</i>	49
3.5	<i>Structure of gallic acid</i>	49
3.6	<i>FT-IR spectrum of 3-pentadecyl cyclohexylamine</i>	56
3.7	<i>^1H NMR spectrum of 3-pentadecyl cyclohexyl amine</i>	57
3.8	<i>^{13}C NMR spectrum of 3-pentadecyl cyclohexyl amine</i>	57
3.9	<i>FT-IR spectrum of 3-pentadecyl cyclohexane carbaldehyde</i>	59

3.10	<i>¹H NMR spectrum of to 3-pentadecyl cyclohexane carbaldehyde</i>	60
3.11	<i>¹³C NMR spectrum of 3-pentadecyl cyclohexane carbaldehyde</i>	61
3.12	<i>FT-IR spectrum of methyl 3, 4, 5-tris octyloxy benzoate</i>	62
3.13	<i>¹H NMR spectrum of methyl 3, 4, 5-tris octyloxy benzoate</i>	63
3.14	<i>¹³C NMR spectrum of methyl 3, 4, 5-tris (octyloxy) benzoate</i>	64
3.15	<i>FT-IR spectrum of methyl 3, 4, 5-tris dodecyloxy benzoate</i>	65
3.16	<i>¹H NMR spectrum of methyl 3, 4, 5-tris dodecyloxy benzoate</i>	66
3.17	<i>¹³C NMR spectrum of methyl 3, 4, 5-tris dodecyloxy benzoate</i>	67
4.1	<i>Stacked plots of ¹H NMR spectra of PVA, PVAS-10, HMPVA-MGC₈₋₂, 3, 4 recorded in DMSO-d₆</i>	78
4.2	<i>Plot of specific viscosity versus polymer concentration (■ PVA, □ PVAS-10, ▲ HMPVA- MGC₈₋₂, ▼ HMPVA- MGC₈₋₃ and Δ HMPVA-MGC₈₋₄)</i>	80
4.3	<i>Master curve obtained from steady-shear data of HMPVA-MGC₈₋₃, C_p = 20 g/L</i>	81
4.4	<i>Master curve for HMPVA-MGC₈₋₃, C_p = 40 g/L, T = 5 – 45 °C, T_{ref} = 25 °C</i>	82
4.5	<i>Comparison of steady shear and complex viscosity for HMPVA-MGC₈₋₃, C_p = 20g/L, 25 °C</i>	84
4.6	<i>Confocal laser scanning microscopy images of (a) HMPVA-MGC₈₋₄ and (b) HMPVA-MGC₁₂₋₃ at C_p = 5 g/L</i>	87
4.7	<i>Strain, frequency and SRFS response of HMPVA-MGC₈₋₄ and HMPVA-MGC₁₂₋₃. (C_p = 20 g/L)</i>	89
5.1	<i>¹³C NMR spectrum of poly(N, N'-dimethyl acryl amide-co-Acrylic acid); 70:30</i>	102
5.2	<i>¹H NMR spectra of Hydrophobically modified poly(N, N'-dimethyl acryl amide-co-Acrylic acid); 70:30 with different contents of 3-PDCA (1, 2, 3 mol%)</i>	103
5.3	<i>Zero shear viscosity (η_0) vs. polymer concentration for precursor and hydrophobically modified poly(N, N'-dimethylacrylamide-co-acrylic acid) (3-PDCA= 1, 2, and 3 mol %, T = 25 °C)</i>	104
5.4	<i>Plot of viscosity vs. shear rate for 70DMA/27AA/3-PDCA-3 (C_p = 5, 10, 15, 25, and 35 g/L)</i>	105
5.5	<i>Shear thickening behavior (1, 4 sample at rest; 2, 3 sample after shaking)</i>	106
5.6	<i>Stress-ramp experiment of 70DMA/27AA/ 3-PDCA-3; C_p = 10 g/L</i>	109
5.7	<i>Evolution of creep compliance at various stress values for the sample</i>	111

	<i>70DMA/27AA/3-PDCA-3; $C_p = 10$ g/L</i>	
5.8	<i>Compliance of the gel at 0.5 Pa after shear-induced gelation at 25 Pa. The recovery of compliance to the equilibrium liquids state starts at a critical time τ_L and follows eq 5.1</i>	113
5.9	<i>Gel to solution transition of a shear-induced gel at various stresses below the critical stress. The modulus of the gel is independent of stress (a), but its viscosity shows a power law dependence on stress (b). The liquefaction happens at a constant critical strain (c), and the critical time for liquefaction decreases with stress (d)</i>	115
5.10	<i>Stress induced change from intra-chain hydrophobic interactions to inter-chain hydrophobic interactions for shear thickening polymers</i>	117
6.1	<i>Chemical structure of chitosan</i>	124
6.2	<i>Plots of 1H NMR of Chitosan, HMC-3-PDCAL-2, HMC-3-PDCAL-5 in $D_2O + CD_3COOD$</i>	129
6.3	<i>Specific viscosity (η_{sp}) as a function of polymer concentration (C_p) for chitosan (■), HMC-3-PDCAL-2 (□), HMC-3-PDCAL-5 (●)</i>	130
6.4	<i>Dynamic frequency sweep data as a function of hydrophobic modification (CS, HMC-3-PDCAL-2, HMC-3-PDCAL-5, $C_p = 2$ wt %)</i>	132
6.5	<i>Plot of $g^1(t)$ vs t (s) for CS, HMC-3-PDCAL-2 and HMC-3-PDCAL-5</i>	133
6.6	<i>Plot of $g^1(t)$ vs t (s) for CS, HMC-3-PDCAL-2 and HMC-3-PDCAL-5</i>	134

ABSTRACT

Novel Hydrophobically Modified Polymers using Hydrophobes Derived from Renewable Resource Materials: Synthesis, Characterization and Rheology

Hydrophobically modified water soluble polymers [HMPs] consist of a water-soluble (hydrophilic) backbone with small amount of (< 5-10 mol %) of covalently bound hydrophobic moieties called 'stickers'. The stickers can be put randomly on the polymer chain or can be small blocks or at the end of the polymer chain. Above a certain polymer concentration, the hydrophobic groups self-associate into micelle-like structures to minimize their exposure to water and form transient networks. The viscosity of such a solution increases several fold as compared to the corresponding solution of the unmodified polymer of same molecular weight. The architectural richness of the random, block or hydrophobically end-capped HMPs give diverse physico-chemical properties and have applications in cosmetics, paints, textile pastes, paper, drilling fluids, detergents and pharmaceuticals.

The present thesis work reports on the design and synthesis of new hydrophobically modified water-soluble polymers [HMPs] using hydrophobic compounds derived/synthesized from renewable resource materials such as, cashew nut-shell liquid [CNSL] and gallic acid [GA], which are the byproducts of cashew processing industry and leather industry respectively. Accordingly, four hydrophobic compounds namely, 3-pentadecyl cyclohexyl amine [3-PDCA], 3-pentadecyl cyclohexane carbaldehyde [3-PDCAL], from CNSL and methyl 3, 4, 5-tris octyloxy benzoate [MGC₈], methyl 3, 4, 5-tris dodecyloxy benzoate [MGC₁₂] from GA were synthesized. The structural elucidation of all the hydrophobic compounds prepared were used for the modification of water-soluble polymers namely, poly(vinyl alcohol) [PVA], poly(N, N'-dimethyl acryl amide-co-acrylic acid) and chitosan [CS].

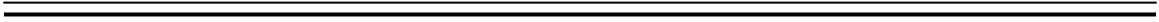
The new HMPs obtained were studied in terms of their structure-property relationship using spectroscopy, rheology and light scattering techniques.

The conclusions from each study are summarized below:

Hydrophobically modified poly(vinyl alcohol) [HMPVA] polymers were prepared using MGC₈ and MGC₁₂. In the semi-dilute regime, the specific viscosity of HMPVAs showed concentration scaling that is typical of polyelectrolytes. However, at higher concentrations, the HMPVA solutions exhibited large increase in specific viscosity and oscillatory experiments showed gel-like behavior which is typical of soft-solids and was probed by strain rate frequency superposition technique.

Hydrophobically modified poly(N, N'-dimethyl acryl amide-co-acrylic acid) polymers were synthesized using 3-PDCA as a hydrophobic compound. Interestingly, at moderate shear rates some of these copolymers exhibited an abrupt shear-induced thickening in which the viscosity of the samples increased several fold. From the creep experiments, it was shown that the thickening occurs only when the shear rate reaches a critical value, $\dot{\gamma}_{crit}$, and that the thickened sample could be trapped in different metastable states by controlling the applied stress. Eventually, the metastable samples reverted back to their equilibrium states at characteristic time which was dependent on (small) probed stress.

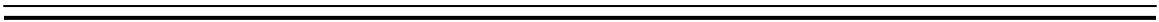
Hydrophobically modified chitosan [HMC] polymers were synthesized using 3-pentadecyl cyclohexane carbaldehyde as a hydrophobic compound. The extent of hydrophobic content was varied from 3 - 7 mol % and the evidence for the incorporation of hydrophobe into chitosan was obtained from ¹H NMR spectroscopy. The solution behavior of unmodified chitosan and HMC was studied using rheology and light scattering techniques. The HMC polymer solutions exhibited enhanced rheological properties as compared to the unmodified chitosan solutions at and above the critical overlap concentrations. This is attributed to the formation of hydrophobic associations in the interacting chains. In the dynamic light scattering studied, comparison of the correlation function of unmodified CS and HMC indicated the slower relaxation/dynamics for HMC due to hydrophobic modifications.



Chapter-I

Hydrophobically Modified Polymers [HMPs]:

A Literature Review



1.1. Introduction:

Water-soluble polymers [WSPs] are an important class of materials to both society and industry due to their specific properties in thickeners, flocculants dispersants or emulsifiers in aqueous based media.^{1, 2, 3} Although WSPs were known in the past, two important events namely, the first legislation of limiting emission of organic solvents in the atmosphere (1966, Los Angeles, USA) and the sharp increase in crude oil price due to Arab-Israel war increased the large usage of WSPs. In the context of water becoming an absolute requirement in food, pharmaceuticals and personal care applications WSPs are gaining more and more attention. Furthermore, due to the environmental hazardous issues, water-based formulations are replacing organic ones in important areas such as drilling fluids, cosmetics and paints.⁴ The key to water solubility lies in positioning sufficient numbers of hydrophilic functional groups along the backbone or side chains. **Figure 1.1** gives some of the major functional groups that possess sufficient polarity, charge or hydrogen bonding capability for hydration.

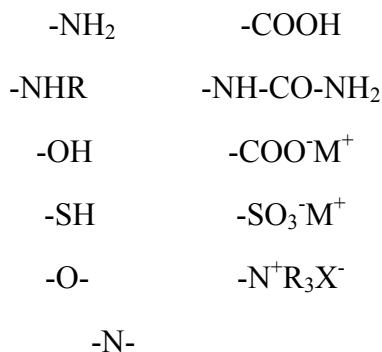


Figure 1.1. Functional groups which impart water solubility to polymer

WSPs are primarily classified into natural and synthetic WSPs depending on their origin. Natural or biopolymers are obtained from plants and animals and some of the examples are proteins,⁵ polypeptides,⁶ polysaccharides⁷ and gums.⁸ Whereas, synthetic WSPs are obtained from monomers of petrochemical origin using suitable polymerization techniques.⁹ Synthetic WSPs are further classified ionic and non-ionic depending on the presence of ionizable/non-ionizable groups in the polymeric chain. Ionic WSPs have been extensively studied as polyelectrolytes¹⁰ and have become increasingly important in large number of industrial applications. Some of the examples of WSPs are poly (acrylic

acid),¹¹ poly(acryl amide),¹² poly(vinyl alcohol),¹³ poly(ethylene oxide)¹⁴ etc. Despite their importance, conventional WSPs suffer from drawbacks since their aqueous solution properties are adversely affected by external working environments such as temperature, pH, shear and the presence of salt.

In order to overcome these problems, Hydrophobically Modified Polymers [HMPs] or also known as Associating Polymers [APs] have emerged as Frontier materials.¹⁵⁻¹⁶ HMPs are basically hydrophilic water-soluble polymers that contain small amount (typically < 2 – 5 mol-%) of hydrophobic groups such as alkyl, perfluoroalkyl or aromatic groups. Above a certain polymer concentration, the hydrophobic groups self-associate into micelle-like structures to minimize their exposure to water. The polymer backbone forms bridges between the micelles leading to the formation of transient network which results into several fold increase in viscosity as compared to the unmodified polymer.

These hydrophobic groups which are also called as “stickers” in HMPs can be incorporated into hydrophilic backbone chain randomly, in a blocky way or at the terminal chain ends (telechelic). Therefore, the architectural richness of HMPs (i. e. random, block or end-capped) gives diverse physico-chemical properties. In aqueous solutions, these polymers exhibit both intra-molecular and inter-molecular interactions which can be manipulated by controlling polymer concentration, molecular weight, ionic strength, pH and temperature. The synthesis of HMPs together with their self-assembling properties in aqueous medium in semi-dilute regime, have been widely reported during the 90's and have formed large number of industrial developments.

1.2. Synthesis of HMPs:

The main objective in synthesizing HMPs is to introduce hydrophobic groups into water-soluble polymers. Basically, there are two ways to incorporate hydrophobic groups into WSP chain: (i) direct copolymerization of hydrophobic and hydrophilic monomers, or (ii) post-modification of the parent water soluble polymer with hydrophobic groups.

Both the methods are described in the following:

1.2.1. Copolymerization:

Copolymerization is routinely used industrial technique for the synthesis of HMPs.¹⁷⁻²³ However, direct copolymerization of hydrophilic monomer with hydrophobic monomer is rather difficult because of the requirement of a common solvent for both the monomers for the reaction to proceed. Furthermore, a limited solubility of monomers often leads to heterogeneous copolymer composition and low hydrophobic modifications.²⁴⁻²⁷ In order to overcome these problems a micellar polymerization/copolymerization technique is routinely used.²⁸⁻³⁵ For example, in the micellar copolymerization of hydrophobic monomer and hydrophilic monomer such as acrylamide the hydrophobic monomer is solubilized within the surfactant micelles, whereas, acrylamide is solubilized in water.²⁵ The heterogeneity in the copolymer or the blockiness of the copolymer can be controlled by the reactivity ratios of hydrophobic and hydrophilic monomers and the concentration of the surfactant.³⁶⁻⁴³ In another route for the synthesis of hydrophobically modified poly(acryl amide) by micellar polymerization, a polymerizable surfactant monomer or surfactant macromonomer (surfmer), n-hexadecyldimethyl-4-vinyl benzyl ammonium chloride, which contains both hydrophilic head and hydrophilic tail is used. (See **Figure 1.2**)

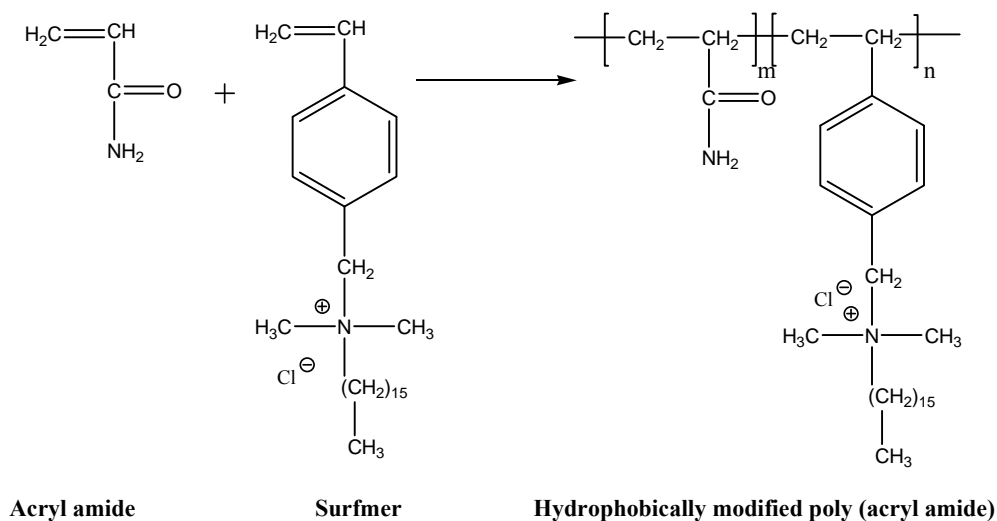


Figure 1.2. Hydrophobically modified poly(acryl amide)

Hydrophobically modified poly(acryl amide)s (HMPAMs) were also synthesized by aqueous micellar copolymerization using poly(propylene glycol) monomethacrylate, PPGMA as hydrophobic monomer and sodium dodecyl sulfate, SDS as surfactant.⁴⁴ Similarly, Dupuis et. al. synthesized HMPs based on 2-acrylamido-2-methylpropane sulfonic acid (AMPS) and dodecyl acrylamide (DAM) using sodium dodecyl sulfonate as surfactant.⁴⁵

1.2.2. Post-polymerization functionalization:

In the second approach of the preparation of HMPs, a hydrophilic polymer is modified with hydrophobic groups using several chemical reaction methods such as coupling reactions. The advantage with this method is that the hydrophobic content of the overall polymer can be easily controlled by taking the known quantity of hydrophobic moiety during the chemical modification reaction. The first studies of the chemical modification of WSPs was reported by Strauss and coworkers in which poly(2-vinyl pyridine) was post-functionalized with n-dodecyl bromide.⁴⁶ Due to the amphiphilic surfactant like nature of the polymer, it was termed as “polysoap”. Similarly, the hydrophobic modification of poly(acrylic acid) [PAA] was performed with alkyl amines in an aprotic solvent, 1-methyl-2-pyrrolidone [NMP] using dicyclohexyl carbodiimide (DCC) as a coupling agent.⁴⁷ A new series of HMPs by grafting highly hydrophobic side chains such as poly(n-butyl acrylate) [PNBA], poly(n-butyl methacrylate) [PNBMA], poly(N-ter butylacrylamide) [PTBA], onto poly(acrylic acid) was prepared by Podhajecka et. al.⁴⁸ Further, natural polymers have been hydrophobically modified using alkyl, aryl halides, isocyanates, aldehydes and anhydrides. Landoll was the first one to modify hydroxyl ethyl cellulose (HEC) using reactive hydrophobic groups.¹⁵⁻¹⁶ Chitosan has been hydrophobically modified using 4-octadecyl benzaldehyde⁴⁹ Recently, Wei and Cheng have reported on the new route for the hydrophobic modification of cellulose.⁵⁰

1.3. Types of HMPs:

Based on the molecular architecture and composition, most of the commercially developed HMPs fall into three categories namely, hydrophobically modified alkali-swellaable/soluble emulsions (HASE), hydrophobically modified ethoxylated urethanes

(HEUR) and hydrophobically modified hydroxyl ethyl cellulose (HMHEC). These systems along with the amphiphilic block copolymers are described in the foregoing:

1.3.1. Hydrophobically modified alkali swellable/soluble emulsion:

HASE were one amongst the first developed HMPs and consists of polyelectrolyte backbone with hydrophobic pendent groups. The polyelectrolyte backbone commonly consists of an ethyl acrylate-methacrylic acid copolymer in such a composition that the polymer is insoluble in water at low pH due to acidic (-COOH) functionality of methacrylic acid (MAA) but becomes highly soluble at high pH because of the ionization of -COOH groups. The solubility is very high at the maximum degree of neutralization of -COOH groups. These materials are prepared by emulsion polymerization at low pH to yield a dispersion which subsequently swells and dissolves upon neutralization with base. They are commonly referred to as HASE thickeners and find extensive applications in paints, textiles and cosmetics. The representative chemical structure of one of the HASE polymer is shown in **Figure 1.3**.

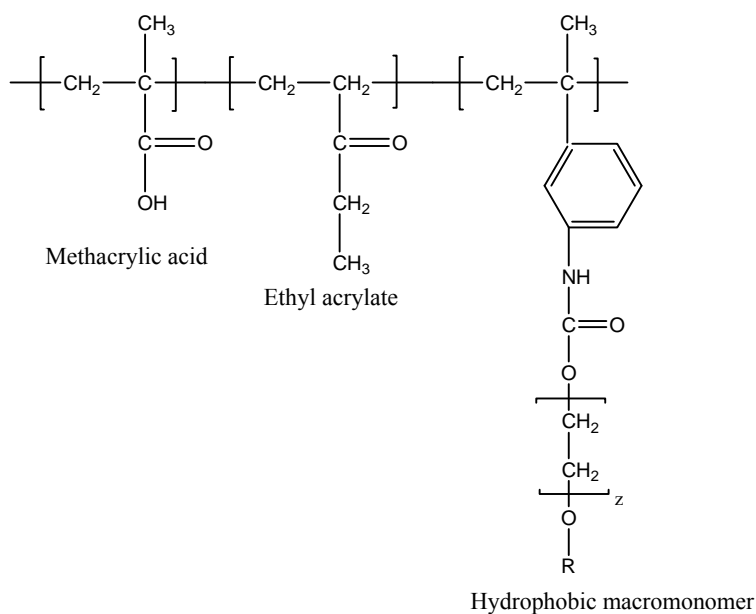


Figure 1.3. Chemical structure of HASE polymer

The thickening effect in these polymers occurs due to the combination of three factors: (i) by dissolution of polymer to form discrete molecules in solution, (ii) by coil-to-expanded conformation at high pH due to electrostatic repulsion and (iii) by intermolecular association of hydrophobic groups leading to the formation of 3-D network structures.

1.3.2. Telechelic polymers:

Telechelic polymers are an important class of HMPs wherein the hydrophobic groups are located only at both ends of the polymer chain.⁵¹ HEUR polymers are classic examples of telechelic polymers and the first reports on HEUR polymers appeared in mid-1980s by Glass and coworkers² and by Sperry and Schaller.⁵¹ Later on this work was reviewed by Howard et. al. with the application of these polymers as rheology modifiers in paint formulations.⁵² Besides their wide industrial applications, telechelic polymers are particularly ideal as model systems for fundamental studies. These polymers consist of poly(ethylene oxide) end-capped with a long hydrocarbon or fluorocarbon alkyl chain. Significant contributions were made by Jenkins to the synthesis and characterization of HEUR polymers.⁵³ HEUR polymers are prepared by chain extension reaction of an oligomeric PEG with diisocyanate, followed by end-capping with an aliphatic alcohol.⁵⁴⁻⁵⁷ The chemical structure of representative HEUR is shown in **Figure 1.4 (a, b)**.

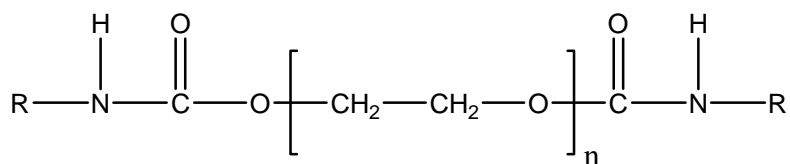


Figure 1.4 a. *Hydrophobically end-capped poly (ethylene glycol)*

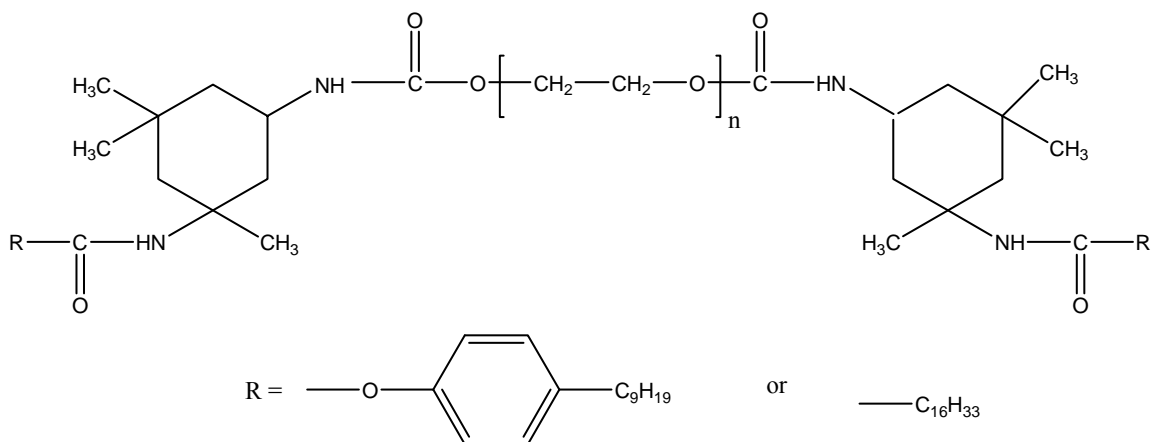


Figure 1.4 b. *Hydrophobically end-capped poly(ethylene glycol)*

Aqueous solutions of these polymers often show enhanced steady-state viscosity and viscoelastic behavior. Under flow, the solution exhibits Newtonian behavior at low shear rates and above some critical shear rates, the solution shows shear thickening behavior and then at high shears rates, the solution shows shear thinning behavior. Large number of publications on the associating behavior of HEUR polymers in aqueous media has been reported in the literature.⁵⁸ Many of the triblock copolymers fall in the category of the telechelic polymers. For example triblock copolymer with sulfonated poly(styrene) as hydrophilic block and poly(*t*-butyl styrene) or poly(butadiene) as hydrophobic endcapping stickers have been reported.⁵⁹ Similarly, different molecular architectures such as comb, block or star HEURs have been synthesized and characterized in the recent past.⁶⁰

1.3.3. Amphiphilic block copolymers:

Amongst the block copolymers, amphiphilic block copolymers have received major attention lately due to their ability to form self-assemblies in aqueous media. For example, PEO-block-PPO and PEO-block-PBO non-ionic, di or triblock and graft copolymers have been widely investigated in aqueous solution.⁶¹ **(Figure 1.5)**

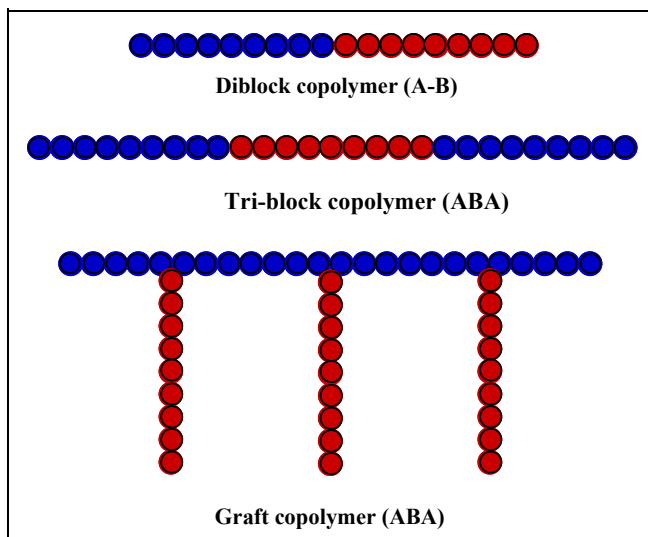


Figure 1.5. Schematic representation of di, tri and graft copolymers

Amphiphilic block copolymers consists of non-ionic (PEO, PPO, PVME etc) or ionic (PAA, PVP, PMA) block linked to hydrophobic blocks such as, poly(styrene), poly (methyl methacrylate) or poly(butylenes oxide).⁶² Many of these amphiphilic polymers are synthesized by living polymerization techniques such as anionic, cationic, atom transfer radical polymerization (ATRP) etc.⁶³ Amphiphilic block copolymers form reversible micellar aggregates due to the hydrophobic associations or electrostatic interactions between different blocks of the copolymers. Nature of the block copolymer, composition of the block copolymer and the temperature gives rise to different micelles (Such as flower-like, star-like and rod-like) and phases (hexagonal, lamellar etc.) in aqueous media.⁶⁴

1.3.4. Hydrophobically modified cellulose:

Hydrophobically modified cellulose derivatives have been widely investigated in terms of their synthesis, characterization and applications.⁶⁵ Particularly, hydroxyethyl cellulose (HEC) containing small amount of n-alkyl substituents (typically C₁₂-C₁₆) was one of the first associating thickeners to be studied.⁶⁶ Hydrophobically modified ethyl hydroxyl ethyl cellulose (HM-EHEC) was synthesized by reacting EHEC with hydrophobic compounds such as long chain alkyl epoxides, alkyl halides, alkyl isocyanates, alkyl anhydrides etc.³ Higher amounts of hydrophobes in these polymers can

lead to insolubility in aqueous media but can be solubilized in the presence of surfactants like SDS.³ The chemical structure of HM-EHEC is shown in **Figure 1.6**.

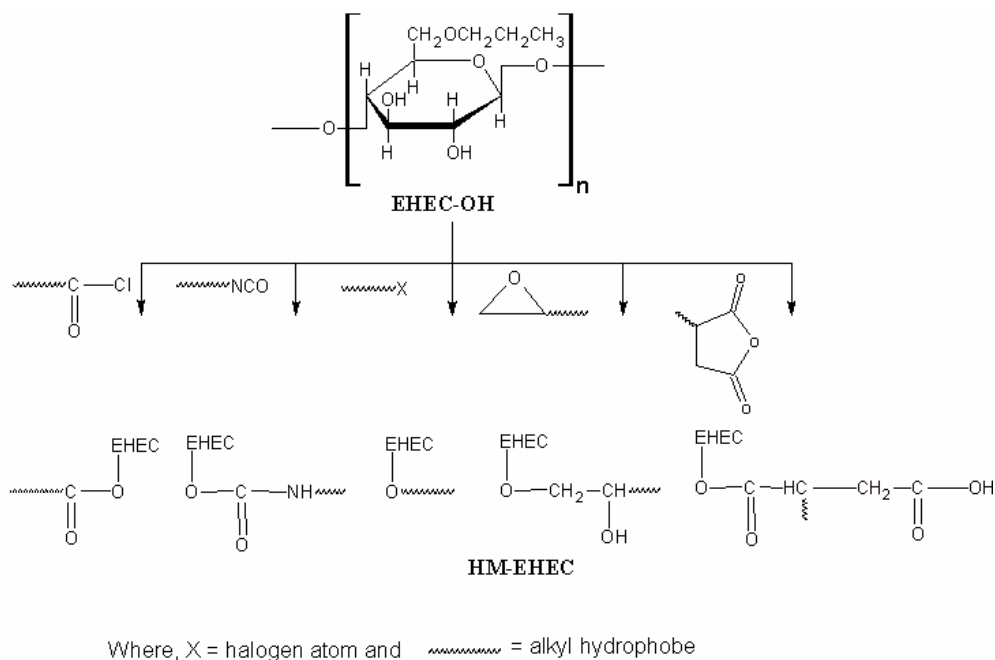


Figure 1.6. Chemical structure of HM-EHEC

Extensive studies on rheology and solution behavior of this class of polymers are reported in the literature.⁶⁷

1.3.5. Hydrophobically modified poly(acryl amide):

Hydrophobically modified poly(acryl amides) (HMPAM) and their partially hydrolyzed analogues have emerged as important HMPs.⁶⁸ These polymers find extensive applications in oil industry for enhanced oil recovery (EOR), drilling fluids, hydraulic fracture and drag reduction.⁶⁹ HMPAMs can be prepared by both micellar copolymerization of acrylamide monomer and hydrophobic monomer (like dodecyl acrylamide) as well as post-functionalization of poly(acrylamide). In the micellar copolymerization, there seems to be a drift in the composition of the copolymer invariably due to the increased reactivity of the hydrophobic comonomer when solubilized in micelles.⁷⁰ Further, with the micellar polymerization, the presence of micro-heterogeneous phase leads to a copolymer with blocky distribution of the

hydrophobes along the polymer backbone. In the case of post functionalization process, a preformed polymer is expected to have statistical arrangement of hydrophobes due to the homogenous medium. Additionally, the hydrophobic content can be controlled in these HMPs with the advantage of using commercially available, well characterized polymers for hydrophobic modification.⁷¹

Many aspects of HMPAMs including synthesis, solution behavior, rheology and applications have been dealt and reported in the literature.⁷² The generalized chemical structure of HMPAM is shown in **Figure 1.7**.

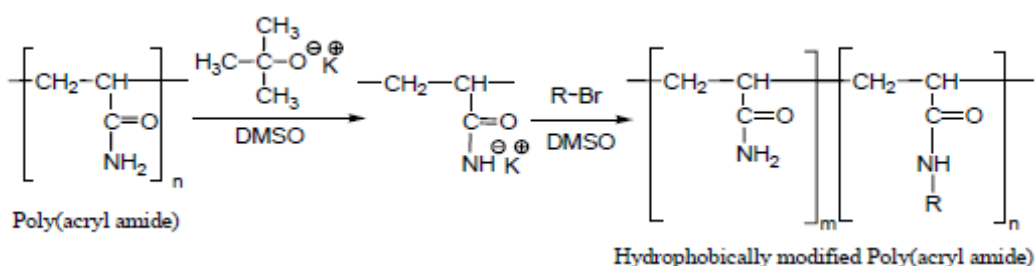


Figure 1.7. Hydrophobically modified poly(acrylamide)

1.4. Rheological behavior of HMPs:

Hydrophobically modified polymers exhibit interesting rheological properties in solution which have large implications in their end applications. When dissolved in aqueous medium, the hydrophobic groups or also termed as “stickers” self-associate yielding intra or intermolecular associations. The driving force for the association process is the interaction between the hydrophobic groups that arises in order to minimize their exposure to water. The resulting micellar association gives rise to 3-D temporary network where it can break and reform continuously due to the thermal fluctuations. The formation of transient network induces a substantial increase in solution viscosity. The viscosity of the polymer solutions strongly depend on the extent of hydrophobic associations, concentration of polymer and the molecular weight of the polymer. Depending on the concentrations, three regimes can be identified namely, the dilute, semi-dilute (semi-dilute can be divided into two) and concentrated which can be seen in **Figure 1.8**.

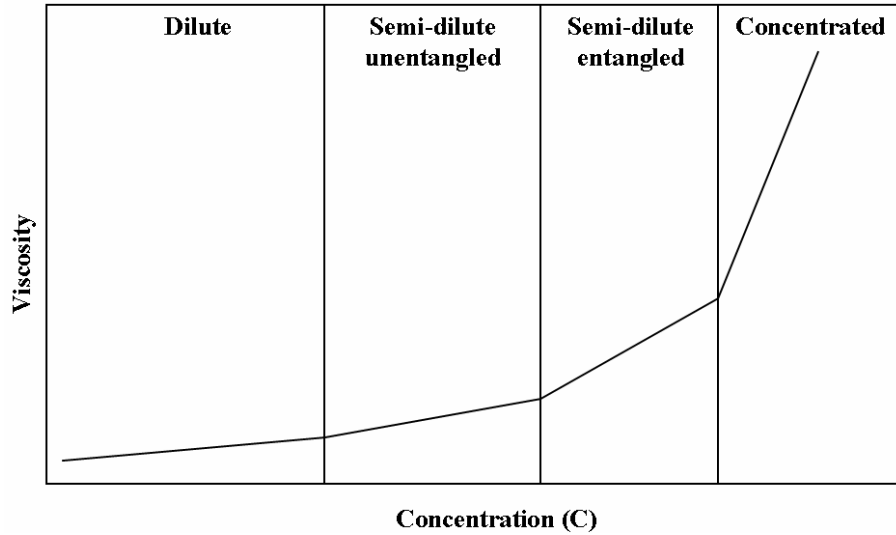


Figure 1.8. Viscosity as a function of concentration [Dilute, semi-dilute (unentangled and entangled) and concentrated regime]

In the dilute regime ($C < C^*$, C^* = overlap concentration), the polymer molecules exist as individual isolated coils having least interactions with each other. At this stage, the viscosity is slightly lower than the corresponding unmodified precursor polymer due to intra-chain interaction leading to compaction of the polymer coils. However, upon increasing the polymer concentrations (at $C = C^*$), polymer coils begin to overlap each other leading to intermolecular interactions. These hydrophobic associations give rise to an increase in viscosity surpassing the viscosity of the unmodified polymer. The intermolecular hydrophobic associations are in dynamic equilibrium where association and dissociation can occur by Rouse relaxation. Further, these associations control the viscoelastic properties of the system and this is considered as the semi-dilute unentangled regime. Here, the viscosity scales with concentration as $\eta \sim C^{1/2}$. With further increase in concentration ($C > C^*$), the density of the entanglements becomes much larger and the intermolecular hydrophobic associations dominate over intramolecular associations. The viscosity rises exponentially, leading to the formation of physical gels. The viscosity scales with concentration as $\eta \sim C^4$ which can be explained using the sticky reptation model.⁷³

1.4.1 Dilute solution viscosity:

The chemical structure and hydrodynamic volume are the key determinants of polymer behavior in solution. The viscosity measurements of dilute solutions give information about the structure or conformation, polymer-solvent interactions and dimensions of polymer chains in solutions.⁷⁴

The relationship between the solution viscosity and polymer concentrations can be given by either Huggins's or Kramer's equations as given below:

Huggins's Eqⁿ:
$$\frac{\eta_{sp}}{C} = [\eta] + k_H [\eta]^2 C \dots\dots\dots (1.1)$$

Kramer's Eqⁿ:
$$\ln \frac{\eta_r}{C} = [\eta]C + k_K [\eta]^2 C \dots\dots\dots (1.2)$$

Huggins's equation is derived from the virial expansion of the specific viscosity in powers of intrinsic viscosity $[\eta]$ whereas the Kramer's equation is obtained from expansion of the inherent viscosity, $\ln \eta_{rel}/C$. Measurements of viscosity are performed using glass capillary viscometer, such as the Oswald-Fenske or the Ubbelohde viscometer.

Practically, the flow of the polymer solution is measured and compared to the flow of the solvent alone. The ratio of the viscosity of a polymer solution, η , to that of the solvent, η_0 , or relative viscosity, η_{rel} , is used to define an important parameter of a polymer in a given solvent, the intrinsic viscosity $[\eta]$ which gives an indication of the hydrodynamic volume (HDV) of an isolated polymer chain in solution.

$$[\eta] = \lim_{c \rightarrow 0} \frac{\eta - \eta_0}{C \eta_0} = \lim_{c \rightarrow 0} \frac{\eta_{sp}}{C} \dots\dots\dots (1.3)$$

In the plots of η_{sp}/C vs. C , the extrapolation to zero concentration is performed to eliminate any influence of molecular interferences likely to happen even in dilute

solutions. In the above equation ‘C’ is the concentration and η and η_0 have the dimension of the viscosity (Poise or Pa.s). η_{sp} and η_{rel} are dimensionless $[\eta]$, η_{red} , η_{inh} all have the dimensions of inverses concentration. A relationship between molecular weight and $[\eta]$ was derived independently by Mark and Houwink in the late 1930s.

$$[\eta] = KM^\alpha \text{ ----- (1.4)}$$

Where, K and α are constants (the Mark-Houwink constants) that vary with solvent and polymer. The exponent α provides a measure of chain rigidity.⁷⁵ For most polymer-solvent pairs, the exponent α ranges between 0.5 and 0.8. In a θ -solvent it takes a value of 0.5, characteristic of the ideal random coil. Further, η can also be used to determine the overlap concentration,

$$C^* \sim \frac{1}{[\eta]} \text{ ----- (1.5)}$$

Wang et. al. studied the viscosity behavior of hydrophobically modified poly(acrylic acid) with long chain alkyl amines.⁷⁶ The study also indicated that the well known viscosity reduction of polyelectrolyte solution in the presence of salt can be prevented by hydrophobic modification of polyelectrolytes. Volpert et. al. reported on the influence of hydrophobe structure on the composition, microstructure and rheology of hydrophobically modified poly(acryl amides) prepared by micellar copolymerization.⁷⁷ Regalado et. al. studied the viscoelastic behavior of semi-dilute solutions of hydrophobically modified poly(acryl amide) having multisticker architecture.⁷⁸ Tan et. al. studied the rheological properties of semi-dilute HASE polymers in the presence of surfactant (SDS) and salt solutions.⁷⁹ There exists an optimum concentration of SDS where the surfactant molecules strengthen the associative network junctions by increasing the aggregation number leading to the enhancement of viscosity and the relaxation time of the network. Similarly, the solution properties of hydrophobically modified ethyl hydroxyl ethyl cellulose (HM-EHEC) in the presence of surfactant (SDS) and salts were investigated by Nystrom et. al.⁸⁰ The rheological behavior of HMPs is often described using transient network model of Tanaka and Edwards.⁸¹ Very clearly two distinct

categories of systems have been identified. The first category describes unentangled network in which the molecular weight between adjacent junctions is smaller than the entanglement molecular weight (M_e) so that the chain follow Rouse dynamics modified by sticky centers. In the second category, entanglement effects play dominant role along with existence of many temporary cross-links. The motions of the chain are described by the sticky reptation, concentration and lifetime of the junction.⁸²

1.4.2. Shear thickening and shear thinning behavior of HMPs:

It is now well established and accepted that the unusual rheological properties of HMPs originate from the formation of a physically cross-linked network formed by the association of hydrophobic groups. Aqueous solutions of these polymers often show enhanced zero shear viscosity and elastic behavior. Under shear, the solutions exhibit Newtonian behavior at low shear rates and interestingly, above some critical shear rate ($\dot{\gamma}_{crit}$), the solutions show shear thickening behavior (i. e. increase in viscosity with increase in shear rate) and then at higher shear rates, the solutions show shear thinning behavior. The shear thickening behavior has been observed in concentrated suspensions,⁸³ mesophases of surfactants,⁸⁴ ionomers in non-polar solvents⁸⁵ and worm-like micelles.⁸⁶ Shear thickening behavior has been reported in associating polymer solutions since 1950's and has attracted increasing attention lately.⁸⁷ Several experimental techniques comprising, rheology,⁸⁸ flow birefringence,⁸⁹ SANS⁹⁰ etc. have been used to explain the shear thickening behavior. The theoretical aspects of shear thickening and the underlying mechanism have been studied by several groups.

In this thesis, a chapter is dedicated to the study of shear thickening polymer and the detailed account of shear thickening polymers will be discussed in that chapter.

1.4.3. Viscoelasticity in HMPs:

The viscoelastic behavior of HMPs is observed in the semi-dilute regime which is beyond the critical concentration of the polymer where intermolecular associations take place. This concentration is in the vicinity or above the critical overlap concentration, C^* . The viscoelastic response of a typical HMP to an applied oscillatory deformation

(Figure 1.9) can be fitted to a simplest model of viscoelastic behaviors namely, the Maxwell model, consisting of an elastic component and a viscous component expressed as:

$$G' = G_0 \frac{\omega^2 \tau^2}{1 + \omega^2 \tau^2} \text{----- (1.6)}$$

$$G'' = G_0 \frac{\omega \tau}{1 + \omega^2 \tau^2} \text{----- (1.7)}$$

Where, G_0 is the plateau modulus, G' is the storage modulus, G'' is the loss modulus, τ is the relaxation time of the network and ω is the angular frequency. (Figure 1.9)

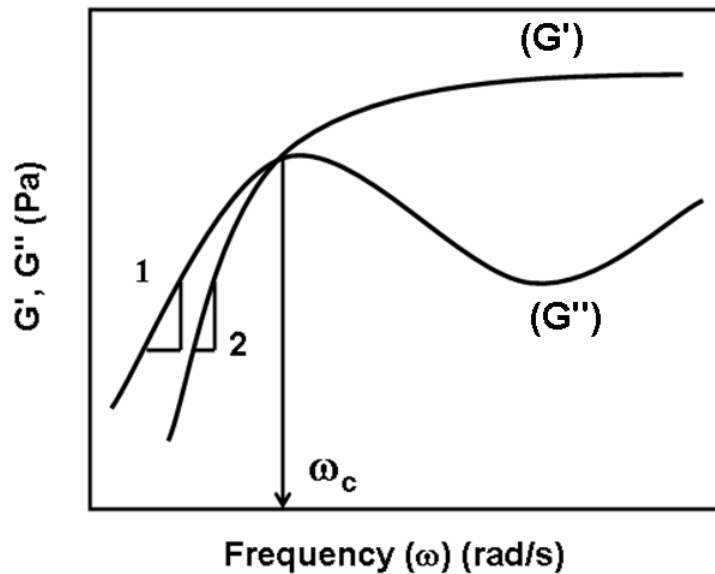


Figure 1.9. Storage modulus (G') and loss modulus (G'') as a function of frequency (ω)

The complex viscosity $[\eta^*]$ can be defined as the ratio of complex modulus, G^* $[G^* = \sqrt{(G')^2 + (G'')^2}]$ to the frequency of the deformation (ω). From the **Figure 1.9** it can be seen that in the high frequency region, an elastic behavior is observed for a short interval of time with almost constant value of storage modulus (G'), which corresponds to a plateau region (G_0). A frequency at which both moduli are equal $[G'(\omega) = G''(\omega)]$ is

referred to as a characteristic frequency and the reciprocal of this frequency corresponds to the relaxation time of the temporary polymer network.

The study of viscoelastic properties by various transient experiments gives insight into the molecular dynamics of polymer network. Since HMPs form transient network due to physical associations between hydrophobic groups, the viscoelastic properties can provide valuable information about the nature and the rate of associations and dissociations of hydrophobes. Volpert et. al. have studied the linear viscoelastic properties of hydrophobically modified poly(acryl amides) and observed that the hydrophobic modification results into enhanced values of G' and G'' compared to the unmodified PAM.⁹¹ In the terminal frequency region, the slopes of G' and G'' were found to be 1.8 and 1.0 which were close to Maxwellian behavior. The crossover frequency was observed only for HMPAM which indicated the slow relaxation of HMPAM chains. However, Regalado et. al. showed that the dynamics of HMPAM can be explained by multiple relaxation process.⁹² Similarly, Jenkins et. al.⁹³ showed that the oscillatory response of HMHEC and HASE polymer exhibited two relaxation processes. Extensive work has been reported on the oscillatory response of HEUR polymers which differ significantly from HASE polymers. Numerous research groups have investigated on the rheology of HEUR polymers. The review by Winnik and Yekta⁹⁴ and a book by Larson⁹⁵ provide a detailed account of these systems, HEUR polymers being telechelic in nature exhibit interesting topological structures in aqueous medium under certain conditions of concentration. The hydrophobic end groups from the same chain can come together in the same micelle and form loop like structures. Alternately, it is possible that the hydrophobic end groups of the same chain can be located in different micelles resulting in bridging of two micelles. These bridging chains can be referred to as elastically active since they become part of the temporary elastic network. One can even expect, under certain conditions only one hydrophobic group getting involved in micelle, leaving the other group unassociated leading to the formation of dangling chains. Therefore, the complex rheological properties of HEUR polymers originate from the dynamical interchange of these loops, bridges and dangling chains as a function of deformation imposed on the network. **(Figure 1.10)**

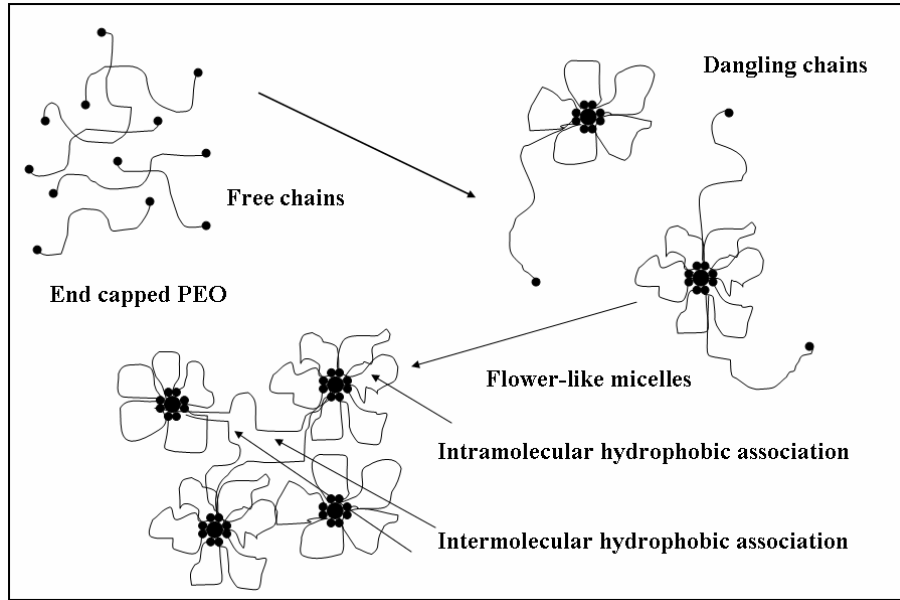


Figure 1.10. *Loops, bridges and dangling chains present in Flower-like micelles of telechelic polymers*

Various parameters such as polymer concentration, molecular weight and degree of hydrophobicity, temperature and shear play an important role in the rheological properties of telechelic polymers.

The salient features of the rheological behavior of HEUR polymers include:

- (i) the ability to form highly viscous solutions at low to moderate concentrations
- (ii) a linear viscoelastic response that obeys Maxwell model with a single relaxation time
- (iii) observation of both shear thickening and shear thinning at moderate and high shear rates, respectively

Annable et. al. studied in detail the linear viscoelastic properties of HEUR solutions which could be fitted to Maxwell model with single relaxation element.⁹⁶ The relaxation time obtained from viscoelastic measurements scaled linearly with respect to hydrophobe chain length at constant polymer concentration and molecular weight.

According to the reports of Ng et. al.⁹⁷ the relaxation spectra obtained from oscillatory data indicates the presence of two relaxation times. The short time relaxation

time corresponded to the lifetime of the hydrophobic junctions and the long relaxation time corresponded to the network. However, Lafleche et. al. attributed slow relaxation to hopping of the micelles. While at higher polymer concentrations, a second relaxation process with long relaxation time corresponded to the detachment of the bridged chains from the micelles.⁹⁸ Tripathi et. al., based on their molecular modeling, explained the dual relaxation behavior for HEUR solutions where short relaxation time (τ_R) corresponded to Rouse relaxation of individual polymer chains ($\sim 5 \times 10^{-5}$ s) and long relaxation time (τ_{eff}) related to the “effective” (elastically active network) network ($\sim 10^{-1}$ s).⁹⁹ Their model predicted that the effective relaxation time (τ_{eff}) depends on the concentration and molecular weight of the chains, the hydrophobic length and the aggregation number. The associating behavior and the dynamics of HEUR solutions have been studied by light scattering,¹⁰⁰ fluorescence spectroscopy,¹⁰¹ NMR self-diffusion and ^2H spin relaxation,¹⁰² small angle neutron scattering (SANS)¹⁰³ experiments and small angle X-ray scattering (SAXS).¹⁰⁴

1.5 Applications of HMPs:

HMPs, because of their excellent viscosity properties are finding increasing applications as thickeners or rheology modifiers in paints and coatings,¹⁰⁵ paper,¹⁰⁶ textiles,¹⁰⁷ food and pharmaceuticals,¹⁰⁸ personal care products,¹⁰⁹ water treatment¹¹⁰ and enhanced oil recovery applications.¹¹¹ The brief details of their applications in various fields are described in the following:

1.5.1. Personal care and cosmetics:

Polymers serve multifarious purposes in cosmetic formulations. They are used as film formers, hair fixatives, as thickeners and rheology modifiers in emulsions, gels, hair colorants, as emulsifiers in lotions, sunscreens, hair colors, as conditioners, moisturizers and dispersants. Conventional polymers such as non-ionic cellulose ethers for example, methyl cellulose, hydroxyl ethyl cellulose, guar gum, xanthan gum and poly(acrylic acid) [carbopols] are used in various applications such as hair care compositions and cosmetic applications. The most commonly used hair fixative polymers are PVP and PVP/VA

copolymers. Hair fixative polymers generally function by performing films that spot-weld and seam-weld the hair in the desired style. Copolymers of acrylates/hydroxy acrylates (Acudyne 255, Rohm & Haas) have been used as hair fixative polymers. HASE (Aculyne polymer, Rohm & Haas) and hydrophobically modified polysaccharides (Natrosol plus, Hercules) have been used in hair dye system and in hair bleaching composition where the precise structure of associative thickener is important in determining the quality of the color imparted to the hair.¹¹² Pemulen polymeric emulsifiers are cross-linked hydrophobically modified polyacrylates marketed by Novean and have been used in cosmetic formulation as emulsifiers and rheology modifiers. Since HEUR polymers are non-ionic in nature, they are compatible with all the cosmetic ingredients and exhibit better salt and acid tolerance. They have been used in hair conditioners, peroxide based hair dyes and sunscreen formulations.¹¹³

1.5.2. Paints and coatings:

HMPs have been extensively used in water based paints and coatings as rheology controlling agents. Particularly, hydrophobically modified hydroxyl ethyl cellulose (HM HEC), hydrophobically modified alkali soluble/swellable emulsions (HASE), hydrophobically modified acrylates and HEUR are used as thickeners in paints and coatings formulations.¹¹⁴ The fundamental purpose of HMPs in paint is that of viscosity control. Paint properties ranging from in-can storage stability to application characteristics to final film performance and film esthetics are all related to the choice of HMPs and their viscosity characteristics at different shear rates. At very low shear rates ($0.01 - 0.1 \text{ s}^{-1}$), viscosity must be high enough to prevent both in-can settling and sagging after application, yet low enough to provide flow and leveling. At moderately low shear rates ($10 - 20 \text{ s}^{-1}$), viscosity must be high enough to provide good brush pick-up. At high shear rates typical of brushing ($5000 - 10,000 \text{ s}^{-1}$ or higher), viscosity must be high enough to give good film build, but not so high as to cause excessive brush drag. Generally, paint formulators aim at obtaining viscosities of 500-1000 P at shear rates of $0.06 - 0.1 \text{ s}^{-1}$, 15 - 40 P at shear rates of $10 - 20 \text{ s}^{-1}$ and 1 - 2 P at shear rates of $10,000 \text{ s}^{-1}$. Besides controlling the flow properties, HMPs also influence processes such as, mixing, pigment dispersion, pumping, coating applications, spreading, sagging and pigment

settling. HMPs impart excellent flow and leveling to latex paints, properties not usually attainable with other thickeners. However, there could be some disadvantages in which paints containing HMPs can take longer time to stabilize and some times, have a tendency to separate.

1.5.3. Enhanced oil recovery: (EOR)

In the crude oil productions, three distinct phases are involved which are primary, secondary and tertiary. Primary recovery typically provides to only a small fraction of reservoir's total oil capacity. Secondary recovery techniques can increase more productivity and tertiary recovery, also called as enhanced oil recovery (EOR) is carried out finally to extract oil to the maximum extent. EOR include miscible techniques such as gas flooding, thermal methods, (steam injection), chemical methods (surfactant/polymer or alkaline injection) and water flooding processes.¹¹⁵ However, many disadvantages still exist in these processes. For example, in water flooding method, due to the higher mobility of water (low viscosity) as compared to oil (high viscosity), create a poor sweep efficiency and this results in viscous fingering instability and hence reduce the efficiency of oil recovery.

In order to overcome this problem, water-soluble polymers have been frequently used in polymer augmented water flooding process.¹¹⁶ The increase in viscosity by addition of these polymers can improve the sweep efficiency during enhanced oil recovery process. Water soluble polymers such as poly(acryl amide) [PAM], xanthan gum and hydrolyzed poly(acrylamide) [HPAM] are the well known rheology modifiers in EOR applications. However, these water-soluble polymers suffer from certain drawbacks in which their solution viscosity is adversely affected by external working environments such as change in pH, presence of salt, shear and temperature. Therefore, HMPs have emerged as improved materials which show enhanced viscosity in the above hostile environments during the EOR operations. Young et. al. introduced hydrophobically modified guar gum as a completion fluid.¹¹⁷ Hydrophobically modified poly(acryl amide) [HM-PAM],¹¹⁸ hydrophobically modified poly(acrylic acid) [HM-PAA],¹¹⁹ hydrophobically modified hydroxyl ethyl or propyl cellulose [HMHEC/HMHPC]¹²⁰ are claimed to have potential in EOR applications.

1.6. Techniques used for the characterization of HMPs reported in this thesis:

1.6.1. Rheology:

Rheology deals with the study of flow and deformation. In 1920, a chemistry Professor at Lehigh University, Eugene Bingham coined a name ‘Rheology’ for the study of flow behavior and described the fundamental relations called constitutive relation between force and deformation in materials, primarily liquids. The simplest relation between the force and deformation in solids is given by Hooke’s law, $\tau = G\gamma$, where τ is the force per unit area or stress and γ is the relative change in the length or strain. G is the elastic modulus which is an intrinsic property of a solid. However, in liquids the relation between the flow and deformation is given by Newton's law of viscosity, $\tau = \eta \dot{\gamma}$ where η is the viscosity and $\dot{\gamma}$ is the rate of shear. In Newtonian fluids, the η will change with temperature but remains independent with shear rate. On the other hand in non-Newtonian fluids the η varies with shear rate. Most of the polymer melts and solutions exhibit non-Newtonian flow behavior especially at high shear rates and found to have both viscous and elastic nature. Therefore, they are also called as visco-elastic fluids. The experimental characterization of a material's rheological behavior is known as rheometry.

1.6.2. Rheometer:

Rheometer is a mechanical device that is capable of subjecting a sample to either a dynamic (sinusoidal) or steady (linear) shear strain (deformation). Then measuring the resultant torque expended by the sample in response to the shear strain (shear strain is applied by the motor and torque is measured by the transducer). Rheometers are of two types: controlled stress rheometer, where the stress is applied electrically via a motor and the strain is measured; and in the controlled strain rheometer, strain is imposed and the stress is computed from the deformation of a calibrated spring system.

1.6.3. Geometry:

A range of different geometries is available which include parallel plates and cone-and-plates (suitable for fluids and melts with $\eta > 10 \text{ m Pa.s}$), couette (for low viscous samples, $\eta < 10 \text{ m Pa.s}$) and double wall couette (for very low viscosity samples, $\eta < 1.0 \text{ m Pa.s}$). (**Figure 1.11**)

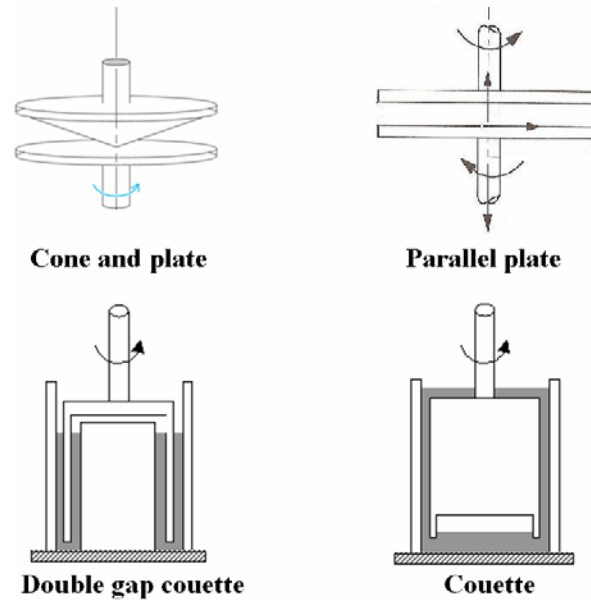


Figure 1.11. Types of geometries used for rheology measurements

1.6.4. Creep:

In case of creep experiments, very low stress is applied to the sample and the strain is calculated. With a constant stress applied, creep compliance $J(t)$ is measured as a function of time (t). When creep compliance $J(t)$ is plotted as a function of time (t) the compliance curve and creep recovery give information about the modulus and relaxation behavior of the sample. (**Figure 1.12**)

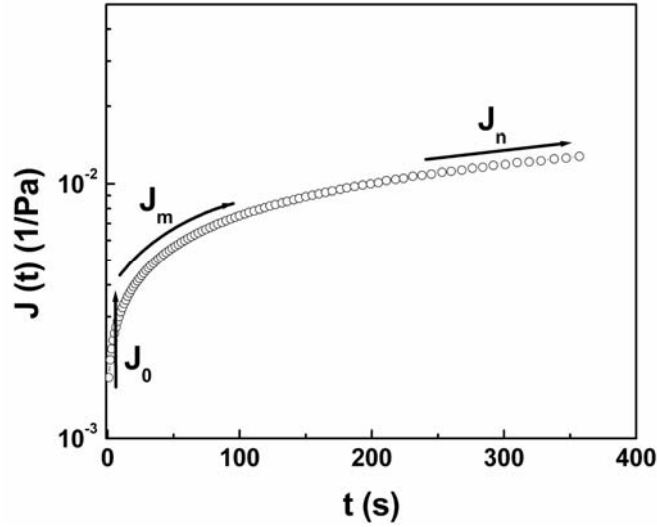


Figure 1.12. Creep measurements

Where,

J_0 = Instantaneous compliance, J_m = Viscoelastic compliance, J_n = Newtonian compliance.

1.6.5. Oscillatory Measurements:

In dynamic oscillatory experiment a sinusoidal strain is applied and resulting stress is measured. The time scale probed is determined by the frequency of oscillation of the shear deformation. Viscous and elastic properties of the sample are simultaneously measured.¹²¹⁻¹²² In a typical case of viscoelastic material, liquid-like response at lowest accessible frequencies is shown (**Figure 1.13**) where the loss modulus (G'') is higher than the storage modulus (G') while at higher frequencies, the storage modulus dominates (G') over the loss modulus (G'').

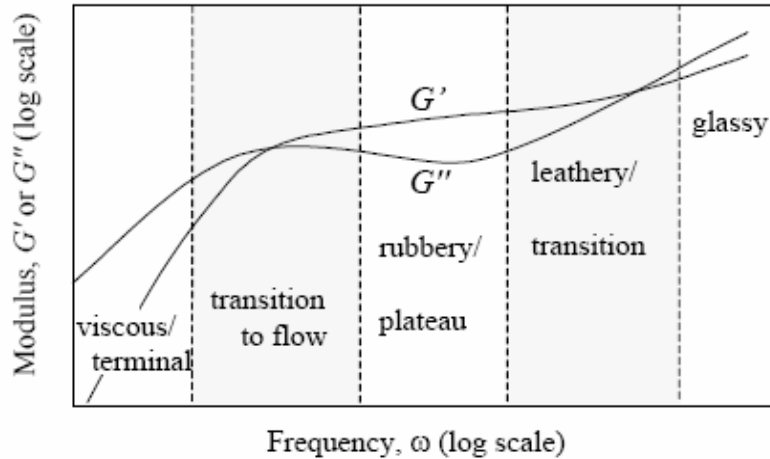


Figure 1.13. Oscillatory test response of viscoelastic material at a range of frequencies

1.6.6. Light scattering:

When a visible light passes through a solution containing solute molecules, part of the light is scattered. The scattered light may be analyzed either in terms of its intensity or in terms of its fluctuations. The former is called static light scattering [SLS] and can be used to find the molecular weight and radius of gyration. $[R_g]$ The scattered light intensity depends on the concentration of the solution and scattering angle.

Dynamic light scattering [DLS], on the other hand, detects the fluctuations of the scattering intensity due to Brownian motion of molecules in solution. DLS gives information about size, shape and interactions of particles in solution. DLS is also sometimes referred to as photon correlation spectroscopy [PCS] or quasielastic light scattering.

Static light scattering measures the intensity of the light scattered of a solution at a single time. The relationship between concentration and intensity of scattered light was derived by Zimm in 1948 which is as follows,

$$\frac{KC}{R_{\theta}^0} = \frac{1}{M_w} + 2A_2c \dots \dots \dots (1.8)$$

Where, C = concentration, M_w = weight average molecular weight, $P(\theta)$ = particle scattering function that depends on the particle shape and R_θ^0 Rayleigh ratio, A_2 = second virial coefficient, constant K is defined to be,

$$K = \frac{4\pi^2 n^2 (dn/dc)^2}{N_A \lambda_0^4} \text{----- (1.9)}$$

Where, n = refractive index, dn/dc = refractive index increment, λ_0 = wavelength of the incident light. $P(\theta)$ describes the large particle size effect and it is a ratio of actual scattering (i_θ) and the scattering that would occur off small particles (i_θ^0).

Rayleigh ratio,

$$R_\theta^0 = \frac{r^2 i_\theta^0}{I_0} \text{----- (1.10)}$$

I_0 = incident polarized light.

$$P(\theta) = \frac{i_\theta}{i_\theta^0} = \frac{R_\theta}{R_\theta^0} \text{----- (1.11)}$$

$\langle s \rangle^2$ = mean squared radius of gyration.

$$\frac{KC}{R_\theta^0} = \frac{1}{M_w} + 2A_2 C \text{----- (1.12)}$$

$$\frac{KC}{R_\theta^0} = \frac{KC}{P(\theta)R_\theta^0} = \left(\frac{1}{M_w} + 2A_2 C \right) \frac{1}{P(\theta)} \text{----- (1.13)}$$

$$\frac{KC}{R_\theta^0} = \left(\frac{1}{M_w} + 2A_2 C \right) \left(1 + \frac{16\pi^2}{3\lambda^2} \langle s \rangle_w^2 \sin^2 \frac{\theta}{2} \right) \text{----- (1.14)}$$

A set of light scattering experiment consists of measuring KC/R_θ for different concentrations and various scattering angles. Plot of KC/R_θ vs. $\text{Sin}^2 \theta/2$ at constant 'C' gives straight line with,

$$\text{slope} = \left(\frac{1}{M_w} + 2A_2c \right) \frac{16\pi^2}{3\lambda^2} \langle S^2 \rangle_w \text{-----} (1.15)$$

$$\text{Intercept} = \left(\frac{1}{M_w} + 2A_2c \right) \text{-----} (1.16)$$

When plot of intercepts with different concentrations give straight line with,

$$\text{slope} = 2A_2 \text{-----} (1.17)$$

$$\text{Intercept} = \frac{1}{M_w} \text{-----} (1.18)$$

One can calculate $\overline{M_w}$ and A_2 . Substituting these values in the slope of the first plot, $(S^2)_w$ can be determined. Alternately, Zimm plot was developed where KC/R_θ vs. $\text{Sin}^2 \theta/2 + KC$ is plotted in which grid is formed. From the grid plot the above parameters can be evaluated.

In dynamic light scattering, speed at which particles are diffusing due to Brownian motion is measured. This is done by measuring the rate at which the intensity of the scattered light fluctuates when detected using a suitable optical arrangement. The rate at which these intensity fluctuations occur will depend on the size of the particles. The small particles cause the intensity to fluctuate more rapidly than the large ones. The intensity fluctuations are measured using a device called digital autocorrelator. The time at which the correlation starts to significantly decay is an indication of the mean size of the sample. If the particles are large the signal will be changing slowly and the correlation will persist for a large time. On the other hand if the particles are small and moving

rapidly then correlation will reduce more quickly. A typical decay of correlation coefficient with time is shown in **Figure 1.14**.

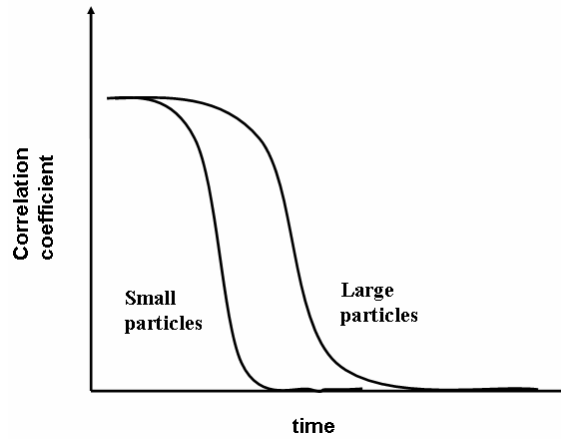


Figure 1.14. Autocorrelation function as a function of particle size

The steeper the line, the more monodisperse the sample is. Conversely, the more extended the decay, the greater is the sample polydispersity. The wave vector determines the length scale, over which molecular motions are detected and is given by,

$$q = 2\pi n \sin(\theta/2)/\lambda \text{ ----- (1.19)}$$

Where, n = refractive index, λ = wavelength of radiation and θ is scattering angle. The resulting correlation function,

$$G(\tau) = \int \frac{I(t)I(t+\tau)}{\langle I(t) \rangle^2} dt \text{ ----- (1.20)}$$

is accumulated over the duration of the measurement of the intensity $I(t)$ as a function of time, and is expected to show under ideal condition a single exponential decay.

$$G(\tau) = 1 + \beta \exp(-D_q^2 \tau) \text{ ----- (1.21)}$$

Where, the decay rate Dq^2 includes the diffusion coefficient of the molecule and the fitting parameter β is related to the ratio of coherent signal to incoherent noise.

The Stokes-Einstein relation may be used to convert the measured diffusion coefficient into hydrodynamic diameter, d_H of the particle.

$$D = \frac{k_B T}{3\pi\eta d_H} \text{----- (1.22)}$$

Where, η is viscosity, k_b = Boltzman constant, and T = absolute temperature.

1.6.7. Confocal microscopy:

The basic concept of confocal microscopy was originally developed by Marvin Minsky in the mid-1950s to visualize neurons in-vivo.¹²³⁻¹²⁵ Illumination is achieved by scanning one or more focused beams of light across the specimen by the laser. Point of illumination is brought to focus by on the specimen by an objective lens and scanned using scanning devices. The sequence of point of light from the specimen is detected by a photomultiplier tube (PMT) through the pinhole and output from PMT is built into image and displayed by the computer. A sample can be labeled with more than one fluorophore by laser scanning confocal microscope (LSCM). Use of red, green and blue color is more informative. Fluorescence is the primary energy source for confocal microscopes.

1.7 Summary:

Water soluble polymers consisting of different types of functional groups (ionic and neutral) are industrially important materials as thickeners, flocculants dispersants or emulsifiers in aqueous based media. There are limitations for WSPs that its solution properties are sensitive to shear, temperature and salt. Thus, HMPs were introduced. These polymers consist of water-soluble backbone polymer with few hydrophobic groups randomly attached through covalent bond. In aqueous medium these hydrophobic groups associate and form network resulting into enhanced viscosity at constant molecular weight. HMPs are prepared by various synthetic methods such as copolymerization and post modification resulting into random or blocky distribution. These polymers are used as thickeners, flocculants dispersants or emulsifiers. Similarly they are used in enhanced oil recovery, paints and coatings, pharmaceutical applications and cosmetics.

References:

1. Glass, J. E. "*Water-Soluble Polymers: Beauty with Performance*," American Chemical Society series 213, Washington DC, **1986**.
2. Glass, J. E. "*Polymers in Aqueous Media: Performance Through Association*", American Chemical Society series 223, **1989**.
3. Dubin, P.; Bock, J.; Davies, R. M.; Schultz, D. N.; Thies, C. "*Macromolecular Complexes in Chemistry and Biology*," Springer-Verlag, Berlin, **1994**.
4. Bock, J.; Valint, P. L.; Pace, S. J.; Siano, D. B.; Schultz, D. N.; Turner, S. R. "*Water-Soluble Polymers for Petroleum Recovery*," Stahl G. A., Schultz D. N., Eds., Plenum Press, New York, chapter 9, 147, **1988**.
5. Shalaby, S. W.; McCormick, C. L.; Buttler, G. B. "*Water-Soluble Polymers: Synthesis, Solution Properties and Applications*," American Chemical Society Symposium 467, Washington D. C. **1991**.
6. Goddard, D. E.; James, G. V. "*Principles of Polymer Science and Technology in Cosmetics and Personal Care*", Cosmetic Science and Technology Series, 22, **1999**.
7. Lapasin, R.; Pricl, S. "*Rheology of Industrial Polysaccharides: Theory and Applications*," AN ASPEN Publication, 1995; Dea I. C M, Pure &App/Chem., 61(7), 1315, **1989**.
8. Whistler, R. L. "*Industrial Gums: Polysachharides and their derivatives*," Bemiller J. N. 3rd edition, Academic Press USA, **1959**.
9. Finch, C. A. "*Chemistry and Industry*," 21, **1981**.
10. Forster, S.; Schmidt, M. "*Polyelectrolytes in Solution*," *Advances in Polymer Science* **1995**, 120, 51.

11. Will, R. K.; Pearson, J.; Yokose, K.; Lochner, U.; Fink, U. “*Synthetic Water-Soluble Polymers*,” Glauser, J.; Blagoev, M. Kumamoto, T. “*Acrylic Acid, Acrylate Esters and Superabsorbent Polymers*,” **2011**.
12. Schmitz, K. S. “*Macroions in Solution and Colloidal Suspension*,” VCH Publishers, **1993**.
13. Finch, C. A. “*Polyvinyl alcohol; properties and applications*,” **1973**, Wiley in London, New York; Finch, C. A. (Ed.), *Polyvinyl Alcohol, Developments*, 2nd Edition - March **1992**.
14. Fink, J. K. poly(ethylene oxide), in “*Handbook of Engineering and Specialty Thermoplastics: Water Soluble Polymers*,” John Wiley & Sons, Inc., Hoboken, N J, USA, **2011**.
15. Landoll, L. M. *US Patent 4228277*, Hercules Incorporation (Wilmington, DE), inv.: **1980**.
16. Landoll, L. M. *US Patent 4 352916A*, Hercules Incorporation (Wilmington, DE), inv. **1982**.
17. Evani, S. *European Patent 57875*, **1982**.
18. Evani, S. *US Patent 4432881*, **1984**.
19. Bock, J.; Siano, D. B.; Kowalik, R. M.; Turner, S. R. *Eur. Patent 115213*, **1984**.
20. Turner, S. R.; Siano, D. B.; Bock, J. *US Patent 4520182*, **1985**.
21. Turner, S. R.; Siano, D. B.; Bock, J. *US Patent 4528348*, **1985**.
22. Turner, S. R.; Siano, D. B.; Bock, J. *US Patent 4521580*, **1985**.
23. Emmons, W. D.; Stevens, T. E. *US Patent 4395524*, **1983**.
24. Biggs, S.; Hill, A.; Selb, J.; Candau, F. *J. Phys. Chem.* **1992**, *96*, 1505.
25. Lacik, I.; Selb, J.; Candau, F. *Polymer* **1995**, *36*, 3197.

26. Bock, J.; Siano, D. B.; Schulz, D. N.; Turner, S. R.; Valint, P. L.; Pace, S. J. *Polym. Mater. Sci. Eng.* **1986**, *55*, 355.
27. Volpert, E.; Selb, J.; Candau, F. *Macromolecules* **1996**, *29*, 1452.
28. McCormick, C. L.; Johnson, C. B. *Polym. Mater. Sci. Eng.* **1986**, *55*, 366.
29. McCormick, C. L.; Nonaka, T.; Johnson, C. B. *Polymer* **1988**, *29*, 731.
30. Hill, A.; Candau, F.; Selb, J. *Prog. Colloid Polym. Sci.* **1991**, *84*, B. C. H. In ref 12, Chapter 19, 365.
31. Hill, A.; Candau, F.; Selb, J. *Macromolecule* **1993**, *26*, 4521.
32. Biggs, S.; Selb, J.; Candau, F. *Polymer* **1993**, *34*, 580.
33. Bock, J.; Varadaraj, R.; Schultz, D. N.; Maurer, J. J. *Polym. Mater. Sci. Engg.* **1987**, *57*, 487.
34. Peiffer, D. G. *Polymer* **1990**, *31*, 2354.
35. Branham, K. D.; Davis, D. L.; Middleton, J. C.; McCormick, C. L. *Polymer* **1994**, *35*, 4429.
36. Idem, In Karunasena, A.; Brown, R. G.; Glass, J. E. "Polymers in Aqueous Media: Performance through Association" ACS symposium series, Washington, DC, 223, chap. 26, 495, **1989**.
37. Ezzell, S. A.; McCormick, C. L. *Macromolecules* **1992**, *25*, 1881.
38. Ezzell, S. A.; McCormick, C. L. "Water-soluble Polymers, Synthesis, Solution Properties and Applications" Ed. Shalaby, S. W.; McCormick, C. L.; Buttler, G. B. ACS Symposium Series 467, ACS, Washington, DC, **1991**.
39. Ezzell, S. A.; Hoyle, C. E.; Creed, D.; McCormick, C. L. *Macromolecules* **1992**, *25*, 1887.
40. Kramer, M. C.; Ezzell, S. A.; McCormick, C. L. *Polym. Prep. Am. Chem. Soc., Div. Polym. Chem.* **1991**, *32*, 108.
41. Valint, Jr. P. L.; Block, J.; Schultz, D. N. *Polym. Mater. Sci.* **1987**, *57*, 482.
42. Idem, In Ezzell, S. A.; McCormick, C. L. "Water-soluble Polymers, Synthesis, Solution Properties and Applications" Ed. Shalaby, S. W.; McCormick, C. L.; Buttler, G. B. ACS Symposium Series 467, ACS, Washington, DC, **1991**, 130, Middleton, J. C.; Cummins, D. F.; McCormick, C. L., 338.

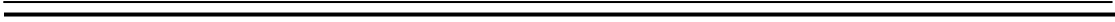
43. Idem, In “*Associative Polymers in Aqueous Media*” Glass, J. E., Ed.; ACS symposium series, Washington, DC, 765, Selb, J.; Candau, F., Chap. 6, 95, **2000**.
44. Gouveia, L. M.; Grassl, B.; Muller, A. J. *J Colloid Interface Sci.* **2009**, *333(1)*, 152.
45. Dupuis, C. *US Patent* 6383472 B1, **2002**.
46. Strauss, U. P.; Jackson, E. G. *J. Polym. Sci.* **1951**, *6*, 649.
47. Wang, T. K.; Iliopoulos, I.; Audebert, R. *Polym. Bull.* **1988**, *20*, 577.
48. Podhajecka, K.; Prochazka, K.; Hourdet, D. *Polymer* **2007**, *48*, 1586.
49. Dowling, M. B.; Kumar, R.; Keibler, M. A.; Hess, J. R.; Bochicchio, G. V.; Raghavan, S. R. *Biomaterials* **2011**, *32*, 3351.
50. Wei, Y.; Cheng, F.; Hou, G.; Sun S. *Reactive & Functional Polymers* **2008**, *68*, 981.
51. Thibeault, J. C., Sperry, P. R., Schaller, E. J. “*Water-Soluble Polymers: Beauty with Performance*,” *Adv. Chem. Series 213*, Glass, J. E. (Ed.), American Chemical Society, Chapter 20, Washington, D.C., **1986**.
52. Howard, P.; Leasure, E.; Rosier, S.; Schaller, E. *J. Coating Technology* **1992**, *64*, 87.
53. Jenkins, R. D. “*The Fundamental Thickening Mechanism of Associative Polymers in Latex Systems: A Rheological Study*” Ph. D. thesis, Lehigh University, Bethlehem, PA, **1990**.
54. Emmons, W. D.; Stevens, T. S. *US Patent* 4079028, **1978**.
55. Hoy, R. C.; Hoy, K. L. *US Patent* 4426485, **1984**.
56. Wang, Y.; Winnik, M. A. *Langmuir* **1990**, *6*, 1437.
57. Yekta, A.; Xu, B.; Duhamel, J.; Adjwadjaja, H.; Winnik, M. A. *Macromolecules*, **1995**, *28*, 956.
58. Cathébras, N.; Collet, M.; Viguier, M.; Berret, J. F. *Macromolecules* **1998**, *31*, 1305.
59. Valint, Jr.; Block, P. L. *Macromolecules* **1988**, *21*, 175.
60. Emmons, W. D.; Stevens, T. S. *US Patent* 4079028, **1978**.
61. Wu, G.; Zhou, Z.; Chu, B. *Macromolecule* **1993**, *26*, 2117.
62. Winzor, C. L.; Mrazek, Z.; Winnik, M. A. *Eur. Polym. J.* **1994**, *30*, 121.

63. Tuzar, Z.; Kratochvil, P. "Micelles of Block and Graft copolymers in solutions in Surface and Colloid Science," 15, E. Matijevic Ed., Plenum Press, New York, **1993**.
64. Landoll, L. M. *J. Polym. Sci. Polym. Chem.* **1982**, 20, 443.
65. Glass, J. E.; Buettner, A. M.; Lowther, R. G.; Young, S. S.; Cosby, L. A. *Carbohydrate Res.*, **1980**, 84, 245.
66. Glass, J. E.; Buettner, A. M.; Lowther, R. G.; Young, S. S.; Cosby, L. A. *Carbohydrate Res.*, **1980**, 84, 245.
67. Evani, S. *European Patent* 57 875, **1982**.
68. Taylor, K. C.; Nasr-El-Din, H. A. *J. Pet. Sci. & Engg.* **1998**, 19, 265.
69. Bock, J.; Siano, D. B.; Schulz, D. N.; Turner, S. R.; Valint, P. L., Jr.; Pace, S. J. *Polym. Mater. Sci. Eng.* **1986**, 55, 355.
70. Hill, A.; Candau, F.; Selb, J. *Macromolecule* **1993**, 26, 4521.
71. Branham, K. D.; Davis, D. L.; Middleton, J. C.; McCormick, C. L. *Polymer* **1994**, 35, 4429.
72. Idem, In Dubin, P.; Block, J.; Davies, R. M.; Schultz, D. N.; Thies, C. "Macromolecular Complexes in Chemistry and Biology" Springer-Verlag, Berlin-Heidelberg, Bock, J.; Varadaraj, R.; Schultz, D. N.; Maurer, J. J., Chap. 3, 33, **1994**.
73. Leibler, L.; Rubinstein, M.; Colby, R. H. *Macromolecules* **1991**, 24, 4701.
74. Van Wazer, J. R.; Lyons, J. W.; Kim, K. Y.; Colwell, R. E. In "Viscosity and Flow Measurements" Wiley Interscience, New York, **1963**.
75. Flory, P. J. "Principles of Polymer Chemistry," Cornell University Press, Ithaca **1953**.
76. Iliopoulos, I.; Wang, T. K.; Audebert, R. *Polym. Prep.*, **1989**, 30, 377.
77. Volpert, E.; Selb, J.; Candau, F. *Polymer* **1998**, 39, 1025.
78. Regalado, E. J.; Selb, J.; Candau, F. *Macromolecules* **1999**, 32, 8580.
79. Tan, H.; Tam, K. C.; Jenkins, R. D. *Langmuir* **2000**, 16, 5600.
80. Nystrom, B; Kjoniksen, A.; Lindmad, B. *Langmuir* **1996**, 12, 3233.
81. Tanaka, F.; Edwards, S. F. *J. Non-Newtonian Fluid Mech.* **1992**, 43, 247.
82. Rubinstein, M.; Semenov, A. *Macromolecules* **2001**, 34, 1058.

83. Barnes, H. A. *J. Rheol.* **1989**, *33*, 329.
84. Oda, R.; Weber, V.; Lindner, P.; Pine, D. J.; Mendes, E.; Schosseler, F. *Langmuir* **2000**, *16*, 4859.
85. Broze, G.; Jerome, R.; Teyssie, P.; Marco, C.; *Macromolecules* **1983**, *16*, 996.
86. Macias, E. R.; Bautista, F.; Soltero, J. F. A.; Puig, J. E.; Attane, P.; Manero, O. J. *Rheol.* **2003**, *47*, 643.
87. Ma, S. X. “*Shear-Thickening Mechanism in Aqueous Solutions of Associating Polymers with Well-Controlled Molecular Architecture*” Ph. D. Thesis, University of Delaware, U. S, **2001**.
88. Jenkins, R. D. “*The Fundamental Thickening Mechanism of Associative Polymers in Latex Systems: A Rheological Study*” Ph. D. thesis, Lehigh University, Bethlehem, PA, **1990**.
89. Le Meins, J. F.; Tassin, J. F. *Macromolecules* **2001**, *34*, 2641.
90. Pedley, A. M.; Higgins, J. S.; Peiffer, D. G.; Rennie, A. R.; Staples, E. *Polym. Commun.* **1989**, *30*, 162.
91. Volpert, E.; Selb, J.; Candau, F. *Polymer* **1998**, *39*, 1025.
92. Regalado, E. J.; Selb, J.; Candau, F. *Macromolecules* **1999**, *32*, 8580.
93. Jenkins, R. D. “*The Fundamental Thickening Mechanism of Associative Polymers in Latex systems: A Rheological Study*” Ph. D. thesis, Lehigh University, Bethlehem, PA, **1990**.
94. Yekta, A.; Xu, B.; Duhamel, J.; Adjwadjaja, H.; Winnik, M. A. *Macromolecules*, **1995**, *28*, 956.
95. Larson, R. G. “*Constitutive Equations for Polymer Melts and Solutions*” Butterworths, Boston, **1988**.
96. Annable, T.; Buscall, R.; Ettelaie, R.; Whittlestone, D. *J. Rheol.* **1993**, *37*, 695.
97. Ng, W. K.; Tam, K. C.; Jenkins, R. D. *J. Rheol.* **2000**, *44*, 137.
98. Lafleche, F.; Durand, D.; Nicolai, T. *Macromolecules* **2003**, *36*, 1331.
99. Tripathi, A.; Tam, K. C.; McKinley, G. H. *Macromolecules* **2006**, *39*, 1981.
100. Gourier, C.; Beaudoin, E.; Duval, M.; Sarazin, D.; Maitre, S.; Francois, J. *J. Colloid and interface Sci.* **2000**, *230*, 41.

101. Yekta, A.; Duhamel, J.; Adiwidjaja, H.; Brochard, P.; Winnik, M. A. *Macromolecules* **1993**, *26*, 1829.
102. Walderhaug, H.; Hansen, F. K.; Abrahmsen-Alami, S.; Persson, K.; Stilbs, P. *J. Phys. Chem.* **1993**, *97*, 8336.
103. Francois, J.; Maitre, S.; Rawiso, M.; Sarazin, D.; Beinert, G.; Isel, F. *Coll. And Surf. A: Physicochem. Eng. Aspects* **1996**, *112*, 251.
104. Abrahmsen-Alami, S.; Alami, E.; Francois, J. *J. Colloid Interface Sci.* **1996**, *197*, 20.
105. Emmons, W. D.; Stevens, T. S. *US Patent* 4 079 028, **1978**.
106. Glass, J. E. “*Water-Soluble Polymers: Beauty with Performance*”, American chemical Society, Washington, DC, 213, **1986**.
107. Taylor, K. C.; Hisham A. Nasr-El-Din. *J. Petroleum and Sci. & Engg.*, *19*, 265, **1998**.
108. Park, T. G.; Hoffmann, A. S. *Biotech. Bio. Engg.* **1990**, *35*, 152.
109. McCornell, G. A.; Gast, A. P.; Huang, J. S.; Smith, S. D. *Phys. Rev. Lett.* **1993**, *71*, 2102.
110. Landoll, L. M. *US Patent* 4 352 916A, **1982**.
111. Block, J.; Valint, Jr.; Pace, S. J.; Siano, D. N.; Schultz, D. N.; Turner, S. R. “*Water-Soluble Polymers for Petroleum Recovery*” Plenum Press, New York, chap. 9, *147*, **1988**.
112. Frederic, L.; Jean, M. *US patent* 6 641 618, **2003**.
113. Lowe, N. J.; Shaath, N. A.; Pathak, M. A., “Hydrafresh” with the right polymer, Exactly your chemistry, Clariant **2/ 2001**; Eds. *Sunscreens: Development, Evaluation, and Regulatory Aspects*, 2nd edition, revised and expanded. New York: Marcel Dekker, **1997**.
114. Hoy, R. C.; Hoy, K. L. *US Patent* 4 426 485, **1984**.
115. Bock, J.; Valint, P. L. Jr.; Pace, S. J. *US Patent* 4 730 028, **1988**.
116. McKennon, K. R. *US Patent* 3 039 529, **1962**.
117. Young, N. W. G.; Williams, P. A.; Meadows, J.; Allen, E. “*A Promising Hydrophobically-Modified Guar for Completion Applications*”, paper SPE 39700

- presented at the SPE/DOE Improved Oil Recovery Symposium, Tulsa, Oklahoma, USA, **1998**.
118. Yabin, N.; Jian, O.; Zhuoyan, Z.; Guijiang, W.; Guanghua, S.; Lijun, S. “*Research on Hydrophobically Associating Water-Soluble Polymer used for EOR*”, SPE International Symposium on Oilfield Chemistry, Houston, TX, USA, **2001**.
 119. Sorbie, K. S. “*Polymer-Improved Oil Recovery*” CRC Press, Boca Raton, Florida, **1991**.
 120. Feng, Y.; Grassi, B.; Billon, L.; Khoukh, A.; Francois, J., “*Effects of NaCl on Steady Rheological Behavior in Aqueous Solutions of Hydrophobically Modified Polyacrylamide and its Partially Hydrolyzed Analogues Prepared by Post-Modification*”, *Polym. Int.*, **2002**, 51, 939.
 121. Macosko, C. W. “*Rheology Principles, Measurements and Applications*,” Wiley-VCH, **1994**.
 122. Larson, R. G. “*Constitutive Equations for Polymer Melts and Solutions*” Butterworths, Boston, **1988**.
 123. Zhang, H.; Tumarkin, E.; Sullan, R. M. A.; Walker, G. C.; Kumacheva, E. *Macromol. Rapid Commun.*, **2007**, 28, 527.
 124. Miao, C.; Chen, X.; Pelton, R. *Ind. Eng. Chem. Res.* **2007**, 46, 6486.
 125. Sam Wells, Basic Principles and Advanced Capabilities of Confocal Microscopy.



Chapter-II
Scope and Objectives



Hydrophobically modified water soluble polymers [HMPs] consist of a water-soluble (hydrophilic) backbone with small amount of covalently bound hydrophobic moieties called 'stickers'. The stickers can be put randomly on the polymer chain or can be in small blocks or at the end of the polymer chain. Maintaining the critical hydrophilic-hydrophobic balance, these HMPs exhibit enhanced solution properties in aqueous medium.¹⁻³ Therefore, the architectural richness of random, block or hydrophobically end-capped HMPs give diverse physico-chemical properties and have applications in cosmetics, paints, textile pastes, paper, drilling fluids, detergents and pharmaceuticals.⁴⁻⁸ Above a certain polymer concentration, the hydrophobic groups self-associate into micelle-like structures to minimize their exposure to water and form transient networks. The viscosity of such a solution increases several fold as compared to the corresponding solution of the unmodified polymer of same molecular weight.

The synthesis of HMPs together with self-associating properties in aqueous medium in semi-dilute regime, have been widely reported in the literature.¹ For example, hydrophobically modified ethoxylated urethanes (HEURs) and hydrophobically modified alkali-swelling emulsions (HASEs) have been developed and commercially produced using both techniques of copolymerization of hydrophilic and hydrophobic monomers as well as post functionalization modification of hydrophilic polymers with hydrophobic compounds.^{1,9}

Different hydrophobic compounds, such as long chain alkyl amines, alkyl isocyanates alkyl halides, and alkyl aldehydes have been used for the hydrophobic modification of both synthetic (viz. poly(acrylic acid) [PAA], polyethylene glycol [PEG]) and natural (viz. carboxy methyl cellulose [CMC], chitosan) water-soluble polymers.¹⁰⁻¹² Despite many studies on HMPs, their industrial development has not taken place to a greater extent. Therefore, there is a need to design and develop newer HMPs aiming at specific end-applications.

The main objective of the present work was to design and synthesize new HMPs using, hydrophobic compounds derived/synthesized from renewable resource materials such as, cashew nut-shell liquid (CNSL) and gallic acid (GA) which are the byproducts of cashew processing industry and leather industry, respectively. Post-functionalization method is

used to modify water-soluble polymers namely, poly(vinyl alcohol), copolymer of N, N'-dimethyl acryl amide-co-acrylic acid and chitosan. The hydrophobic compounds, 3-pentadecyl cyclohexylamine (3-PDCA) and 3-pentadecylcarbaldehyde (3-PDCAL) were synthesized from CNSL and two other hydrophobic compounds, 3, 4, 5-tris (n-octyloxy benzoate) (MGC₈) and 3, 4, 5-tris(n-dodecyloxy benzoate) (MGC₁₂) were synthesized from gallic acid and used to hydrophobically modify the above mentioned water-soluble polymers. The physico-chemical properties of the synthesized HMPs were studied using techniques like viscometry, rheometry and light scattering. Viscosity scaling as a function of polymer concentration, extent of hydrophobic modification and the type of polymer was studied in detail using different scaling concepts.¹³⁻¹⁷ The formation of transient network structure as a result of the associations of hydrophobic groups is largely manifested in macroscopic property, viscosity.¹⁸ The gel-like, soft-solid behavior of the HMPs was probed using rheology and imaging techniques such as SEM/confocal microscopy.¹⁹ Structure property relationship was explained using light scattering technique.²⁰

The network structure in HMPs is shear sensitive and can break and reform under flow. As a result HMPs largely exhibit shear thinning behavior. However, thermo thickening and shear thickening i. e. viscosity enhancement at higher temperature and higher shear can also be observed in aqueous solutions of certain HMPs. Bokias et. al. have reported a thermo thickening phenomenon in hydrophobically modified amphiphilic copolymer based on N-isopropyl acrylamide (NIPAm) and N, N'-[(dimethyl amino) propyl methacrylamide] (MADAP).⁸ Similarly, Cadix et. al. and Wang et. al. reported shear thickening property in hydrophobically modified poly (N, N'-dimethyl acryl amide-co-acrylic acid).²¹⁻²²

An abrupt and large shear induced thickening in the aqueous solutions of hydrophobically modified poly(N, N'-dimethyl acrylamide-co-acrylic acid) is also demonstrated in the present work. The structural attributes which are responsible for the observed shear thickening originate from the critical balance of hydrophilic/hydrophobic groups, charges in the polymer and the shear rates. Using renewed experiments and scientific understanding the shear thickening phenomenon has been explained.

The specific objectives of the thesis are given below,

Specific objectives:

- To synthesize novel hydrophobic compounds namely, 3-pentadecyl cyclohexyl amine (3-PDCA), 3-pentadecyl cyclohexane carbaldehyde (3-PDCAL) from CNSL and methyl 3, 4, 5 tris(n-octyloxy benzoate) (MGC₈) and methyl 3, 4, 5 tris(n-dodecyloxy benzoate) (MGC₁₂) from gallic acid.
- To synthesize hydrophobically modified water soluble polymers using 3-PDCA, 3-PDCAL, MGC₈ and MGC₁₂.
- To establish chemical structure of new hydrophobic compounds and HMPs prepared using spectroscopic techniques.
- To study structure-property relationship of HMPs by rheology, confocal microscopy and light scattering techniques.
- To understand and correlate the structural attributes which are responsible for exhibiting shear thinning and abrupt shear thickening in HMPs.

References:

1. Glass, J. E. "*Polymers in Aqueous Media: Performance Through Association*", American Chemical Society series 223, **1989**.
2. Glass, J. E. "*Associative Polymers in Aqueous Media*" Ed.; ACS symposium series, Washington, DC, 765, **2000**.
3. Karunasena, A.; Brown, R. G.; Glass, J. E. "*Polymers in Aqueous Media: Performance Through Association*," ACS symposium series, Washington, DC, **1989**, 223, chap. 26, 495.
4. Bock, J.; Valint, P. L.; Pace, S. J.; Siano, D. B.; Schultz, D. N.; Turner, S. R.; "Water-Soluble Polymers for Petroleum Recovery," Stahl, G. A.; Schultz, D. N.; Eds., Plenum Press, New York, chapter 9, 147, **1988**.
5. Goddard, D. E.; James, G. V. "*Principles of Polymer Science and Technology in Cosmetics and Personal Care*", Cosmetic Science and Technology Series, 22, **1999**.
6. Schultz, D. N. "*Polymer as Rheology Modifiers*" Glass, J. E., Ed.; Advances in Chemistry Series, American Chemical Society, Washington, DC, No. 462, **1991**.
7. Maver, T. L. *Journal of Coatings Technology* **1992**, 64, 45.
8. Bokias, G.; Hourdet, D.; Iliopoulos, I. *Macromolecules* **2000**, 33, 2929.
9. Emmons, W. D.; Stevens, T. S. *US Patent* 4079028, **1978**.
10. Wang, T. K.; Iliopoulos, I.; Audebert, R. *Polymer Prep.* **1989**, 30 (2), 377.
11. Landoll, L. M. *US Patent* 4228277, **1980**.
12. Desbrieres, J.; Martinez, C.; Rinaudo, M. *International Journal of Biological Macromolecules* **1996**, 19, 21.
13. Dobrynin, A. V.; Colby, R. H.; Rubinstein, M. *Macromolecules* **1995**, 28, 1859.
14. Dobrynin, A. V.; Rubinstein, M. *Macromolecules* **1999**, 32, 915.
15. Leibler, L.; Rubinstein, M.; Colby, R. H. *Macromolecules* **1991**, 24, 4701.
16. Rubinstein, M.; Semenov, A. *Macromolecules* **2001**, 34, 1058.
17. Semenov, A. N.; Rubinstein, M. *Macromolecules* **2002**, 35, 4821.
18. Tsitsilianis, C.; Iliopoulos, I.; Ducouret, G. *Macromolecules* **2000**, 33, 2936.
19. Wyss, H. M.; Miyazaki, K.; Mattsson, J.; Hu, Z.; Reichman, D. R.; Weitz, D. A. *Phys. Rev. Lett.* **2007**, 98, 238303.

20. Esquenet, C.; Terech, P.; Boue, F.; Buhler, E. *Langmuir* **2004**, *20*, 3583.
21. Cadix, A.; Chasseneux, C.; Lafuma, F.; Lequeux, F. *Macromolecule* **2005**, *38*, 527.
22. Wang, J.; Benyahia, L.; Chassenieux, C.; Tassin, J.; Nicolai, T. *Polymer* **2010**, *51*, 1964.

Chapter III

Synthesis of Hydrophobic Compounds Derived from

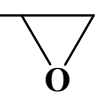
Natural Resource Materials

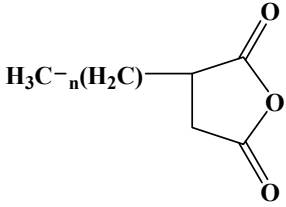
3.1 Introduction:

Various hydrophobic compounds have been used in the past to synthesize HMPs.¹ For example, long chain alkyl amines such as dodecyl amine, hexadecyl amine and octadecyl amine have been used in the hydrophobic modification of synthetic water-soluble polymer such as, poly(acrylic acid) [PAA], n-butyl methacrylate, n-butyl acrylate, dodecyl methacrylate, octadecyl methacrylate. Long chain alkyl epoxides namely, 1, 2-epoxydecane/1, 2-epoxydodecane, alkyl halides, acyl halides, alkyl isocyanates, alkyl anhydrides or aliphatic acid chlorides have been used to hydrophobically modified ethyl hydroxyl ethyl cellulose (EHEC) and carboxymethyl cellulose.² (CMC, Natural polymers)

The replacement of hydrocarbons with perfluoroalkyl groups in the synthesis of HMPs is also of specific interest, since the hydrophobic character of perfluoroalkyl groups is more pronounced compared to their hydrocarbon analogues and are found to be more effective for hydrophobic associations. Fluorocarbon modified EHEC have been reported in the literature.³ Details of some of the hydrophobes along with their chemical structure and hydrophobic modification using specific polymers is given in **Table 3.1**.

Table 3.1. Different hydrophobic compounds used for the modification of water-soluble polymers along with references.

Hydrophobes and chemical structure	Water-soluble polymers	References
$\text{H}_3\text{C}-(\text{CH}_2)_n-\text{NH}_2$ <p>Long chain alkyl amines n = 1, 2, 3.....</p>	Poly(acrylic acid), poly(aspartic acid), alginates	4-6
$\text{H}_3\text{C}-(\text{CH}_2)_n-\text{O}$  <p>Long chain alkyl epoxides n = 1, 2, 3.....</p>	Ethyl hydroxyl ethyl cellulose (EHEC), carboxy methyl cellulose (CMC)	7, 8
$\text{H}_3\text{C}-(\text{CH}_2)_n-\text{X}$	Ethyl hydroxyl ethyl cellulose (EHEC), carboxymethyl	7, 8, 9

<p>Long chain alkyl halides</p> $n = 1, 2, 3, \dots$	cellulose (CMC), poly(vinyl alcohol)	
<p>$R/Ar-CO-X$</p> <p>Long chain acyl/aryl halides</p> $n = 1, 2, 3, \dots$	Ethyl hydroxyl ethyl cellulose (EHEC), carboxymethyl cellulose (CMC), poly(ethylene glycol)	7, 8, 10
<p>$H_3C-(CH_2)_n-NCO$</p> <p>Long chain alkyl isocyanates</p> $n = 1, 2, 3, \dots$	Poly(ethylene glycol)	11
<p>$F_3C-(CF_2)_n-NH_2$</p> <p>$F_3C-(CF_2)_n-NCO$</p> <p>Long chain perfluoro compounds</p> $n = 1, 2, 3, \dots$	Ethyl hydroxyl ethyl cellulose (EHEC), poly(acrylic acid), poly(ethylene glycol)	7, 12, 13
<p>  </p> <p>Long chain alkyl anhydrides</p> $n = 1, 2, 3, \dots$	Ethyl hydroxyl ethyl cellulose (EHEC), carboxymethyl cellulose (CMC)	7, 8
<p>$H_3C-(CH_2)_n-OH$</p> <p>Long chain alcohol</p> $n = 1, 2, 3, \dots$	Ethyl hydroxyl ethyl cellulose (EHEC)	7
<p>$H_3C-(CH_2)_n-CHO$</p> <p>Long chain aldehyde</p> $n = 1, 2, 3, \dots$	Chitosan	14

$\begin{array}{c} \text{H}_3\text{C}-(\text{CH}_2)_n \\ \quad \quad \quad \diagdown \\ \quad \quad \quad \text{NH} \\ \quad \quad \quad \diagup \\ \text{H}_3\text{C}-(\text{CH}_2)_n \end{array}$ <p>N, N'-dimethyl-N-alkyl group</p> <p>n = 1, 2, 3.....</p>	Cellulose	15
--	-----------	----

Although large number of hydrophobic compounds have been synthesized and used in the preparation of HMPs/APs, our interest has been in the design and synthesis of new hydrophobic compounds from renewable resource materials such as, cashew nut-shell liquid (CNSL) and gallic acid (GA).

3.1.1 Cashew nut-shell liquid [CNSL]:

Cashew nut-shell liquid is a byproduct in the cashew processing industry and abundantly available. The total production of CNSL worldwide amounts to ~ 1, 25, 000 TPA. CNSL is a product of cashew tree, *Anacardium occidentale* and present in the pericarp of the cashew nut. Cashew tree is cultivated globally in tropical areas such as Brazil, India, Bangladesh, Tanzania, Kenya, tropical regions of Africa and South East and Far-East Asia. Number of methods such as hot-oil bath and roasting are used to extract CNSL from nuts. Steam distillation, solvent extraction techniques are also used to obtain oil from nuts.¹⁶⁻¹⁷ (Figure 3.1)

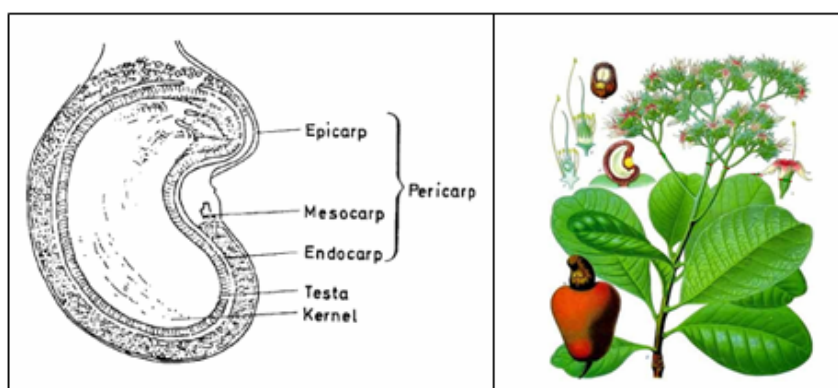


Figure 3.1. Source of CNSL.

Industrial grade CNSL is reddish brown in colour and consists of naturally occurring non-isoprenoid phenolic compounds such as: anacardic acid, cardanol and 2-methyl cardol. (**Figure 3.2**)

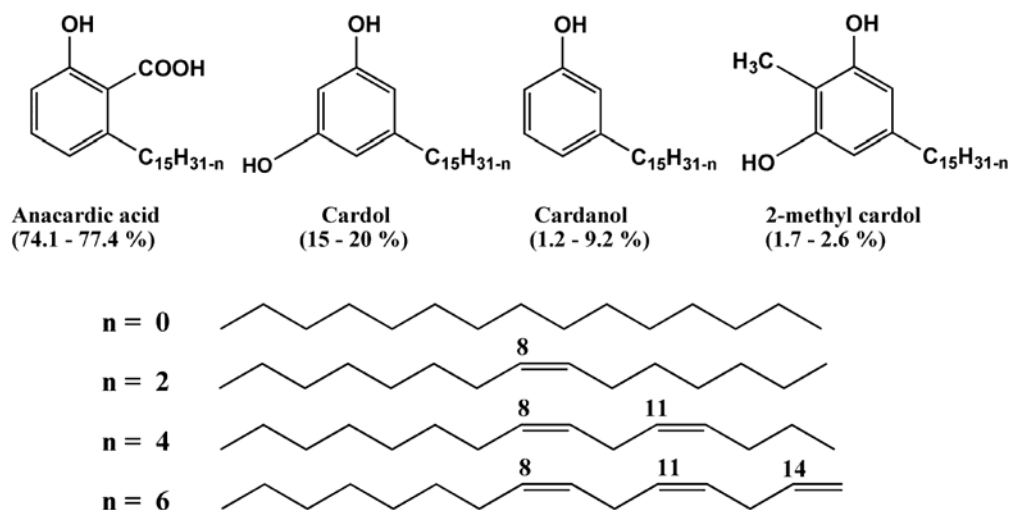


Figure 3.2. Constituents of cashew nut-shell liquid. (CNSL)

Commercial grade CNSL contains hardly any anacardic acid because of decarboxylation during roasting process, which converts anacardic acid to cardanol. The unsaturated C-15 chain along with the phenolic moiety in CNSL has offered variety of possibilities of reaction of CNSL such as, hydrogenation, sulfonation, nitration, halogenation, etherification, esterification, epoxidation, phosphorylation which have been documented in the literature.¹⁸⁻²³

3.1.2 Gallic acid:

Gallic acid (3, 4, 5-trihydroxybenzoic acid) is found in nature in gallnuts, sumac, tea leaves and oak bark in the form of gallotannins (**Figure 3.3**). This class of tannins is also called as hydrolysable tannins. Gallotannins are simple polygalloyl esters of glucose that has five ester linkages and consists of aliphatic hydroxyl groups of the core sugar of gallic acid.



Figure 3.3. Source of gallic acid.

Harad, Harda, Indian gall-nut, Ink nut are the common names for the tree shown in **Figure 3.3**. Botanical name of the plant is *Terminia chebula*, available in Northern and Central India. The fruit of the plant is called Mayrabolan.

Hydrolysis of gallotannins (pentagalloyl glucose) with strong acid such as H_2SO_4 results into gallic acid and the core polyol. Gallic acid (F. W. = 170.12, M. P. = $253\ ^\circ C$) is a white or yellowish-white solid and is soluble in alcohol, ether and in boiling water. It is odorless and has acid taste. It is used in inks, photography and pharmaceuticals. It has antifungal, antiviral activity and used as antioxidant. It is also used in ointments.²⁴⁻²⁵
(Figure 3.4, 3.5)

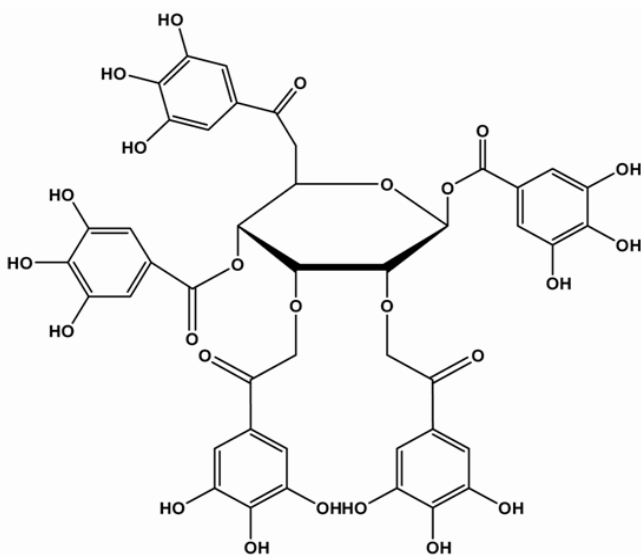


Figure 3.4 Structure of gallotannins.

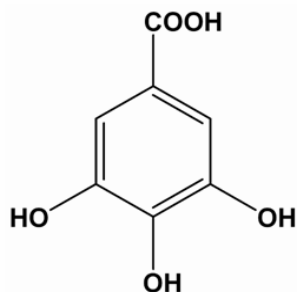


Figure 3.5 Structure of gallic acid.

In this chapter, the synthesis and characterization of four hydrophobic compounds namely, (I) 3-pentadecyl cyclohexyl amine [3-PDCA], (II) 3-pentadecyl cyclohexane carbaldehyde [3-PDCAL] from CNSL and (III) methyl 3, 4, 5-tris (n-octyloxy) benzoate [MGC₈], (IV) methyl 3, 4, 5-tris (n-dodecyloxy benzoate) [MGC₁₂] from gallic acid have been reported.

3.2 Experimental:

3.2.1 Materials:

3-Pentadecyl phenol [3-PDP], ruthenium on carbon [Ru-C], lithium aluminium hydride [LiAlH₄], n-octyl bromide [n-C₈H₁₇Br] and n-dodecyl bromide [n-C₁₂H₂₅Br], methoxy methyl triphenyl phosphonium chloride [C₂₀H₂₀OCIP] were purchased from Aldrich chemical company, USA and used as received. Analytical grade pyridine, chromium trioxide [CrO₃], Celite-545, pyridinium chlorochromate [C₅H₆NO₃ClCr], potassium t-butoxide [t-BuOK], tetrabutyl ammonium bromide [C₁₆H₃₆NBr], potassium carbonate, p-toluene sulfonic acid, sodium sulfate, sodium bicarbonate, silica gel, hydroxyl amine hydrochloride, hydrochloric acid, isopropanol, ethanol, dichloromethane, diethyl ether, dioxane were procured from Merck, India and were used as received.

3.3 IR and NMR spectroscopy:

¹H and ¹³C NMR spectra were recorded using spectrometers operating at ¹H NMR frequency of 200, 400 and 500 MHz. (Bruker AV-200, DRX-400, DRX-500 NMR) All the spectra were recorded in CDCl₃. IR spectra were obtained using FT-IR spectrometer. (Schimatzu, Perkin Elmer)

3.4 Synthesis of 3-PDCA:

3-PDCA was synthesized from 3-pentadecyl phenol (3-PDP) in four steps: (i) reduction of 3-PDP to 3-pentadecyl cyclohexanol (ii) oxidation of 3-pentadecyl cyclohexanol to 3-pentadecyl cyclohexanone (iii) conversion of 3-pentadecyl cyclohexanone to 3-pentadecyl cyclohexane oxime (iv) reduction of 3-pentadecyl cyclohexane oxime to 3-pentadecyl cyclohexyl amine.

3.4.1 Reduction of 3-pentadecyl phenol (1) to 3-pentadecyl cyclohexanol (2):

Into a Paar reactor, 3-pentadecyl phenol (35.0 g, 0.115 mol) was dissolved in propan-2-ol (140 ml). To the above solution, ruthenium on carbon (Ru-C, 1.05 g) was added under stirring. Reactor was maintained at hydrogen (H₂) pressure of 900 psi and 100 °C temperature for 2 h. Catalyst was separated by passing the reaction mixture through a bed of silica gel. Filtrate containing 3-pentadecyl cyclohexanol was concentrated on rotary evaporator to obtain dry powder. Conversion of 3-pentadecyl phenol to 3-pentadecyl cyclohexanol is shown in **Scheme 3.1**. *Yield* = 35.4 g (99 %).

3.4.2 Oxidation of 3-pentadecyl cyclohexanol (2) to 3-pentadecyl cyclohexanone (3):

Into a 5 liter three necked round bottom flask equipped with a mechanical stirrer, 3-pentadecyl cyclohexanol (125.0 g, 0.04 mol) was dissolved in 1.5 liter dichloromethane. To this solution pyridinium chlorochromate (PCC) (130.0 g 0.66 mol) mixed with silica gel (130 g) was added at 0 °C and stirred vigorously for 8 h at room temperature. Dichloromethane solution was filtered through a bed of mixture of silica gel and Celite-545 to remove the PCC residue. Dichloromethane solution was neutralized by washing with aqueous sodium bicarbonate solution followed by washing with water. Organic layer was dried over sodium sulfate. Solvent was evaporated on a rotary evaporator to obtain a white solid, 3-pentadecyl cyclohexanone. Crude product was recrystallized from methanol. Conversion of 3-pentadecyl cyclohexanol to 3-pentadecyl cyclohexanone is shown in **Scheme 3.1**. *Yield* = 117.0 g (94 %).

3.4.3 Conversion of 3-pentadecyl cyclohexanone (3) to 3-pentadecyl cyclohexane oxime (4):

Into a 500 ml three necked round bottom flask, 3-pentadecyl cyclohexanone (20.0 g, 64.82 mmol) was dissolved in ethanol (250 ml). To the above solution hydroxyl amine hydrochloride (9.01 g, 129.65 mmol) and pyridine (7.75 g, 114 mmol) were added and the reaction mixture was refluxed for 2 h. The reaction mixture was allowed to cool to room temperature and 100 ml distilled water was added with continuous stirring over a period of 0.5 h. The reaction mixture was extracted with diethyl ether (3 x 50 ml). Ether

solution was washed with brine, water, separated and dried over anhydrous sodium sulfate. Solvent was removed using rotary evaporator and the product obtained was purified by recrystallization from methanol. Conversion of 3-pentadecyl cyclohexanone to 3-pentadecyl cyclohexane oxime is shown in **Scheme 3.1**. *Yield* = 16.8 g (81 %).

3.4.4 Reduction of 3-pentadecyl cyclohexane oxime (4) to 3-pentadecyl cyclohexyl amine (5):

Into a 500 ml three necked round bottom flask equipped with a magnetic stirring bar, a reflux condenser, an addition funnel and an inlet for nitrogen gas was added lithium aluminium hydride (37.95 g, 278.2 mmol) and dry diethyl ether (250 ml). The reaction mixture was maintained at 0 °C and 3-pentadecyl cyclohexanone oxime (15.0 g, 46.36 mmol) dissolved in diethyl ether (200 ml) was added drop-wise over a period of 0.5 h under the nitrogen atmosphere. Reaction mixture was allowed to attain room temperature and further refluxed for 2 h under the nitrogen atmosphere. Reaction mixture was allowed cool to 0 °C and saturated aqueous solution of sodium sulfate (100 ml) was added. Resulting slurry was filtered through a Celite-545 column and the filtered semi-solid was washed with chloroform (3 x 100 ml). Combined filtrate and washings were dried over sodium sulfate and concentrated on rotary evaporator to obtain product. Conversion of 3-pentadecyl cyclohexane oxime to 3-pentadecyl cyclohexyl amine is shown in **Scheme 3.1**. *Yield* = 14.06 g. (98 %).

3.5 Synthesis of 3-PDCAL:

The hydrophobic compound 3-PDCAL was also synthesized from 3-PDP. Same steps used for the preparation of 3-PDCA were followed till the preparation of 3-pentadecyl cyclohexanone. Then, the 3-pentadecyl cyclohexanone was converted to (E/Z)-1-(methoxy methylene)-3-pentadecyl cyclohexane which was further converted to 3-PDCAL.

3.5.1 Conversion of 3-pentadecyl cyclohexanone (3) to (E/Z)-1-(methoxy methylene)-3-pentadecyl cyclohexane (4):

Into a 1 liter three necked round bottom flask equipped with a reflux condenser, a suspension of methoxymethyl triphenyl phosphonium chloride (MMTPC) (54.72 g, 0.2

mole) in dioxane (560 ml) was stirred at 20 °C. A suspension of MMTPC in dioxane was stirred and potassium tertiary butoxide (18.18 g, 0.2 mole) was added to the mixture which changed reaction mixture red. (Slightly exothermic reaction) Reaction mixture was allowed to stir for 3 h and 3-pentadecyl cyclohexanone (10 g, 0.032 mole) was added. Reaction mixture was stirred at 20 °C for 1 h and then heated to reflux for 3 h. The mixture was allowed to cool, diluted with water (560 ml), extracted with diethyl ether. The conversion of the reaction was monitored by IR by the disappearance of the carbonyl frequency. (1711 cm⁻¹) Organic extracts were washed twice with water, dried over sodium sulfate and concentrated on rotary evaporator. Conversion of 3-pentadecyl cyclohexanone to (E/Z)-1-(methoxy methylene)-3-pentadecyl cyclohexane is shown in **Scheme 3.2**. *Yield = 7.5 (75 %)*.

3.5.2 Conversion of (E/Z)-1-(methoxy methylene)-3-pentadecyl cyclohexane (4) to 3-pentadecyl cyclohexane carbaldehyde (5):

Into a 1 liter three necked round bottom flask equipped with a reflux condenser (E/Z)-1-(methoxy methylene)-3-pentadecyl cyclohexane (6.5 g, 0.019 mole) was dissolved in dioxane (400 ml). To the above mixture, p-toluene sulfonic acid (0.75 g, 0.0044 mole) was dissolved in water (80 ml) and added. Reaction mixture was refluxed for 16 h followed by cooling and dilution with water. (400 ml) The product was extracted with diethyl ether. All the extracts were washed with water, dried over sodium sulfate and concentrated on rotary evaporator. Product was yellow viscous oil. Conversion of (E/Z)-1-(methoxy methylene)-3-pentadecyl cyclohexane to 3-pentadecyl cyclohexane carbaldehyde is shown in **Scheme 3.2**. *Yield = 5.85, (90 %)*.

3.6 Preparation of hydrophobic compounds from gallic acid:

3.6.1 Synthesis of methyl 3, 4, 5-tris octyloxy benzoate [MGC₈]:

Synthesis of MGC₈ consists of two steps:

- (i) Conversion of gallic acid to methyl 3, 4, 5-trihydroxy benzoate (methyl gallate).
- (ii) Conversion of 3, 4, 5-trihydroxy benzoate to methyl 3, 4, 5-tris (octyloxy) benzoate.

3.6.1.1 Preparation of methyl 3, 4, 5-trihydroxybenzoate (methyl gallate):

Into a 250 ml single necked round bottom flask equipped with a reflux condenser, gallic acid (10 g, 0.058 mol) was dissolved in methanol (150 ml). To the reaction mixture, thionyl chloride (9 ml, 0.076 mol) was added drop-wise through the addition funnel with stirring at 0 °C. The reaction mixture was refluxed at 65 °C for 4 h. Methanol was evaporated to obtain solid product which was dissolved in ethyl acetate and treated with NaHCO₃ solution (3 x 100 ml), saturated NaCl solution (2 x 100 ml) and water. Ethyl acetate solution was dried over sodium sulfate and then filtered through a short column of silica. Filtrate was concentrated using rotary evaporator and the product was dried under vacuum at room temperature. Conversion of gallic acid to methyl gallate is shown in **Scheme 3.3**. *Yield* = 82 %.

3.6.1.2 Preparation of methyl 3, 4, 5-tris(n-octyloxy) benzoate (MGC₈):

Into a 250 ml three necked round bottom flask equipped with a reflux condenser, methyl gallate (2 g, 0.0107 mol) was dissolved in 2-butanone (150 ml). A mixture of K₂CO₃ (8.99 g, 0.065 mol) and TBAB (0.17 g, 0.0054 mol) was triturated and added to the above solution. To the reaction mixture 1-bromooctane (6.29 g, 0.033 mol) was added and refluxed at 80 °C for 2 h. The progress of the reaction was monitored by TLC. Obtained brown mixture was allowed to cool to room temperature and water (120 ml) was added. Separated organic layer was washed with water (2 x 120 ml), 1 M HCl solution (2 x 120 ml) and again with water (2 x 120 ml). Organic layer was separated, dried over anhydrous sodium sulfate, filtered and concentrated using rotary evaporator to obtain yellow viscous oily product. Product was purified by flash column chromatography with hexane/ethyl acetate mixture (96:4, v/ v) as an eluent. Purified product was yellow, viscous liquid. Conversion of methyl gallate to methyl 3, 4, 5-tris (octyloxy) benzoate and methyl 3, 4, 5-tris (dodecyloxy) benzoate is shown in **Scheme 3.3**. *Yield* = 92.5 %.

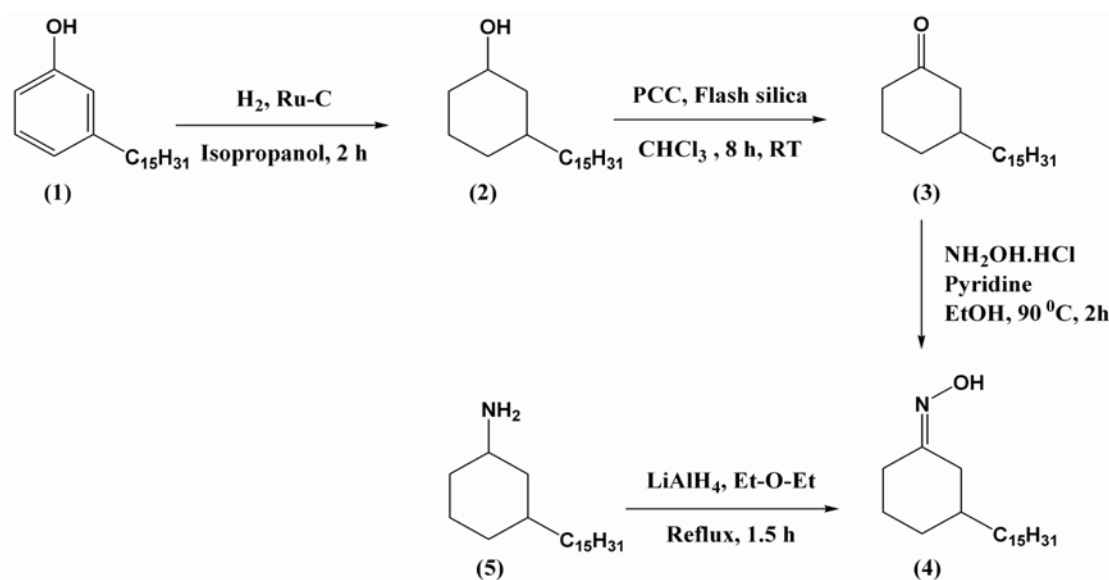
3.6.1.3 Synthesis of methyl 3, 4, 5-tris(n-dodecyloxy) benzoate [MGC₁₂]:

Using the same procedure mentioned above and replacing 1-bromo octane with 1-bromo dodecane, MGC₁₂ was prepared.

3.7 Results and Discussion:

3.7.1 Preparation of 3-Pentadecyl cyclohexyl amine [3-PDCA]:

3-PDCA was synthesized from 3-pentadecyl phenol [3-PDP]. 3-pentadecyl phenol was hydrogenated using hydrogen (H_2) as a reducing agent and ruthenium on carbon (Ru/C) as a catalyst. The obtained 3-pentadecyl cyclohexanol was oxidized to 3-pentadecyl cyclohexanone using pyridinium chlorochromate and silica gel as an oxidizing agent. 3-Pentadecyl cyclohexanone was then converted to 3-pentadecyl cyclohexane oxime using hydroxyl amine hydrochloride. Finally, 3-pentadecyl cyclohexane oxime was reduced to 3-pentadecyl cyclohexyl amine using lithium aluminium hydride as a reducing agent. The reaction pathway is shown in **Scheme 3.1**.



Scheme 3.1. Synthesis of 3-pentadecyl cyclohexylamine.

FT-IR spectrum of 3-PDCA (**Figure 3.6**) showed amine group ($-NH_2$) stretching frequency at 3392 cm^{-1} . Aliphatic side chain appeared at $2849 - 2924\text{ cm}^{-1}$. $-C-N$ bond stretching appeared in the range of $1033 - 1356\text{ cm}^{-1}$.

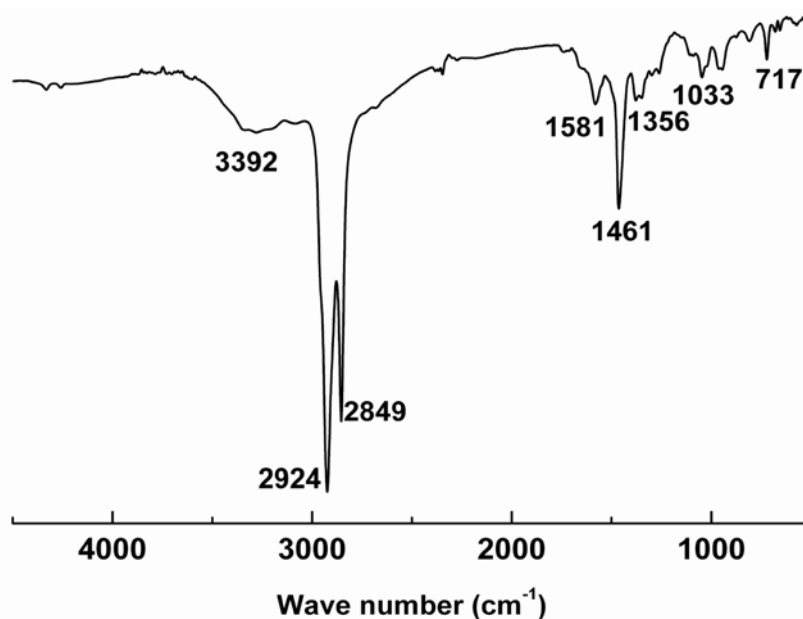


Figure 3.6. FT-IR spectrum of 3-pentadecyl cyclohexylamine

¹H NMR spectrum of 3-PDCA (**Figure 3.7**) showed the terminal methyl (–CH₃) protons of the pentadecyl side (–C₁₅H₃₁) chain attached to the cyclohexyl ring at 0.82 ppm (triplet, –CH₃, 3 H). Methylene and methyne protons of the pentadecyl side chain and the cyclohexyl ring appeared in the range of 1.2 - 1.83 ppm (multiplet, (–CH₂)₁₃, 36 H). Proton of the cyclohexyl ring to which –NH₂ is attached, appeared at 2.55 and 3.00 ppm. (Singlet of singlet, (–CH), 1 H) Proton denoted as C exist in its equatorial and axial (C_{e,a}) conformation due to the ring flipping and experience different chemical environment. Therefore, for this proton two chemical shifts are observed (2.55 and 3.00 ppm).

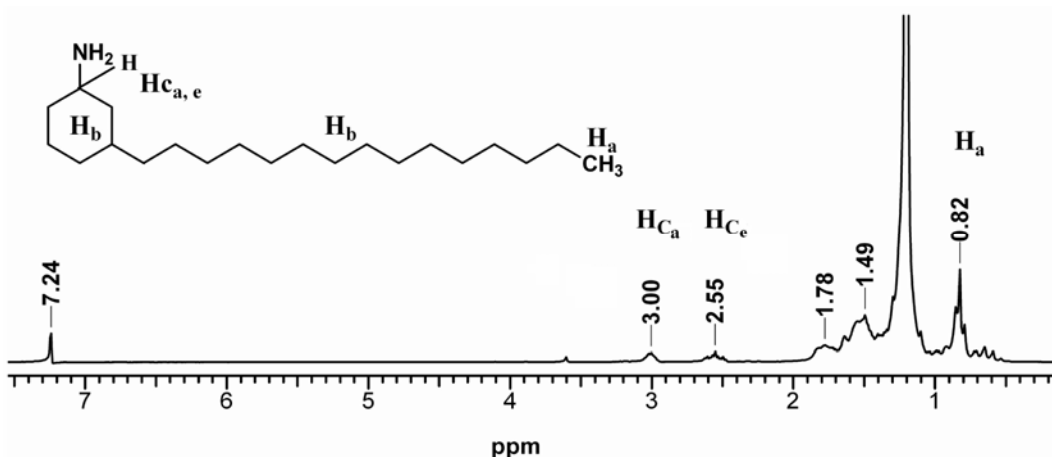


Figure 3.7. ^1H NMR spectrum of 3-pentadecyl cyclohexyl amine

^{13}C NMR spectrum of 3-PDCA (**Figure 3.8**) showed the terminal methyl carbon of the pentadecyl side chain ($-\text{C}_{15}\text{H}_{31}$) of 3-PDCA at 14.02 ppm. Methylene carbons of the pentadecyl side chain and cyclohexyl ring appeared in the range of 20 - 45.94 ppm. Carbon to which amine group is attached appeared at 50.64 ppm.

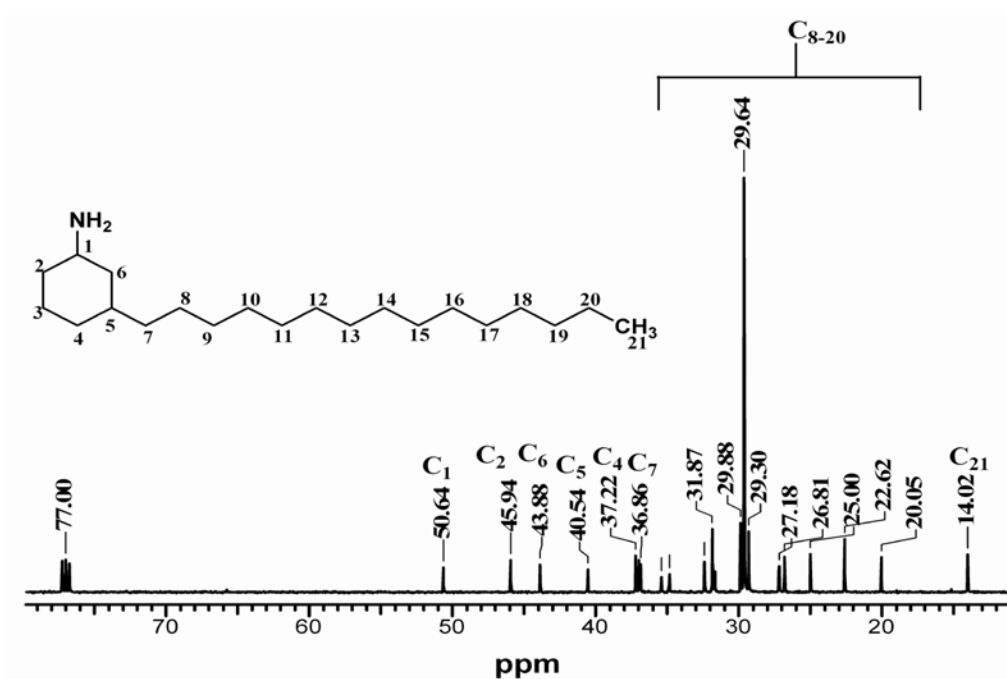
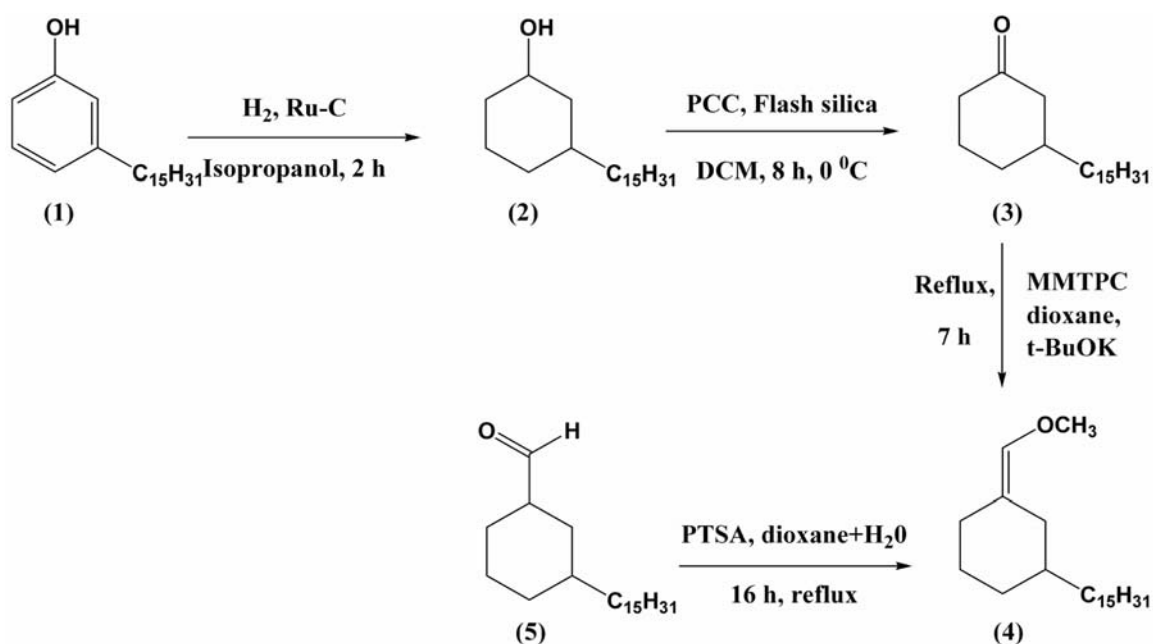


Figure 3.8. ^{13}C NMR spectrum of 3-pentadecyl cyclohexyl amine

The assignments of peaks in both ^1H and ^{13}C NMR spectra confirmed the structure of 3-PDCA.

3.7.2 Preparation of 3-pentadecyl cyclohexane carbaldehyde (3-PDCAL):

The hydrophobic compound, 3-pentadecyl cyclohexane carbaldehyde was prepared from 3-PDP a constituent of CNSL. The synthesis of 3-PDCAL from 3-PDP consists of 4 steps: (i) conversion of 3-PDP to 3-pentadecyl cyclohexanol using hydrogenation reaction with Ru/C as a catalyst under high pressure. (ii) in the second step, 3-pentadecyl cyclohexanol was converted to 3-pentadecyl cyclohexanone using pyridinium chlorochromate as an oxidizing agent. (iii) in the third step, 3-pentadecyl cyclohexanone was converted to (z)-1-(methoxy methylene)-3-pentadecyl cyclohexane using suspension of methoxy methyl triphenyl phosphonium in dioxane and potassium t-butoxide as a base. Finally, in step (iv) (z)-1-(methoxy methylene)-3-pentadecyl cyclohexane was converted to 3-PDCAL in the presence of p-toluene sulfonic acid using dioxane water mixture as a solvent. The reaction pathway is shown in **Scheme 3.2**.



Scheme 3.2. Synthesis of 3-pentadecyl cyclohexane carbaldehyde

FT-IR spectrum of 3-PDCAL (**Figure 3.9**) showed carbonyl of the aldehyde group ($>\text{C}=\text{O}$, $-\text{CHO}$ stretching vibrations) attached to the cyclohexyl ring at 1723 cm^{-1} .

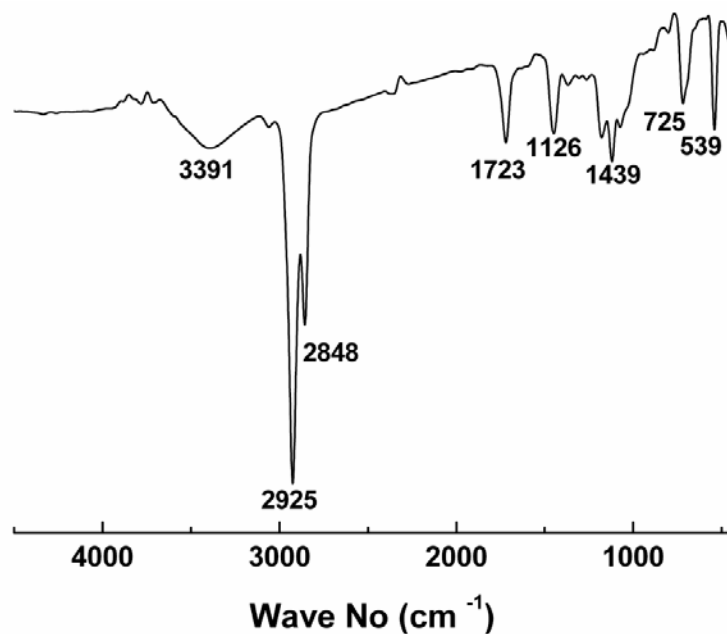


Figure 3.9. FT-IR spectrum of 3-pentadecyl cyclohexane carbaldehyde

^1H NMR spectrum of 3-PDCAL (**Figure 3.10**) showed terminal methyl ($-\text{CH}_3$) protons of the pentadecyl chain at 0.84 ppm (triplet, 3H, $-\text{CH}_3$), methylene ($-\text{CH}_2$) protons of the pentadecyl chain, the cyclohexyl ring and the methine proton attached to the carbon to which the pentadecyl chain is attached appeared in the range of 1.22 - 2.43 ppm (multiplet, 41 H), aldehyde proton ($\text{O}=\text{C}-\text{H}$) (singlet of singlet, 1H) attached to the cyclohexyl ring appeared at 9.56 ppm and 9.66 ppm which can be attributed to the axial and equatorial flipping of the cyclohexyl ring, respectively.

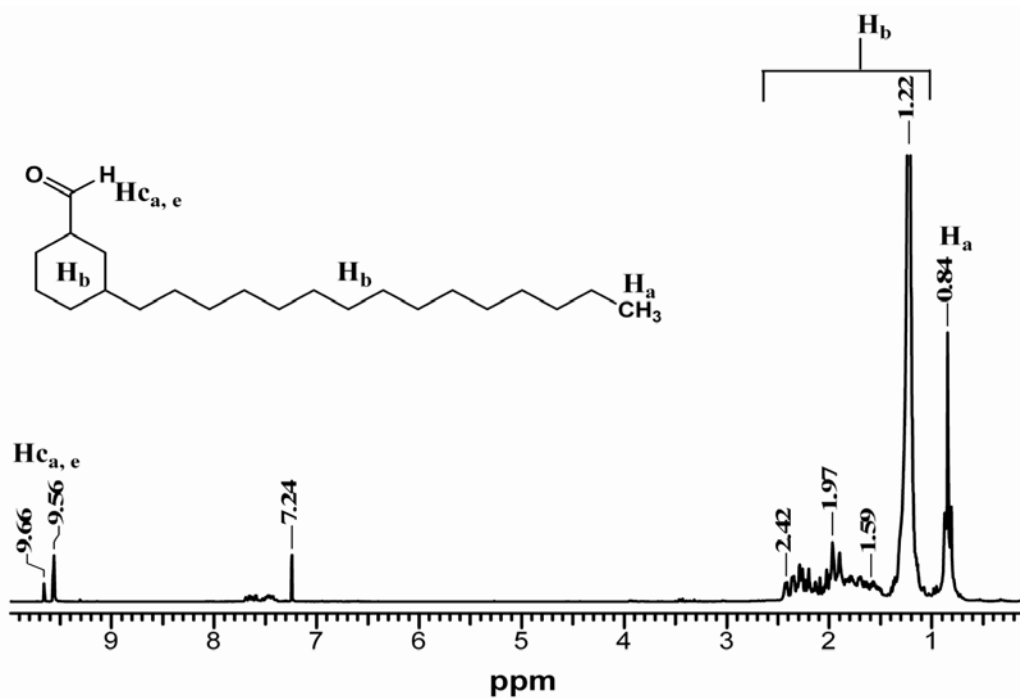


Figure 3.10. ^1H NMR spectrum of 3-pentadecyl cyclohexane carbaldehyde

^{13}C NMR spectrum of 3-PDCAL (**Figure 3.11**) showed terminal methyl carbon ($-\text{CH}_3$, C_1) of the pentadecyl side chain attached to the cyclohexyl ring appeared at 14.13 ppm. Methylene ($-\text{CH}_2$) carbons of the pentadecyl chain, the cyclohexyl ring and the methine carbons ($-\text{CH}-\text{CHO}$, C_{2-20}) of the cyclohexyl ring appeared in the range of at 22.7 - 48.25 ppm. The aldehyde carbon ($\text{O}=\text{C}-\text{H}$, C_{21}) attached to the cyclohexyl ring appeared at 212.75 ppm.

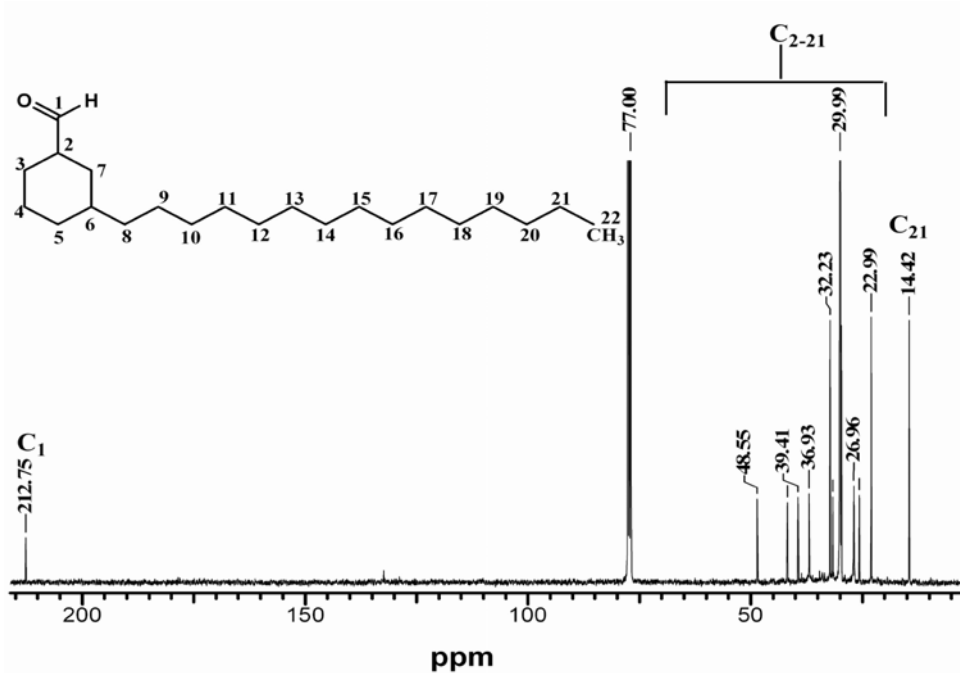
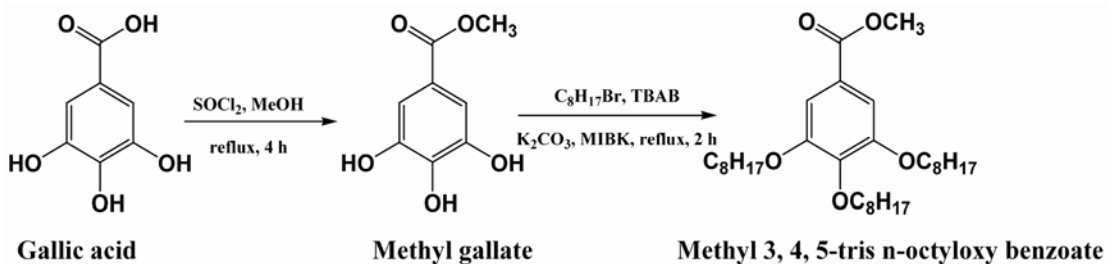


Figure 3.11. ¹³C NMR spectrum of 3-pentadecyl cyclohexane carbaldehyde

The analysis of FT-IR spectrum and the assignment of peaks in both ¹H and ¹³C spectra confirmed the structure of 3-PDCAL.

3.7.3 Synthesis of hydrophobic compounds from gallic acid: [MGC₈ and MGC₁₂]

Synthesis of MGC₈ and MGC₁₂ from gallic acid is shown in **Scheme 3.3**. In order to prevent any side reaction from the –COOH groups of gallic acid, it was first converted to methyl gallate using thionyl chloride and methanol. Methyl gallate was then converted to alkoxy substituted methyl gallate derivatives (MGC₈/MGC₁₂) by Williamson ether synthesis using alkyl bromide (C₈H₁₇Br/C₁₂H₂₅Br). Tetrabutyl ammonium bromide (TBAB) was used as a phase transfer catalyst and K₂CO₃ was used as a base.



Scheme 3.3. Preparation of methyl 3, 4, 5-tris octyloxy benzoate

FT-IR spectrum of methyl 3, 4, 5-tris (octyloxy benzoate) (**Figure 3.12**) showed ester carbonyl attached to the benzene ring of MGC_8 at 1727 cm^{-1} . The C-O bond of the ester appeared at $1017 - 1334 \text{ cm}^{-1}$. Out of plane $-\text{C}-\text{H}$ bend of the aromatic ring appeared at 760 cm^{-1} .

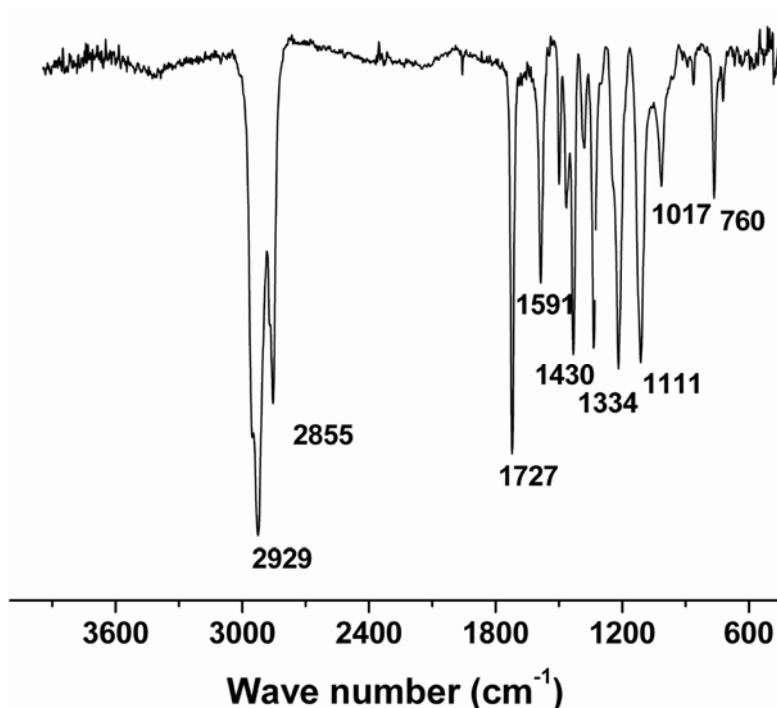


Figure 3.12. FT-IR spectrum of methyl 3, 4, 5-tris octyloxy benzoate

^1H NMR spectrum of methyl 3, 4, 5-tris octyloxy benzoate [MGC_8] (**Figure 3.13**) showed the terminal methyl protons of the octyl side chain, $[(-\text{CH}_2)_7-\text{CH}_3]$, attached to the aromatic ring at 0.87 ppm (t, $-\text{CH}_3$, 9H). Methylene protons $[(-\text{CH}_2)_5-\text{CH}_3]$ of the octyl side chain appeared at $1.27 - 1.80 \text{ ppm}$ (m, $-\text{CH}_2$, 36H). Methyl protons of the ester group attached to aromatic ring appeared at 3.87 ppm (s, $-\text{COOCH}_3$, 3H). Methylene

protons of the octyl side chain $[(-\text{CH}_2)_5-\text{CH}_3]$ attached to the oxygen of the aromatic ring appeared at 4 ppm (t, $-\text{OCH}_2$, 6H) and the aromatic protons appeared at 7.2 ppm (s, 2H, Ar-H).

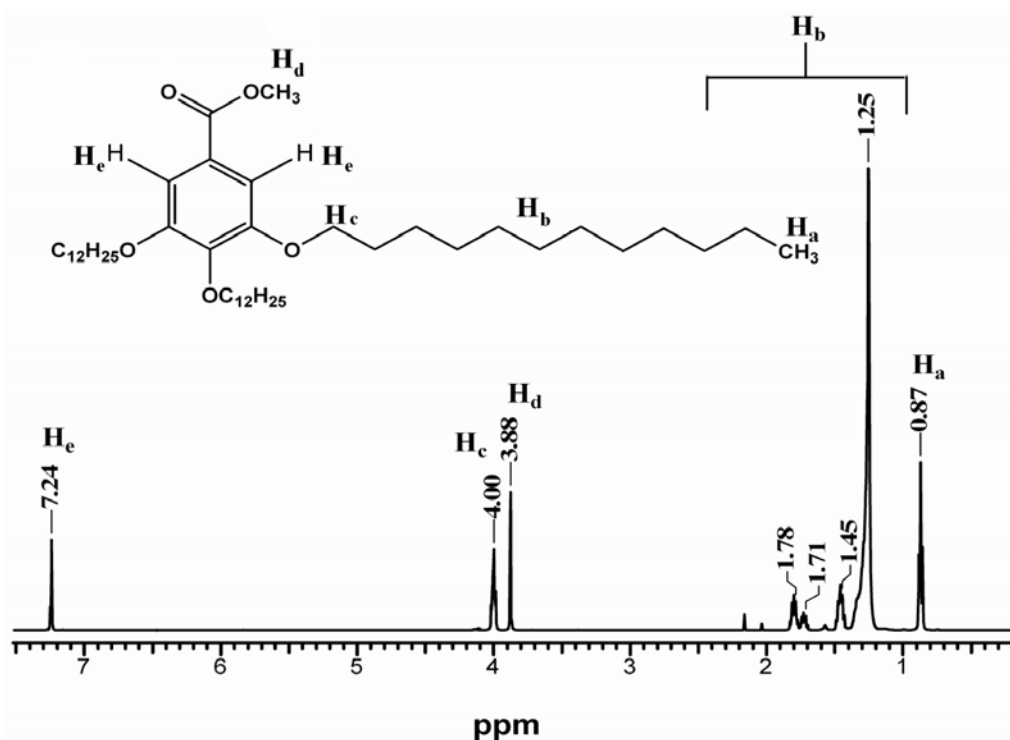


Figure 3.13. ^1H NMR spectrum of methyl 3, 4, 5-tris octyloxy benzoate

^{13}C NMR spectrum of MGC₈ (**Figure 3.14**) showed the methyl carbons of the methyl gallate ester at 52.04 ppm (C_1 , $-\text{COOCH}_3$). Carbonyl carbons of the methyl ester appeared at 166.91 ppm (C_2 , $\text{O}=\text{C}-\text{OCH}_3$). Carbon of the aromatic ring to which methyl ester group is attached appeared at 124.66 ppm. (C_3 , $-\text{C}-\text{Ar}$) Aromatic carbons ortho with respect to methyl ester (C_{4-8} , $-\text{C}-\text{Ar}$) appeared at 108.02 ppm. Aromatic meta carbons with respect to methyl ester (C_{5-7} , $-\text{C}-\text{Ar}$) appeared at 152.83 ppm. Aromatic carbons para with respect to methyl ester (C_6 , $-\text{C}-\text{Ar}$) appeared at 142.41 ppm. C_9 carbons appeared at of 69.16 ppm ($-\text{OCH}_2$, 3C). C_{10-15} carbons appeared in the range of 22.65 – 31.82 ppm ($-\text{OCH}_2$, 6C). C_{16} methyl carbon of the aliphatic side chain appeared at 14.06 ppm. (C_{16} , $-\text{CH}_3$, 1C)

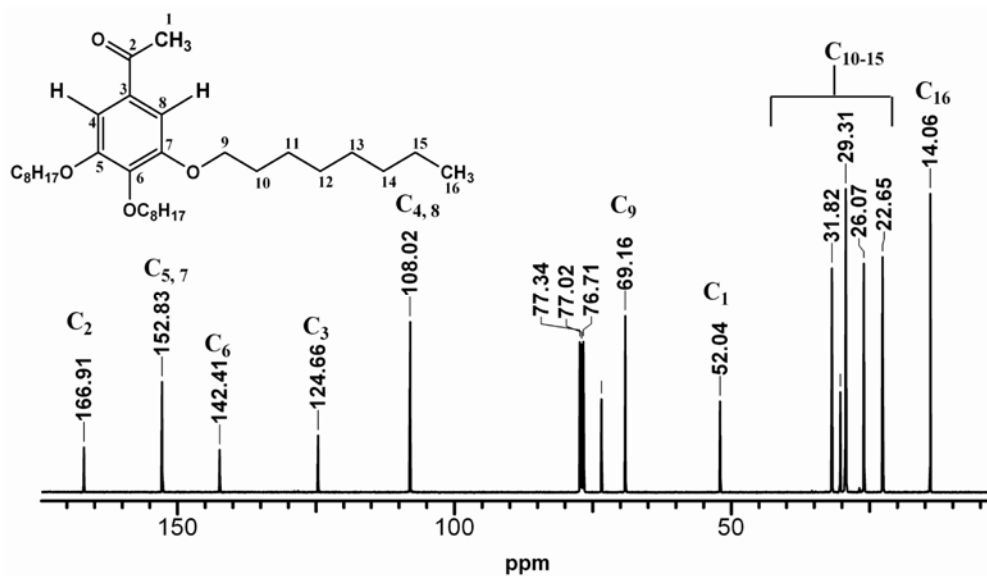
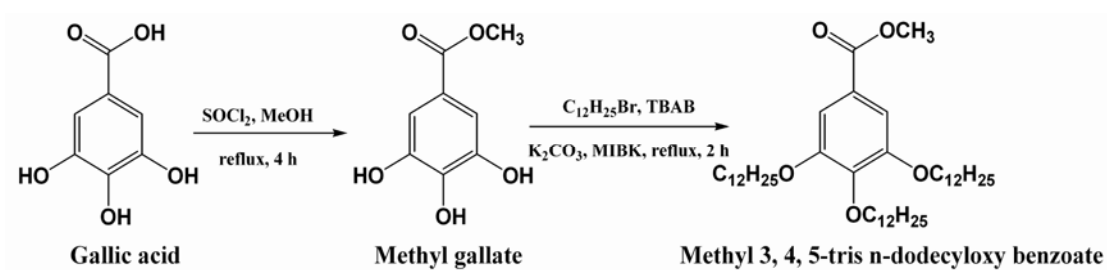


Figure 3.14. ^{13}C NMR spectrum of methyl 3, 4, 5-tris (octyloxy) benzoate

The analysis of FT-IR spectrum and the assignments of the peaks in both ^1H and ^{13}C spectra confirmed the structure of MGC_8 .

3.7.4 Methyl 3, 4, 5 tris-octyloxy benzoate [MGC_{12}]:

In order to increase the hydrophobicity, methyl gallate with C_{12} alkyl chain (MGC_{12}) was synthesized using the same procedure of MGC_8 synthesis. During the reaction, octyl bromide was replaced by dodecyl bromide. The reaction pathway is shown in **Scheme 3.4**.



Scheme 3.4. Preparation of methyl 3, 4, 5-tris dodecyloxy benzoate

FT-IR spectrum of methyl 3, 4, 5-tris (dodecyloxy benzoate) (**Figure 3.15**) showed aliphatic side chain attached to aromatic ring through ether linkage at 2850-2917 cm^{-1} . Ester carbonyl attached to the benzene ring of MGC_{12} appeared at 1723 cm^{-1} . The carbon-carbon double bond ($\text{C}=\text{C}$) of the aromatic ring stretch appeared at 1583 cm^{-1} . The C–O bond of the ester appeared at 1015 - 1335 cm^{-1} . Out of plane C–H bend of the aromatic ring appeared at 761 cm^{-1} .

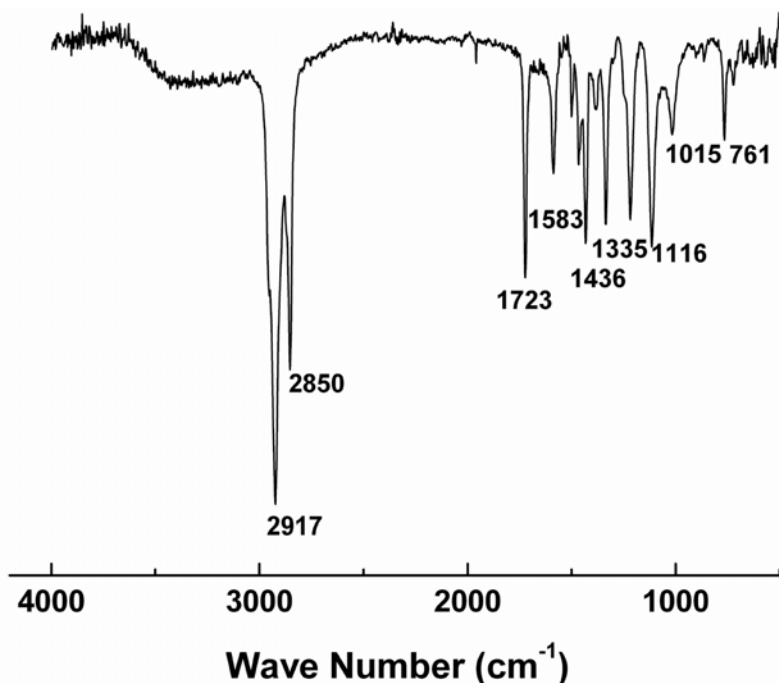


Figure 3.15. FT-IR spectrum of methyl 3, 4, 5-tris dodecyloxy benzoate

^1H NMR spectrum of methyl 3, 4, 5-trisdodecyloxy benzoate (**Figure 3.16**) showed terminal methyl protons of the dodecyl side chain [$\text{CH}_3(-\text{CH}_2)_7$] attached to the aromatic ring at 0.87 ppm (t, $-\text{CH}_3$, 9 H). Methylene protons [$(-\text{CH}_2)_5-\text{CH}_3$] of the dodecyl side chain attached to the aromatic ring appeared at 1.25 – 1.78 ppm (m, $-\text{CH}_2$, 60 H). Methyl protons of the ester group attached to aromatic ring appeared at 3.88 ppm (s, $-\text{COOCH}_3$, 3H). Methylene protons of the dodecyl side chain [$(-\text{CH}_2)_{10}-\text{CH}_3$] attached to the oxygen of the aromatic ring appeared at 4.0 ppm (t, $-\text{OCH}_2$, 6H). Aromatic protons of MGC_{12} appeared at 7.24 ppm (s, 2H, Ar–H).

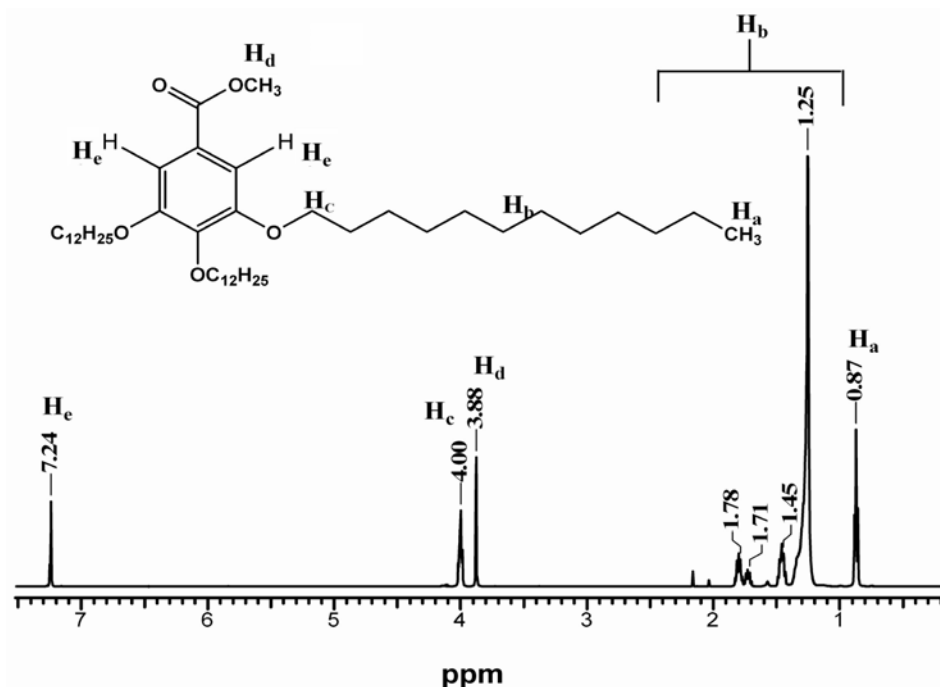


Figure 3.16. ¹H NMR spectrum of methyl 3, 4, 5-tris dodecyloxy benzoate

¹³C NMR spectrum of MGC₁₂ (**Figure 3.17**) showed the methyl carbons of the methyl gallate ester at 52.11 ppm (C₁, –COOCH₃). Carbonyl carbons of the methyl ester appeared at 166.98 ppm (C₂, O=C–OCH₃). Carbon of the aromatic ring to which methyl ester group is attached appeared at 124.66 ppm. (C₃, –C–Ar) Aromatic carbons ortho with respect to methyl ester (C₄₋₈, –C–Ar) appeared at 108 ppm. Aromatic carbons meta with respect to methyl ester (C₅₋₇, –C–Ar) appeared at 152.84 ppm. Aromatic carbons para with respect to methyl ester (C₆, –C–Ar) appeared at 142.39 ppm. C₉ carbons appeared at of 69.19 ppm (–OCH₂, 3C). C₁₀₋₁₅ carbons appeared in the range of 22.71 – 31.94 ppm (–OCH₂, 6C). C₁₆ terminal carbon of the aliphatic side chain appeared at 14.12 ppm. (C₁₆, –CH₃, 1C)

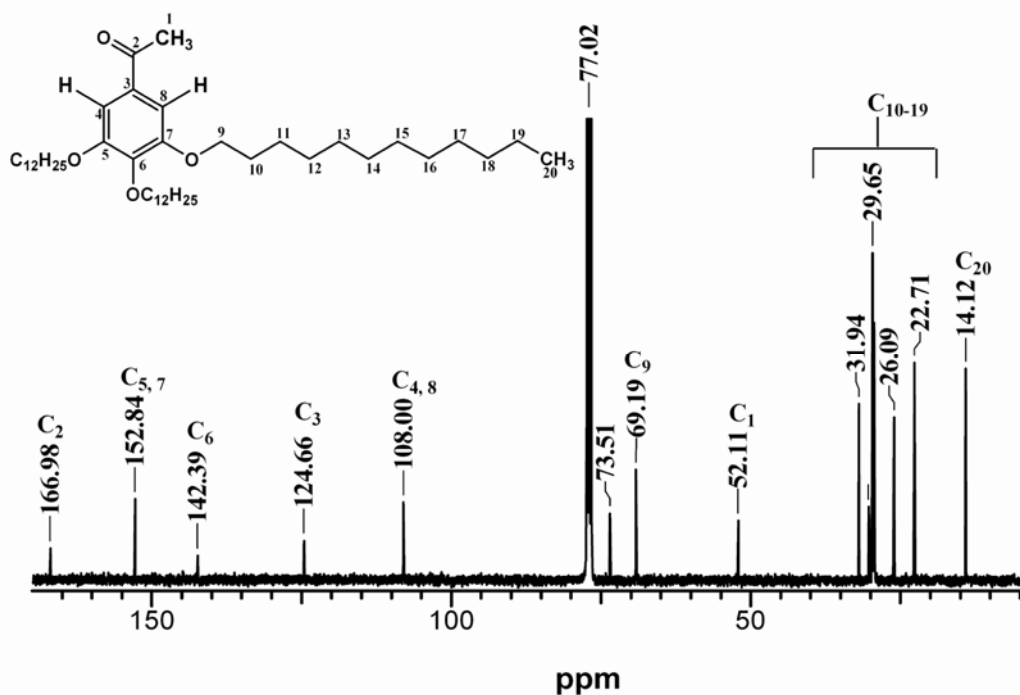


Figure 3.17. ^{13}C NMR spectrum of methyl 3, 4, 5-tris (dodecyloxy) benzoate

The analysis of FT-IR spectrum and the assignments of the peaks in both ^1H and ^{13}C spectra confirmed the structure of MGC_{12} .

3.8 Conclusion:

Hydrophobic compounds from natural resource materials such as cashew nut-shell liquid and gallic acid were prepared. Starting from 3-pentadecyl phenol two hydrophobic derivatives namely, 3-pentadecyl cyclohexyl amine and 3-pentadecyl cyclohexane carbaldehyde were prepared. From gallic acid, two hydrophobic derivatives were prepared namely, methyl tris-octyloxy benzoate and methyl tris-dodecyloxy benzoate. The structural elucidation of all the hydrophobic compounds were performed using IR and NMR spectroscopy. The hydrophobic compounds were later used in synthesizing HMPs which are given in the subsequent chapters.

References:

1. Glass, J. E. “*Polymers in Aqueous Media: Performance Through Association*”, American Chemical Society series 223, **1989**.
2. Landoll, L. M. *US Patent* 4 228 277, Hercules Incorporation (Wilmington, DE), inv. **1980**.
3. Hogen-Esch, T. E.; Amis, E. *Trends in Polym. Sci.* **1995**, 3, 98; Hwang, F. S.; Hogen-Esch, T. E. *Macromolecules* **1993**, 26, 3 156.
4. Wang, T. K.; Iliopoulos, I.; Audebert, R. *Polym. Bull.* **1988**, 20, 577.
5. Nakato, T.; Tomida, M.; Suwa, M.; Morishima, Y.; Kusuno, A.; Kakuchi T. *Polymer, Bulletin*, **2000**, 44, 385.
6. Sinquin, A.; Hubert, P.; Dellacherie, E. *Polymer*, **1994**, 35, 3557.
7. Dubin, P.; Block, J.; Davies, R. M.; Schultz, D. N.; Thies, C. “*Macromolecular Complexes in Chemistry and Biology*” Springer-Verlag, Berlin-Heidelberg, **1994**.
8. Landoll, L. M. *US Patent* 4 352 916A, **1982**; Landoll, L. M. *J. Polym. Sci. Polym. Chem.* **1982**, 20, 443.
9. Marstokk, O.; Roots, J. *Polym. Bull.* **1999**, 42, 527.
10. Hoy, R. C.; Hoy, K. L. *US Patent* 4 426 485, **1984**.
11. Jenkins, R. D. “*The Fundamental Thickening Mechanism of Associative Polymers in Latex Systems: A Rheological Study*” Ph. D. thesis, Lehigh University, Bethlehem, PA, **1990**. Emmons, W. D.; Stevens, T. S. *US Patent* 4 079 028, **1978**.
12. Tian, Q.; Zhao, X.; Tang, X.; Zhang Y. *J. of Appl. Polym. Sc.* **2003**, 89, 1258.
13. Desbrieres, J.; Martinez, C.; Rinaudo, M. *International Journal of Biological Macromolecule* **1996**, 19, 21.
14. Rangelov, S.; Tsvetanov, C. *Polymer Bulletin*, **2001**, 46, 471.
15. Tyman, J. H. P. *J. Chromatogr.*, **1975**, 111, 277.
16. Gedam, P. H.; Sampathkumaran, P. S. *Prog. Org. Coatings* **1986**, 14, 115; Trox, J.; Vadivel, V.; Vetter, W.; Stuetz, W.; Scherbaum, V.; Gola, U.; Nohr, D.; Biesalski, H. K. *J. Agric. Food Chem.* **2010**, 58, 5341.
17. Lubi, M. C.; Thachil, E. T. *Designed monomers and polymers* **2000**, 3, 123.
18. Suresh, K. I.; Kishanprasad, V. S. *Ind. Eng. Chem. Res.* **2005**, 44, 4504.
19. Shingte, R. D.; Wadgaonkar, P. P. *US Patent* 6 790 993, **2004**.

20. Avadhani, C. V.; Wadgaonkar, P. P.; Sivaram, S. *US Patent* 6 255 439, **2001**.
21. Rodriguez, F. H. A.; Feitosa, J. P. A.; Ricardo, N. M. P. S.; de Franca, F. C. F.; Lubi, M. C.; Thachil, E. T. *Designed monomers and polymers* **2000**, 3, 123.
22. Bhunia, H. P.; Jana, R. N.; Basak, A.; Lenka, S.; Nando, G. B. *J. Polym. A Polym. Chem.* **1998**, 36, 391.
23. Bate-Smith and Swain “*Flavonoid compounds: Comparative Biochemistry*,” Florkin, M. Mason H. S. Eds.; Academic Press, New-York, **1962**.
24. Nonaka, G. I.; Sakai, T.; Nakayama, S.; Nishioka, I. *J. Nat. Prod.* **1990**, 53, 1297.
25. Singh, O. V.; Steven, H. P. “*Sustainable Biotechnology: Sources of Renewable Energy*,” Springer, **2010**.

Chapter-IV

**Hydrophobically modified poly(vinyl alcohol): Synthesis,
Characterization and Solution properties**

4.1 Introduction:

There are various water-soluble polymers which can be hydrophobically modified.¹ Poly(vinyl alcohol) [PVA] is one of the largest volume synthetic water-soluble polymers manufactured and contains reactive –OH groups which can easily be modified to incorporate hydrophobic groups into it. Furthermore, PVA has good chemical stability and is non-toxic and biocompatible. Because of these advantages and coupled with ease of availability, PVA is attracting increasing attention lately as a starting material for hydrophobically modified polymers. Yahya et. al.² have reported on the hydrophobic modification of PVA using urea (hydrophilic) and long chain acid chlorides. Their study emphasized on the surface and interfacial activities of hydrophobically modified PVA as a function of polymer concentration, salt (NaCl) concentration, time and average length of the hydrophobic group. Subsequently, Lauten et. al.³ reported the dynamics of aqueous solutions of hydrophobically modified PVA using viscometry and dynamic light scattering techniques. The decreased water solubility of hydrophobically modified PVA was regained by incorporating anionic groups in the polymer chain. Competition between electrostatic and hydrophobic interactions on the polymer chains influenced the dynamics of the aqueous solutions. While exploring different routes for the chemical modification of PVA, Jialanella and Piirma⁴ reported on the synthesis of poly(vinyl alcohol-co-vinyl gallate) by transesterification reaction between PVA and methyl gallate. The advantage of gallate group as a metal chelating agent was utilized to synthesize PVA with improved stabilizing property in latex formulations.

In the present work, we report on the hydrophobic modification of PVA using 3, 4, 5-tris(n-octyloxy) benzoate [MGC₈] and 3, 4, 5-tris(n-dodecyloxy) benzoate [MGC₁₂]. Our emphasis was on deriving hydrophobic compounds from natural resource materials and therefore, both MGC₈ and MGC₁₂ were synthesized from gallic acid which is obtained from gal-nut, a renewable resource material. The details of synthesis and characterization of MGC₈ and MGC₁₂ are given in chapter III. In order to retain the aqueous solubility of HMPVAs upon hydrophobic modification, an ionic moiety was incorporated in the polymer chain using 1, 3-propane sultone during the hydrophobic modification. The influence of hydrophobic modification (MGC₈ and MGC₁₂) (yet

retaining the aqueous solubility) on the rheological behavior of HMPVA solutions was studied by performing creep, steady shear and oscillatory experiments.

4.2 Experimental:

4.2.1 Materials:

Poly(vinyl alcohol) with an average molecular weight of 2.05×10^5 g/mol and degree of hydrolysis, 86 % was obtained from Fluka chemicals, USA and used as received. Gallic acid, n-octyl bromide ($C_8H_{17}Br$), n-dodecyl bromide ($C_{12}H_{25}Br$) were purchased from Aldrich chemicals, USA and used as received. Potassium t-butoxide (t-BuOK), tetrabutyl ammonium bromide (TBAB), potassium carbonate (K_2CO_3) and 1-methyl-2-pyrrolidone (NMP) were procured from Merck, India and used as received. All other reagents were of analytical grade. De-ionized water (Q-Millipore, 18 Ω) was used for preparation of all the polymer solutions.

4.2.2 Hydrophobic modification of PVA with MGC₈:

Into a 250 ml, three necked round bottom flask equipped with an addition funnel, PVA (5 g, 113.63 mmol) and NMP (100 ml) were added. The dissolution was carried out at 120 °C under nitrogen atmosphere. After complete dissolution (2 h), the temperature was decreased to 50 °C and 1, 3-propane sultone (1.38 g, 11.36 mmol) dissolved in 20 ml NMP was added. The solution of t-BuOK (1.27 g, 11.36 mmol) dissolved in 20 ml NMP was added drop-wise through the addition funnel. The reaction was continued at 60 °C for 3 h. To the reaction mixture, MGC₈ (2.36g, 4.54 mmol) dissolved in 30 ml NMP was added and the second lot of t-BuOK (0.51 g, 4.54 mmol) dissolved in 10 ml NMP was added drop-wise through the addition funnel over a period of 90 min. The reaction was continued at 60 °C for an additional 4 h. The polymer was precipitated in acetone and dried under vacuum at room temperature. The dry product was dissolved in water and dialyzed against water for five days and freeze dried to dry polymer. (4.64 g) HMPVAs with different hydrophobic content of MGC₈ were prepared. Using the above procedure, HMPVA with MGC₁₂ was also prepared. Poly(vinyl alcohol) was also modified with 1, 3-propane sultone with 10 mol % modification. (PVAS-10)

4.2.3 Characterization:

^1H and ^{13}C NMR spectra of PVA, PVAS-10, and HMPVAs were recorded on Bruker DRX-400 NMR spectrometer operating at ^1H frequency of 400 MHz. HMPVA samples were recorded in DMSO- d_6 (concentration of polymer = 100 mg.ml). All the HMPVA samples were homogenized for at least 7 days before recording the NMR spectra.

4.2.4 Gel permeation chromatography (GPC) and light scattering (LS):

Molecular weights of PVA, PVAS-10 were determined by GPC using 0.1M NaNO_3 as a mobile phase and pectin as GPC standard. 10 mg of polymer was dissolved in 10mL of 0.1M NaNO_3 , and solution was filtered through a 0.45 μm filter [Instrument with simple and double detection RD-UV, GPC column: HF-PW-5000 (60 cm)]. Light scattering measurements were performed in the presence of 100 mM NaCl solution with different polymer concentrations ($C_p = 0.1 - 40$ g/L). Static and dynamic light scattering measurements were performed to calculate absolute molecular weight.

4.2.5 NMR spectroscopy:

^1H and ^{13}C NMR spectra of MGC_8 , PVA, PVAS-10 and HMPVAs were recorded on Bruker AV-200, DRX-400 NMR spectrometers operating at ^1H frequency of 200 and 400 MHz, respectively. ^1H and ^{13}C NMR spectra of MGC_8 were recorded in CDCl_3 whereas, HMPVA samples were recorded in DMSO- d_6 . (Concentration of polymer = 100 mg.ml^{-1}) All the HMPVA samples were homogenized for at least 7 days before recording the NMR spectra.

4.2.6 Sample preparation:

Polymer solutions of desired concentrations (C_p , g/L) were prepared by dissolving a known amount of polymer in water with gentle stirring. The solutions were homogenized for at least one week before using them for measurements.

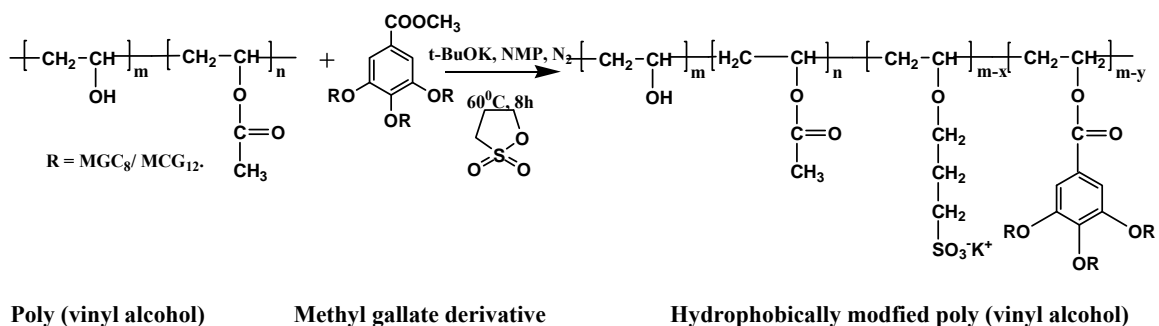
4.2.7 Rheology:

Rheological measurements were performed using two rheometers namely, MCR-301 (Anton Paar, stress and strain controlled) and ARES (Rheometric Scientific, strain control). Creep measurements were performed on the MCR-301 using a cup and bob fixture (cup radius = 9 mm, bob radius = 8.33 mm, gap length = 25 mm, and cone angle 120°) and a cone and plate geometry (cone = 25 mm / 2° , plate 50 mm) depending on the viscosity of polymer solutions. Zero shear viscosities were calculated from the long time creep compliance, and they were used further to calculate the specific viscosity. Steady-shear experiments were performed using ARES rheometer at 25, 35, 45, and 55 $^{\circ}\text{C}$. For dilute solutions, a cup and bob geometry was used, whereas for viscous solutions and gels, a cone and plate geometry (cone radius = 25 mm / angle 4° , plate radius 50 mm) was used. Small amplitude oscillatory shear experiments were performed at 10 $^{\circ}\text{C}$ intervals over a temperature range of 5 - 45 $^{\circ}\text{C}$ using ARES rheometer fitted with a cone and plate geometry. Temperature control on ARES rheometer was achieved using a peltier system. Evaporation of water from the free surface of the sample was minimized by a solvent trap and also by spreading a thin layer of low viscosity silicon oil on the edges of the sample. To determine the linear viscoelastic regime, a strain sweep experiment was performed before every frequency sweep experiment.

4.3 Results and Discussion:

4.3.1 Synthesis of hydrophobically modified PVA using MGC_8 :

Hydrophobically modified PVAs were synthesized with three different contents (2, 3 and 4 mol %) of MGC_8 . The transesterification reaction between PVA and MGC_8 with small amount of t-BuOK as a base catalyst was utilized to modify PVA. The reaction pathway is shown in **scheme 4.1**.



$x = \text{mol \% of 1, 3-propane sultone}$ and $y = \text{mol \% of MGC}_8$.

Scheme 4.1. Reaction mechanism for the preparation of HMPVA

The hydrophobic modification alone results into products which are insoluble in water due to strong hydrophobic nature. Therefore, in order to retain the solubility of HMPVA in water, a hydrophilic compound, 1, 3-propane sultone was incorporated into HMPVAs which enabled the polymer to dissolve in aqueous medium. In the presence of a base t-BuOK, 1, 3-propane sultone ring opens up and couples to the PVA backbone through -OH groups.

In order to study the influence of chain length of the hydrophobic sticker, PVA was modified with 3 mol % of MGC₁₂. The reaction stoichiometry is shown in **Table 4.1**. HMPVAs with different contents of MGC₈ (2, 3 and 4 mol %) were denoted as HMPVA-MGC₈-2, HMPVA-MGC₈-3 and HMPVA-MGC₈-4, respectively. Similarly, HMPVAs with two different contents of MGC₁₂ (2 and 3 mol %) were denoted as HMPVA-MGC₁₂-2, HMPVA-MGC₁₂-3, respectively. The amount of 1, 3-propane sultone was kept constant at 10 mol % for all the samples. PVA with only 1, 3-propane sultone was also prepared separately (10 mol %) and denoted as PVAS-10 (**Table 4.1**)

Table 4.1. Stoichiometry of the reaction between PVA, 1, 3-propane sultone and MGC_8

Samples	PVA (g)	MGC_8/ MGC_{12} (mol %)	$MGC_8/$ MGC_{12} (g)	1, 3- propane sultone (mol %)	1, 3- propane sultone (mmol)
HMPVA- MGC_8 -2	5	2	1.18	10	1.38
HMPVA- MGC_8 -3	5	3	1.77	10	1.38
HMPVA- MGC_8 -4	5	4	2.36	10	1.38
HMPVA- MGC_{12} -2	5	2	1.54	10	1.38
HMPVA- MGC_{12} -3	5	3	2.32	10	1.38
PVAS-10	5	-		10	1.38

Molecular weights of PVA and PVAS-10 were calculated from GPC and static light scattering measurements and found to be comparable. Intrinsic viscosities of poly(vinyl alcohol) and poly(vinyl alcohol) modified with 10 mol % of 1, 3-propane sultone were calculated in the presence of 100 mM NaCl. Intrinsic viscosity was used for the calculation of the Benoit factor (B). Molecular weight of poly(vinyl alcohol) and poly(vinyl alcohol) modified with 10 mol % of 1, 3-propane sultone from GPC measurements were converted to absolute molecular weight using Benoit factor (B).⁵

The molecular weight obtained for PVA was with respect to pectin equivalent with the viscosity of the standard, $\eta = 96.21 \text{ cm}^3/\text{g}$. The viscosity of the standard was divided by the intrinsic viscosity of the poly(vinyl alcohol) which gave the Benoit factor for PVA. (**Table 4.2**)

Table 4.2. GPC data obtained for PVA and PVAS-10

GPC data	Polymer	
	PVA	PVAS-10
M_w (pectin equivalent)	3.31×10^5	4.66×10^5
M_w (absolute)	2.57×10^5	2.44×10^5
M_n	2.08×10^5	2.66×10^5
Viscosity (cm^3/g)	96.214	119.041
l	1.592	1.75
dn/dc (cm^3/g)	0.13	0.12

4.3.2 ^1H NMR spectra of PVA, PVAS-10, HMPVAs:

The structural characterization of the precursor and HMPVAs was carried out using ^1H NMR spectroscopy. The stacked plots of ^1H NMR spectra of PVA, PVAS-10, HMPVA-MGC₈-2, HMPVA-MGC₈-3, HMPVA-MGC₈-4 recorded in DMSO- d_6 are shown in **Figure 4.1**. The various proton chemical shifts in the spectra have been assigned. (**Figure 4.1**) In the case of PVA spectrum, the methylene protons of the backbone appeared in the range 1.37 - 1.94 ppm and the methine proton attached to carbon to which -OH and -OCOCH₃ groups are attached appeared at 3.35 ppm and 3.83 ppm, respectively. The -OH protons appeared at 4.25/4.49/4.68 ppm (atactic) due to the formation of inter-molecular H-bonding in the polymer. Upon comparison of spectra of modified and unmodified PVAs, it can be readily seen that, the modified PVAs show the distinct peaks of the hydrophobe, MGC₈. The terminal methyl (-CH₃) protons of the hydrophobic side chain of MGC₈ appeared at 0.86 ppm. The methylene (-CH₂) protons of PVA backbone and the pendent chain of MGC₈ merge and appeared in the range 1.44 - 1.96 ppm. The aromatic protons of the MGC₈ appeared at 7.17 ppm. The

enlargement of the peaks coming from MGC₈ is shown in the inset of the **Figure 4.1**. This clearly indicates the incorporation of hydrophobic, MGC₈ into the polymer, PVA.

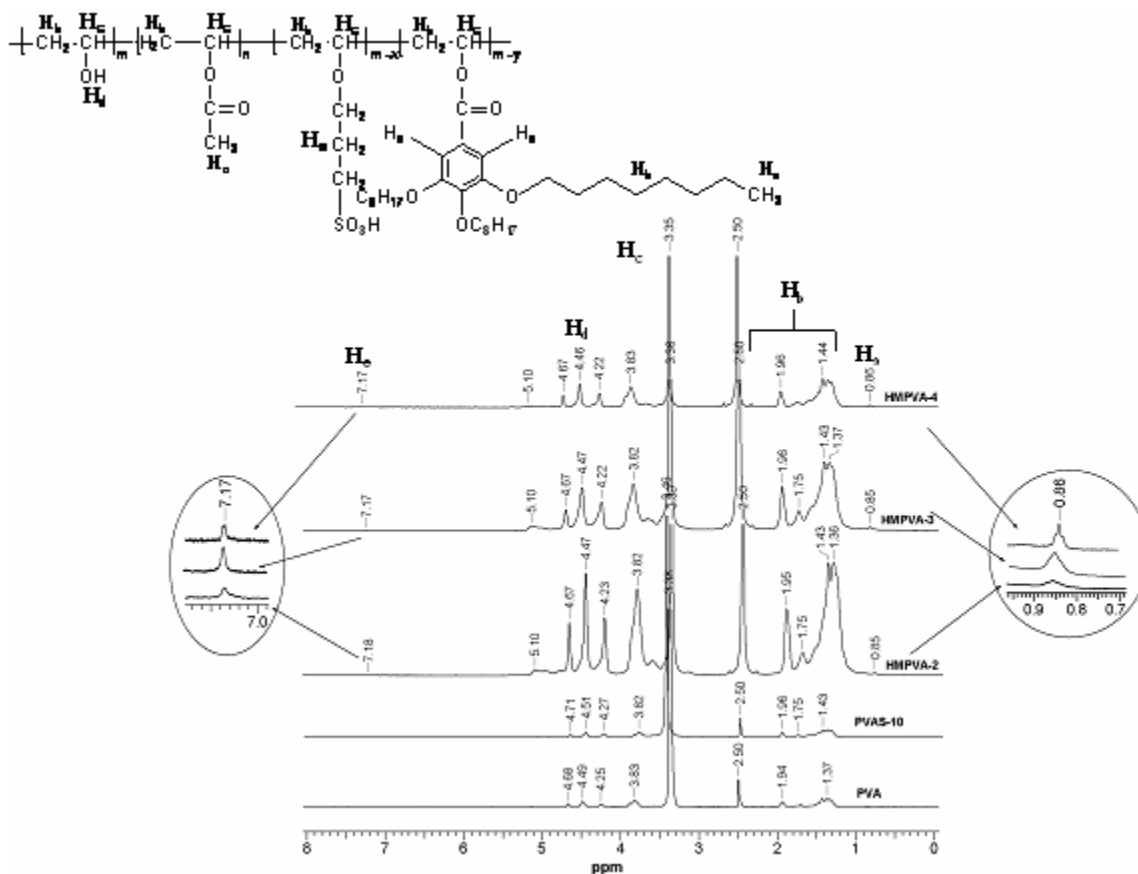


Figure 4.1. Stacked plots of ¹H NMR spectra of PVA, PVAS-10, HMPVA-MGC₈-2, 3, 4 recorded in DMSO-d₆

Furthermore, the incorporation of hydrophobe is well manifested in the macroscopic rheological properties, wherein the combination of hydrophobic (MGC₈/MGC₁₂) and hydrophilic (1, 3-propane sultone) groups in the polymer conferred the multitude of properties to aqueous solutions of HMPVAs. Upon dissolution of HMPVAs in water at moderate concentrations (2 - 40 g/L), the hydrophobic groups in the polymer associate to form transient networks, which give enhanced viscosity properties when compared with their unmodified precursors. The details of the rheological behavior are discussed in the subsequent sections.

4.4 Rheology:

4.4.1 η_{sp} vs. C_p :

The concentration dependent specific viscosities of aqueous solutions of PVA, PVAS-10, HMPVA-MGC₈-2, HMPVA-MGC₈-3, and HMPVA-MGC₈-4 are shown in **Figure 4.2**. The inset shows a magnified view of the data at lower polymer concentrations along with concentration scaling of the specific viscosity for each polymer. The viscosity of PVA solution (uncharged polymer) scaled linearly with concentration indicating the dilute regime. PVAS-10 containing 10 mol % 1, 3-propane sultone exhibited polyelectrolyte behavior and the viscosity was higher than that of the unmodified PVA at similar concentrations, suggesting chain stretching due to intra-chain charge repulsion. The scaling exponent was found to be 0.5 till a polymer concentration of about 15 g/L. This is in accordance with the empirical Fuoss law, wherein the viscosity of a polyelectrolyte solution in the semi-dilute, unentangled regime scales with square root of concentration ($\eta \approx C^{1/2}$).⁶⁻⁸ The concentration, $C_p = 15$ g/L could be considered as the entanglement concentration, C_e , because above this concentration, the scaling exponent was observed to be 1.5, which is typical of a polyelectrolyte solutions in semi-dilute, entangled regime ($\eta \approx C^{3/2}$).⁶⁻⁸ For HMPVA-MGC₈-2 and HMPVA-MGC₈-3, the specific viscosity at low polymer concentrations was found to be less than that of the PVAS-10, indicating chain compaction as a result of intra-chain hydrophobic interactions. The viscosity scaled as the square root of polymer concentrations indicating an unentangled, semi-dilute regime. However, at higher polymer concentrations (>10 g/L), the viscosity of HMPVA-MGC₈-2 scaled as 1.5 power of the polymer concentration, indicating a crossover ($C_p = 5$ g/L) from semi-dilute, unentangled regime to semi-dilute, entangled regime. The crossover concentration ($C_p = 5$ g/L) was lower when compared with PVAS-10, indicating viscosity build up due to hydrophobic associations. The HMPVA-MGC₈-3 also showed concentration scalings of $C_p^{0.5}$ and $C_p^{1.5}$ at lower polymer concentrations. However, compared with HMPVA-MGC₈-2, the HMPVA-MGC₈-3 solution showed a stronger concentration dependence above $C_p = 6$ g/L. The sample HMPVA-MGC₈-4 with still higher content of hydrophobe exhibited a gel-like behavior at higher polymer concentrations; the concentration scalings

of specific viscosity for HMPVA-MGC₈-3 and HMPVA-MGC₈-4 were found to be $C_p^{5.6}$ and $C_p^{7.9}$, respectively. Various scaling laws for the concentration dependence of specific viscosity of associating polymers (APs) have been suggested.⁹⁻¹⁰ Strong concentration dependence of specific viscosity has also been reported for other polymers.¹¹⁻¹² The strong concentration dependence shown in **Figure 4.2** might arise from aggregation.

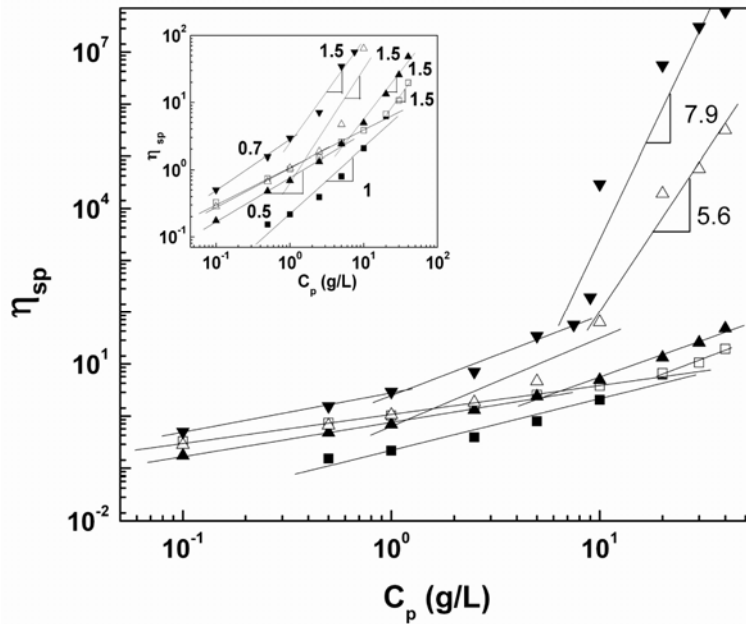


Figure 4.2. Plot of specific viscosity versus polymer concentration (■ PVA, □ PVAS-10, ▲ HMPVA- MGC₈-2, ▼ HMPVA- MGC₈-3 and Δ HMPVA-MGC₈-4)

4.4.2 Steady shear data:

Steady shear experiments were performed to understand the shear rate dependence of viscosity at different polymer concentrations. Although PVAS-10 and HMPVA-MGC₈-2 solutions showed Newtonian behavior over the entire concentration (80 - 100 g/L) and shear rate ranges (0.2 - 800 s⁻¹) studied HMPVA-MGC₈-3 at $C_p = 20$ g/L showed a Newtonian behavior at low shear rates ($\dot{\gamma} = 0.02 - 2$ s⁻¹) and shear thinning behavior at higher shear rates (**Figure 4.3**). A small extent of shear thickening was also observed before shear thinning. This could be attributed to the formation of shear-induced intermolecular hydrophobic associations at moderate shear rates.

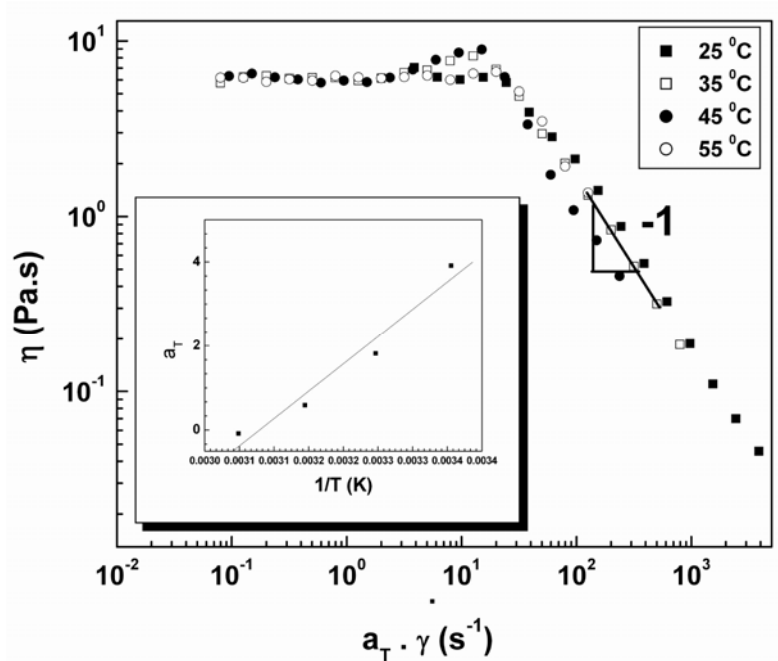


Figure 4.3. Master curve obtained from steady-shear data of HMPVA-MGC₈₋₃,
 $C_p = 20 \text{ g/L}$

4.4.3 Time temperature superposition-Master curve:

Horizontal and vertical shifting of η versus $\dot{\gamma}$ data for HMPVA-MGC₈₋₃ ($C_p = 20 \text{ g/L}$) at different temperatures (25 - 55 °C) resulted into a master curve as shown in **Figure 4.3**. The shift factors at various temperatures were found to follow Arrhenius dependence from which the activation energy for flow was calculated (**Figure 4.3 and Table 4.3**). It is interesting to note that in the shear thinning regime, the viscosity showed power law decay with the shear rate ($\eta = m \dot{\gamma}^{n-1}$). The observed exponent of -1 indicated that the shear stress was constant in this shear rate range, which is an indication of an apparent yielding or structure breakage at high shear rates.

4.4.4 Oscillatory Measurements:

In a typical viscoelastic material, liquid-like response is shown at low frequencies where the loss modulus (G'') is higher than the storage modulus (G'). However, at higher frequencies the storage modulus dominates over the loss modulus and exhibit dominance

of elastic behavior. Generally, strain sweep is performed before every frequency sweep experiment in order to find the linear viscoelastic regime. Many of the HMPs exhibit viscoelastic behavior at moderate concentrations.

Here the linear viscoelastic behavior of HMPVA solutions was studied using isothermal dynamic frequency sweep experiments at different temperatures (5 - 45 °C). The samples PVAS-10 and HMPVA-MGC₈-2 solutions ($C_p = 40$ g/L) were viscous in nature, and their storage modulus (G') was too small to be accurately measured. However, HMPVA-MGC₈-3 solutions ($C_p = 20$ g/L) showed measurable viscoelasticity, indicating network formation by hydrophobic associations. In **Figure 4.4** the master curves for HMPVA-MGC₈-3 solution at $C_p = 40$ g/L is reported. The isothermal frequency sweep data was horizontally superposed using the time-temperature superposition (TTS) principle to obtain master curves and the corresponding shift factors are shown in the inset in **Figure 4.4**.

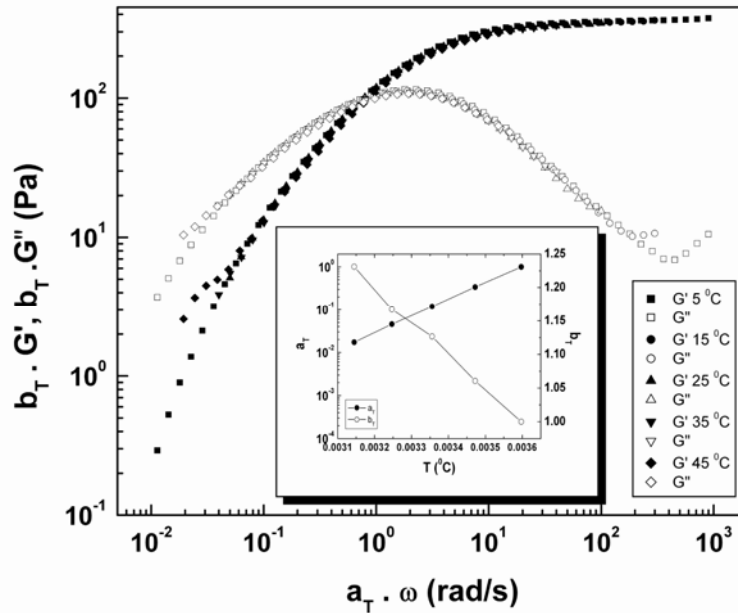


Figure 4.4. Master curve for HMPVA-MGC₈-3, $C_p = 40$ g/L, $T = 5 - 45$ °C, $T_{ref} = 25$ °C

The master curve shown in **Figure 4.4** can be fitted with a multimode Maxwell model. In the low frequency limit, the classical linear viscoelastic behavior ($G'' > G'$ and $G'' \sim \omega$; $G' \sim \omega^2$) was observed, while at high frequency the storage modulus became frequency independent and correspondingly the loss modulus decreased. The maximum

in G'' represents a dominant relaxation mode whose time scale is approximately equal to the inverse of the crossover frequency. This time scale represents the relaxation time of the associating network and corresponds typically to the life time of the association. The plateau modulus, G_e was taken to be approximately equal to the value of G' at the frequency where the G'' exhibited a minimum. Over a narrow concentration range of $C_p = 20 - 40$ g/L, we found that the plateau modulus, the terminal relaxation time (Estimated as the inverse of the crossover frequency), and the low frequency complex viscosity scaled with polymer concentration according to $G_e \sim C_p^{2.5}$, $\tau \sim C_p^{2.5}$, $\eta^* \sim C_p^{7.8}$ respectively. In this context, the following points are worth noting: (i) in the same concentration range of 20 - 40 g/L, the precursor polymers, namely PVA and PVAS-10, are essentially Newtonian liquids and do not show measurable elasticity. On the contrary, the HMPVAs are viscoelastic with a measurable storage modulus. Therefore, it might seem that the plateau modulus of HMPVAs can be considered to arise from hydrophobically associated structures, which form a network of chains and not from chain entanglements. However, the temperature dependence of the plateau modulus was found to be weak, indicating that entanglements contribute significantly to the observed elasticity. Such apparently contradictory behavior was explained by invoking the effectiveness of entanglements. Caputo et. al.¹² argued that at a given polymer concentration, the physical associations such as hydrophobic interactions trap chains in the neighborhood, thereby increasing the effective number of entanglements for every chain and hence the plateau modulus. Thus, the origin of elasticity is still entropic in nature, despite the fact that the network is formed by hydrophobic associations. Hence, the plateau modulus has weak temperature dependence. However, the hydrophobic associations modify the relaxation time, which therefore has strong temperature dependence. This is clearly seen in the large horizontal shift factors shown in **Figure 4.4**.

(ii) Above $C_p = 20$ g/L, the specific viscosity was calculated as $\eta_{sp} = \eta_0 / C_p$ where, η_0 , the zero shear viscosity, was determined from the long time slope of creep experiments. The zero shear viscosity so measured agreed with the low frequency complex viscosity measured from dynamic experiments which indicates that the Cox-Merz rule (where the correspondence between the steady shear viscosity and the complex viscosity exists) is

followed by these APs at low shear and low frequencies. This is shown in **Figure 4.5** and is in line with the earlier observations made for APs.^{12, 13} However, the concentration scaling of the complex viscosity ($\eta^* \sim C_p^{7.8}$) did not agree with the concentration scaling of the specific viscosity ($\eta_{sp} \sim C_p^{5.6}$, **Figure 4.2**). The reason for this disagreement of concentration dependence of η_{sp} and η^* is not known at present. As seen from **Figure 4.5**, the Cox-Merz rule is not obeyed at higher shear rates and higher frequencies, which is in agreement with the previous reports.¹²⁻¹⁴

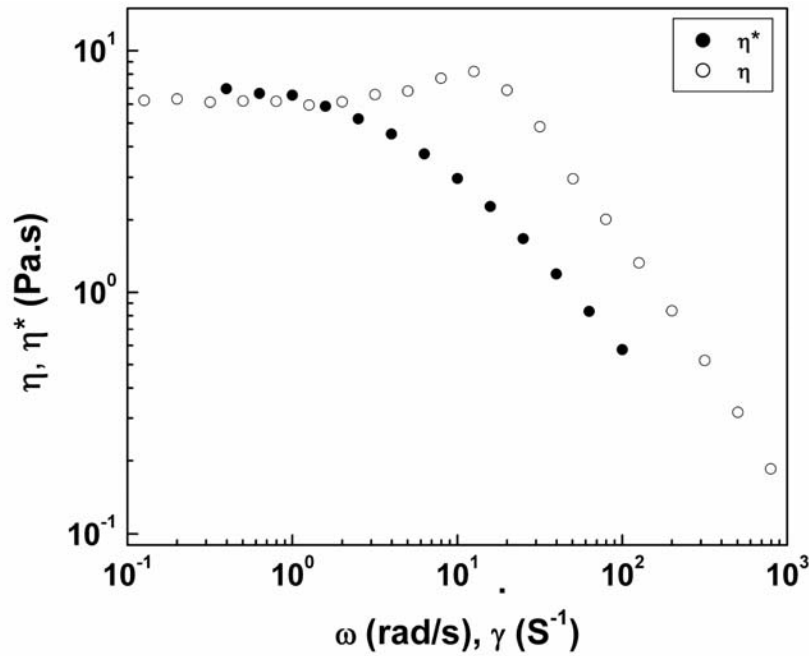


Figure 4.5. Comparison of steady shear and complex viscosity for HMPVA-MGC₈₋₃, $C_p = 20 \text{ g/L}$, 25°C

4.4.5 Activation Energy (E_a):

The shift factors for HMPVA-MGC₈₋₃ at different concentrations were found to follow Arrhenius dependence, and the activation energy, E_a , obtained is presented in **Table 4.3**. The E_a was calculated using the relation:

$$\ln aT = \ln \frac{\eta_0(T)}{\eta_0(T_{ref})} = \frac{E_a}{R} \left(\frac{1}{T} - \frac{1}{T_{ref}} \right) \text{----- (4.1)}$$

aT = horizontal shift factor, η_0 = zero shear viscosity, T = absolute temperature, E_a = activation energy, R = gas constant. The activation energy values obtained from steady-shear and dynamic frequency sweep experiments at different polymer concentrations were found to be in reasonable agreement with each other. It can also be seen that the E_a values obtained from the dynamic frequency sweep experiments are nearly independent of polymer concentration, indicating that they correspond to the intrinsic energy required to overcome hydrophobic interactions and disengage the hydrophobic groups from the associations.

Table 4.3. Comparison of activation energy calculated from steady-shear and oscillatory shear data

HMPVA-MGC ₈ -3 C _p (g/L)	SRST E _a (KJ/mol)	TTS (DFS) E _a (KJ/mol)
20	108	74.4
30	86.4	75.5
40	90.5	81
50	75.3	76.5

Based on the empirical formula ($E_a = 7 n_c - 41$), where ' n_c ' is the number of carbon atoms in the alkyl chain length] derived from the discussions reported by Annable et al.¹⁴ and Kadam et. al.,¹¹ the activation energies obtained here are consistent ($\pm 10\%$) with the molecular structure of the hydrophobic moieties used. Nevertheless, the position of the hydrophobic groups, stereochemical effects may influence the activation energy.

4.4.6 Strain-Rate Frequency Superposition: [SRFS]

Aqueous solutions of HMPVAs containing higher hydrophobe content such as the HMPVA-MGC₈-4 or HMPVA-MGC₁₂-3 did not follow TTS; horizontal shifting of their dynamic frequency sweep data at different temperatures did not yield master curves. Therefore, these solutions were not thermo-rheologically simple fluids. It was noticed

that at high polymer concentrations, these solutions had a tendency to form microgels because of strong inter polymer hydrophobic interactions. The term “microgels” is commonly used for partially/lightly cross-linked chemical gels. Nevertheless, the formation of microgels in HMPs/APs has been reported by several research groups.^{13, 15} Microgel formation (a class of HMPs) is caused because of large number of physical cross-links formed due to hydrophobic associations.

These microgels appear to exist in the form of colloidal particles or colloidal aggregates, which were readily observed by confocal laser scanning microscopy (CLSM). **Figure 4.6** shows the CLSM images of HMPVA-MGC₈-4 and HMPVA-MGC₁₂-3 samples at $C_p = 5$ g/L. To observe the microgel particles clearly, it was required to dilute the sample to a suitable extent; in this case, the 20 g/L solution was diluted to 5 g/L. The sample was stained by Pyren-1-ylmethanol, and the blue particles in **Figure 4.6** are microgels of size 20 - 25 μ m. One can expect an increase in microgel concentration with an increase in polymer concentration or an increase in the hydrophobic chain length as shown in **Figure 4.6** ^(a, b). Thus, the microstructure of HMPVA-MGC₈ and HMPVA-MGC₁₂ solutions of high polymer concentrations ($C_p > 10$ g/L) can be expected to comprise closely packed soft microgels suspended in the AP solution.

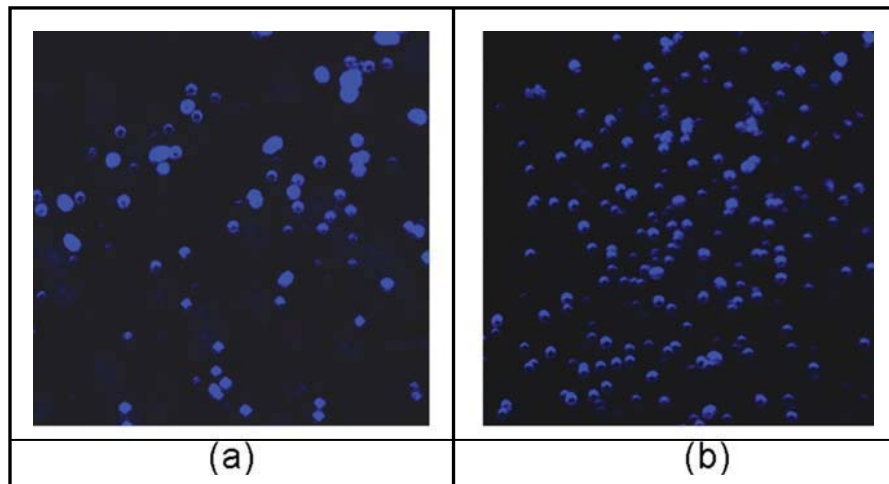


Figure 4.6. Confocal laser scanning microscopy images of (a) HMPVA-MGC₈-4 and (b) HMPVA-MGC₁₂-3 at $C_p = 5$ g/L

Microgel suspensions are typically non-ergodic systems and exhibit soft glassy rheology. The rheological behavior of such materials is expected to be dominated by inter particle friction and deformability of the particles. The salient rheological signatures of soft solids are as follows: (i) in a frequency sweep experiment, the storage modulus is greater than the loss modulus ($G' > G''$), the storage modulus shows weak frequency dependence, and the loss modulus shows a shallow minimum at an intermediate frequency; (ii) in a strain sweep test, the storage modulus exceeds the loss modulus ($G' > G''$) at low strains, while the loss modulus becomes greater than the storage modulus at high strains ($G' < G''$), and at intermediate strain the loss modulus (G'') shows a characteristic maximum; (iii) soft solids exhibit an apparent yield stress; and (iv) they also show distinct thixotropic behavior. Recently, Wyss et. al.¹⁶ proposed a new approach to characterize the rheological response of such materials. In this so called strain-rate frequency superposition (SRFS) approach, the material is subjected to an oscillatory shear test in which the effective shear rate, defined as the product of the strain amplitude “ γ_0 ” and the frequency “ ω ”, is maintained constant. Tests are performed at various constant values of the effective shear rates. The SRFS methodology is based on the hypothesis that the relaxation time of a soft glassy material is a function of the imposed shear rate as per **equation 4.2** below,

$$b(\dot{\gamma}) = \frac{\tau_{ref}}{\tau} = 1 + \tau_0 k \left(\frac{\dot{\gamma}}{\dot{\gamma}_{ref}} \right)^n \text{----- (4.2)}$$

In **equation 4.2**, ‘k’ is a constant, ‘ $\dot{\gamma}$ ’ is the effective shear rate, ‘n’ is the power law index and τ_{ref} is the relaxation time of the soft solid at a reference shear rate $\dot{\gamma}_{ref}$.

τ_{ref} becomes equal to the microscopic relaxation time τ_0 when, $\dot{\gamma}_{ref} \rightarrow 0$, i. e., under near quiescent conditions. Higher shear rate enables the breakage of ‘cages’ around any particle thus enabling it to sample larger configurational space more effectively. In other

words, the characteristic relaxation time of soft solids decreases with increase in shear rate. This behavior is enshrined in **equation 4.2**.

Since the microstructure of the HMPVA-MGC₈₋₄ and HMPVAMGC₁₂₋₃ polymers comprises dense suspensions of microgels, the use of SRFS technique becomes relevant for these polymers. In **Figure 4.7** the strain and frequency sweep responses and SRFS master curves for two samples are shown: HMPVA-MGC₈₋₄ and HMPVA-MGC₁₂₋₃ at the same concentration, C_p = 20 g/L. Many of the characteristic rheological responses of a soft solid are seen in **Figure 4.7 (a-d)** for these two polymer solutions. The HMPVA-MGC₁₂₋₃ solution even shows a distinct G'' maximum in strain sweep experiment [**Figure 4.7 (b)**]. Compared to the HMPVA-MGC₈₋₄ solution, the HMPVA-MGC₁₂₋₃ solution can be expected to have higher concentration of microgel particles. This is indeed evidenced from the confocal microscopy images presented earlier.

The SRFS experimental data were obtained by performing frequency sweep experiments in which the product $\dot{\gamma} = \omega\gamma_0$ was maintained constant. SRFS experiments were performed at various effective shear rates ranging from 0.05 - 5 s⁻¹. Data so obtained was then horizontally and vertically shifted using a horizontal shift factor b ($\dot{\gamma}$) defined by **equation 4.3** and a vertical shift factor defined as,

$$a(\dot{\gamma}) = G_0(\dot{\gamma}) / G_0(\dot{\gamma}_{ref}) \text{ ----- (4.3)}$$

Here, G₀ $\dot{\gamma}$ is the high-frequency storage modulus at a shear rate $\dot{\gamma}$ and G₀($\dot{\gamma}_{ref}$) is the high-frequency storage modulus at the reference shear rate, $\dot{\gamma}_{ref}$. The master curves shown in **Figure 4.7 (e, f)** were obtained by shifting the raw data to the reference shear rate of $\dot{\gamma}_{ref} = 0.05 \text{ s}^{-1}$. It was found that the vertical shift factors were unity and the horizontal shift factors were linearly dependent on the effective shear rate. From the above studies, it can be realized that SRFS method works for both the solutions, indicating that perhaps highly concentrated and highly hydrophobically associating

polymer solutions that have a tendency to form microgels ought to be characterized by this new approach.

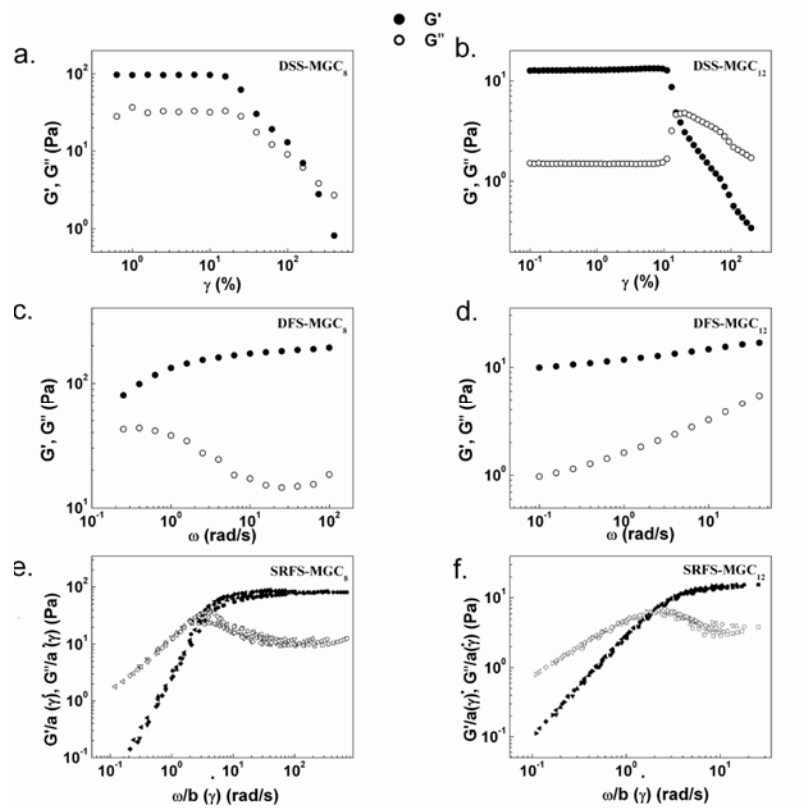


Figure 4.7. Strain, frequency and SRFS response of HMPVA-MGC₈-4 and HMPVA-MGC₁₂-3, $C_p = 20$ g/L

4.5 Conclusions:

In conclusion, hydrophobic compounds namely, MGC₈ and MGC₁₂ were prepared from gallic acid, a renewable resource material and used to synthesize hydrophobically modified poly(vinyl alcohol) [HMPVAs]. The hydrophobic nature of MGC₈/MGC₁₂ results into HMPVAs (above 1 mol % of MGC₈/MGC₁₂) insoluble in water. In order to retain the aqueous solubility of these HMPVAs, an ionic moiety namely 1, 3-propane sultone was incorporated (10 mol %) in the polymer backbone. HMPVAs with different contents of MGC₈ (2, 3 and 4 mol %) and MGC₁₂ (2, 3 mol %) were prepared and the rheological properties were studied. In the dilute regime, the specific viscosities of HMPVA-MGC₈-2 and HMPVA-MGC₈-3 were found to be lower than the viscosity of PVAS-10 polymer. At higher polymer concentrations the HMPVA-MGC₈-2 solutions

showed signature of the semi-dilute entangled regime with respect to Fous law ($\eta_{sp} \sim C_p^{1.5}$), while HMPVA-MGC₈-3 showed a network-like response with a much stronger dependence on concentration. The specific viscosities of HMPVA-MGC₈-4 solutions showed higher viscosities than the PVAS-10 solutions. At higher concentrations, HMPVA-MGC₈-4 and HMPVA-MGC₁₂-3 exhibited highly viscoelastic nature with the presence of microgels in the system. This could be explained by the confocal microscopy and a new approach of SRFS. These systems have potential applications as thickeners in cosmetic creams, lotions and also as drug carriers in pharmaceutical formulations.

References:

1. Glass, J. E. Water-Soluble Polymers, Beauty with Performance, Advances in Chemistry Series No. 213; American Chemical Society: Washington, **1986**, Glass, J. E. Associative Polymers in Aqueous Media, American Chemical Society Symposium Series No. 765; American Chemical Society: Washington, **2000**.
2. Yahaya, G. O.; Ahdab, A. A.; Ali, S. A.; Abu-Sharkh, B. F.; Hamad, E. Z. *Polymer* **2001**, *42*, 3363.
3. Lauten, R. A.; Marstokk, O.; Kjoniksen, A. L.; Nystrom, B. *Polym. Bull.* **2002**, *49*, 281.
4. Jialanella, G.; Piirma, I. *Polym. Bull.* **1987**, *18*, 385.

5. Hersmis, M. C.; Spiering, A. J. H.; Waterval, R. J. M.; Meuldijk, J.; Vekemans, J. A. J. M.; Hulshof, L. A. *Org. Process Res. Dev.* **2001**, *5*, 645.
 6. Dobrynin, A. V.; Colby, R. H.; Rubinstein, M. *Macromolecules* **1995**, *28*, 1859.
 7. Dobrynin, A. V.; Rubinstein, M. *Macromolecules* **1999**, *32*, 915.
 8. Leibler, L.; Rubinstein, M.; Colby, R. H. *Macromolecules* **1991**, *24*, 4701.
 9. Rubinstein, M.; Semenov, A. *Macromolecules* **2001**, *34*, 1058.
 10. Semenov, A. N.; Rubinstein, M. *Macromolecules* **2002**, *35*, 4821.
 11. Kadam, V. S.; Badiger, M. V.; Wadgaonkar, P. P.; Ducouret, G.; Hourdet, D. *Polymer* **2008**, *49*, 4635.
 12. Caputo, M.; Selb, J.; Candu, F. *Polymer* **2004**, *45*, 231.
 13. English, R. J.; Raghavan, S. R.; Jenkins, R. D.; Khan, S. A. J. *Rheol.* **1999**, *43*, 1175.
 14. Annable, T.; Buscall, R.; Ettelaie, R.; Whittlestone, D. *J. Rheol.* **1993**, *37*, 695.
 15. Yekta, A.; Xu, B.; Duhamel, J.; Adiwidjaja, H.; Winnik, M. A. *Macromolecules* **1995**, *28*, 956.
 16. Wyss, H. M.; Miyazaki, K.; Mattsson, J.; Hu, Z.; Reichman, D. R.; Weitz, D. A. *Phys. Rev. Lett.* **2007**, *98*, 238303.
-
-

Chapter-V

Hydrophobically Modified Poly(N, N'-dimethyl acryl amide-co-acrylic acid): Synthesis, Characterization and Rheology

5.1 Introduction:

In general, most polymer melts and solutions display shear thinning behavior. The opposite behavior of an increase in viscosity with an increase in shear, i.e. shear thickening, is less commonly encountered. The phenomenon of shear thickening is often observed in physically cross-linked networks of polymer chains having a few localized, energetically favored interactions such as in ionomers¹ and aqueous solutions of hydrophobically modified polymers.²⁻³ Certain shear thickening polymers are industrially important as viscosity modifiers for polymer augmented water flooding in enhanced oil recovery (EOR). Shear thickening has also been observed in worm-like micellar solutions⁴ and concentrated suspensions.⁵ Several theoretical models have been proposed to explain the viscoelastic behavior of associating polymer solutions. The mathematical

framework for these models was first provided by Tanaka and Edwards (TE),⁶⁻⁹ who developed a transient network theory based on the affine network model of Green and Tobolsky.¹⁰ In the TE model for telechelic associating polymers containing two hydrophobic “sticker” groups at chain ends, the cross-links under quiescent conditions have a finite lifetime, which decreases with imposed shear deformation. Consequently, the model predicts shear thinning but fails to describe the shear thickening property of associating polymer solutions. The molecular cause of shear thickening phenomenon in polymer solutions was suggested to be shear-induced transfer of intra-molecular interactions to intermolecular interactions.^{11, 12} Wang¹³ argued that free polymer chains, under the action of shear, can join the transient network first as dangling chains and eventually as bridging chains which are elastically active. This model predicted shear thickening albeit at shear rates much higher than the experimentally observed range. Marucci et. al.¹⁴ suggested that a bridging chain would pull out of its associations only when shear is able to stretch it to nearly its full extent such that the accompanying non-Gaussian chain stretching might cause shear thickening before thinning occurs. Similar observations were also made by others.¹⁵ However, the predicted extent of thickening was much smaller than experimental observations. In the same paper the authors also suggested an alternative mechanism in which bridging chains relax only partially upon breakage of associations since they are likely to be trapped into other associations before complete relaxation. Brownian dynamic simulations¹⁶ supported this idea and suggested that the rate of associations in fact depends on the chain extension. Subsequently, Vaccaro and Marucci¹⁷ revised the earlier model and were able to predict shear thickening at intermediate shear rates in qualitative agreement with experiments. Ahn and Osaki¹⁸ proposed alternative kinetics for the rates of network creation and destruction. Lele and Mashelkar¹⁹ used this model to predict anomalous gelation effects in transient networks. Further refinements of the network model by Tripathi et. al.²⁰ allowed nearly quantitative model fits to experimental shear thickening data in both shear and extension. Some researchers have also explained the mechanism of shear thickening on the basis of association of aggregates containing many chains under shear.^{21, 22} The above theoretical models predict a gradual shear thickening with increase in shear rate followed by shear thinning, in agreement with most experimental observations. However, Bokias et al.²³

recently reported on the shear rheology of a copolymer of poly(N-isopropyl acrylamide-co-N, N'-[(dimethyl amino) propyl]-methacryl amide) of high molecular weight and demonstrated an abrupt shear thickening effect of large magnitude at a critical shear rate, $\dot{\gamma}_{crit}$ which decreased with increasing polymer concentration and decreasing temperature. Subsequently, Cadix et. al.²⁴ investigated the rheology of high molecular weight poly(N, N'-dimethyl acrylamide-co-acrylic acid) which was hydrophobically modified using linear alkyl amines. In the linear viscoelastic regime the copolymer showed scaling laws that were in apparent agreement with the so-called “sticky reptation” model²⁵ where as at high shear rates abrupt shear-induced thickening was observed at critical shear rates which decreased with polymer concentration as, $\dot{\gamma}_{crit} \sim C_p^{-3}$ and also with increasing hydrophobic content. More recently, Wang et. al.²⁶ investigated the nonlinear rheological properties of the same solutions in a dynamic mode and concluded that shear thickening is caused by an increase in the lifetime of associations.

On the basis of the observations made from earlier reports, it appears that the prerequisites for associating polymers to exhibit an abrupt shear thickening effect in experimentally observable range of shear rates are,

- (i) The polymer should possess an appropriate balance of hydrophobic and hydrophilic interactions such that in a solution it is on the threshold of phase separation yet shows complete solubility.
- (ii) The concentration of the polymer should be close to a critical aggregation concentration, C_{agg} .
- (iii) Furthermore, the nature of the hydrophobic compound, the charges on the polymer chain, the molecular weight of the polymer, and the presence of salt and surfactants largely influence the shear thickening behavior.

Despite a few interesting studies on such polymer solutions, the abrupt shear-thickening phenomenon remains largely not understood. None of the transient network models for associating polymers mentioned above can predict an abrupt shear thickening effect in associating polymers. In most previous rheological studies on associating polymer solutions, the shear thickening effect has been investigated using a strain-

controlled rheometer in a rate-ramp mode. The intrinsic difficulty with this experiment, especially in the case of solutions that show abrupt thickening, is that the large imposed strain tends to rupture the thickened samples or eject it out of the geometry. On the other hand, if similar experiments were to be done in a stress-ramp mode, the rate of deformation tends to decrease as the sample thickens, thereby minimizing the chances of damage to the sample. In this work, creep experiments were performed to demonstrate several interesting features of the abrupt shear thickening phenomenon in hydrophobically modified polymer solutions. In particular, it has been shown that the creep experiments provide a facile control on trapping the thickened sample in different meta-stable states. The results also show that upon reduction of the imposed stress the thickened sample undergoes an increase in stiffness. Eventually at low stress, the thickened sample relaxes to its equilibrium state after a critical liquefaction time and at a critical strain. In this study a high molecular weight poly(N, N'-dimethyl acrylamide-co-acrylic acid) copolymer which is modified with a hydrophobic compound, 3-pentadecyl cyclohexylamine [3-PDCA] has been used. This particular hydrophobe contains a -C₁₅H₃₁ side chain attached to an aliphatic six-membered ring²⁷ and is prepared from a renewable resource material namely, cashew nutshell liquid (CNSL) (As discussed in chapter III). According to some literature reports²⁸ aliphatic ring compounds are more hydrophobic as compared to linear and aromatic hydrophobic compounds with a similar number of carbon atoms. Therefore, it is presumed that a small amount of 3-PDCA is sufficient to provide the requisite hydrophobicity for observing shear thickening behavior in copolymers. The backbone copolymer poly(N, N'-dimethyl acrylamide-co-acrylic acid) is similar to that used in earlier studies^{25, 26} and it is easy to synthesize with high molecular weights. Further, it allows for tunable hydrophilic-hydrophobic properties and exhibit limited solubility in water, which seems to be a prerequisite for the occurrence of abrupt shear thickening.

5.2 Experimental:

5.2.1 Materials:

N, N'-Dimethyl acrylamide (DMA), acrylic acid (AA), sodium metabisulfite (Na₂S₂O₅), and ammonium per sulfate [(NH₄)₂S₂O₈] were purchased from Aldrich Chemicals.

Dicyclohexyl carbodiimide (DCC), N-methyl-2-pyrrolidone, dichloromethane and diethyl ether were purchased from Merck, India. All the chemicals were of synthesis grade and used as received. The polymer samples were prepared in DI-water (18 Ω) with a required concentration.

5.2.2 Synthesis:

5.2.2.1 Preparation of poly(N, N'-dimethyl acrylamide-co-acrylic acid) and its hydrophobic modification using 3-PDCA:

The synthesis of polymer involves two steps: In the first step, precursor copolymer poly(N, N'- dimethyl acrylamide-co-acrylic acid) was prepared, and in the second step, some of the acrylic acid units in the copolymer were modified using 3-PDCA. The detailed procedure for the synthesis of precursor polymer and its subsequent hydrophobic modification is described below.

5.2.2.2 Synthesis of poly(N, N'-dimethyl acrylamide-co-acrylic acid) [(70 mol % DMA/30 mol % AA)]:

Into a 500 ml three-necked jar reactor, 26 g (0.26 mol) of N, N'-dimethyl acrylamide (DMA) and 8.1 g (110 mmol) of acrylic acid (AA) were added in 220 ml of water. The pH was adjusted between 8 and 10 by adding 20 ml of 1 M NaOH. The homogeneous mixture obtained by stirring was deaerated with argon gas for 30 min. 0.72 g (3.1 mmol) of ammonium persulfate and 18 mg (0.095 mol) of sodium meta-bisulfite were added. The polymerization was allowed to proceed for 90 min at 30 $^{\circ}$ C. The reaction was quenched by adding 10 ml of 3 M HCl, and the polymer was dialyzed against pure water for 1 week and finally recovered by freeze-drying. The yield of the copolymer was found to be 70-%. The content of AA incorporated in the copolymer was estimated by 13 C NMR spectroscopy.

5.2.2.3 Hydrophobic modification of poly(N, N'-dimethyl acrylamide-co-acrylic acid) using 3-PDCA:

Into a 500 ml two-neck round-bottom flask, 6 g of precursor polymer was dissolved in 200 ml of N-methyl-2-pyrrolidone (NMP) at 70 $^{\circ}$ C for 12 h. To this solution

0.59 g (1.9 mmol) of 3-PDCA (dissolved in 10 ml of NMP) and 1.98 g (9.6 mmol) of DCC (dissolved in 10 ml of NMP) were added, and the reaction was continued at 70 °C for 12 h. The reaction pathway for the hydrophobic modification is shown in **scheme 5.1**. Then the reaction mixture was allowed to cool to room temperature and precipitated in 3 L of diethyl ether. The precipitated polymer was filtered and dried under vacuum at 50 °C. In order to purify the polymer, the dry polymer was again dissolved in 300 ml of chloroform and precipitated in 3 liter of diethyl ether. This process was repeated thrice to get pure polymer, which was dried at 50 °C under vacuum. The dry polymer was then dissolved in de-ionized water and the carboxylic groups in the polymer were neutralized with 1M NaOH.

5.3 Gel permeation Chromatography:

Molecular weight of precursor polymer was determined using 0.1M NaNO₃ as a mobile phase and pectin as GPC standard. 10 mg of polymer was dissolved in 10 ml of 0.1M NaNO₃, and solution was filtered through a 0.45 µm filter [instrument with simple and double detection RD-UV, GPC column: HF-PW-5000 (60 cm)].

5.4 ¹H and ¹³C NMR Spectroscopy:

The structural characterization and the composition of the precursor copolymer were determined by ¹³C NMR spectroscopy. The spectra were recorded in DMSO-d₆ using a Bruker DRX-500 spectrometer operating at a ¹H frequency of 500 MHz. For hydrophobically modified polymers, structural characterization was done by ¹H NMR spectroscopy. ¹H NMR spectra were recorded in DMSO-d₆ using a Bruker AV-400 spectrometer operating at a ¹H frequency of 400 MHz. All samples were allowed to dissolve for 4-5 days for homogenization before recording the spectra (polymer concentrations for ¹H NMR and ¹³C NMR were 20 mg/0.7 ml and 100 mg/0.9 ml, respectively).

5.5 Sample Preparation:

Polymer solutions of desired concentrations (C_p ; g/L) were prepared by dissolving a known amount of polymer in water with gentle stirring. The solutions were homogenized for at least 7 days before use. Samples were designated as follows:

70DMA/27AA/3-PDCA-3 implies a hydrophobically modified poly(N, N'-Dimethyl acrylamide-co-acrylic acid) containing 70 mol % DMA, 27 mol % AA, and 3 mol % of 3-PDCA. The polymer concentration for each solution is specified separately.

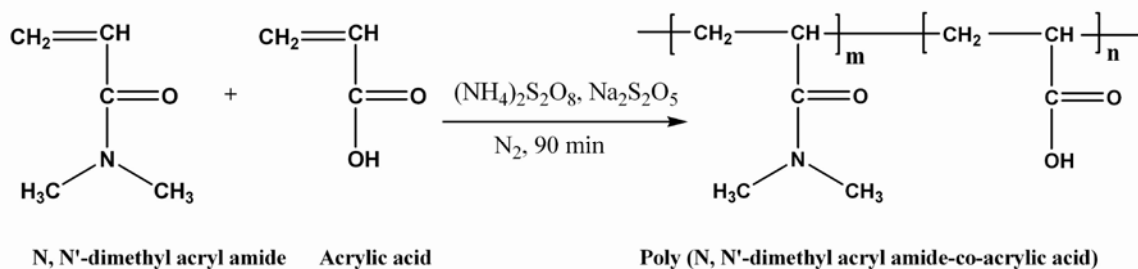
5.6 Rheology:

Rheological properties of the copolymer solutions were studied using two rotational rheometers: a stress controlled rheometer MCR-301 (Anton Paar) and a strain-controlled rheometer ARES (Rheometric Scientific). Isothermal steady shear experiments were performed in a rate-ramp mode on the ARES and in a stress-ramp mode on the MCR-301. A majority of the rheological studies performed in this work were based on isothermal creep experiments, which were carried out on the MCR-301. Compliance data obtained using small values of the applied stress were used to determine the zero-shear viscosity (η_0). Concentric cylinder geometries and Peltier heating systems were used in all experiments in both rheometers.

5.7 Results and Discussion:

5.7.1 Synthesis of poly(N, N'-dimethyl acrylamide-co-acrylic acid) [(70 mol % DMA/30 mol % AA)]:

N, N'-Dimethyl acrylamide (DMA) and acrylic acid (AA) were copolymerized in the presence of ammonium persulfate and sodium meta-bisulfite as redox initiators in aqueous medium under inert atmosphere at 30 °C. The reaction pathway for copolymerization is shown in **scheme 5.1**.



Scheme 5.1. Reaction pathway for the preparation of poly (N, N'-dimethyl acryl amide - co-Acrylic acid)

Although the reactivity ratios of DMA and AA are not known, an analogy can be made with the pair of acrylamide/ acrylic acid due to similarity in the chemical structures of acrylamide and N, N'-dimethyl acrylamide. The reactivity ratios of acrylamide and acrylic acid in basic pH are known to be respectively $r_1 = 1.32$ and $r_2 = 0.35$. As a consequence, one can expect blocks of DMA to some extent in addition to the random structure in the copolymer. However, the sequence lengths of DMA and AA units in the copolymers were not analyzed in this work. The weight-average molecular weight of the copolymer as determined by GPC was found to be $M_w = 1254$ kg/mol (pectin standards) with a PDI of 2.7. This solution was dialyzed against water and recovered by freeze-drying. Using the above procedure, polymers with different hydrophobic content (1-3 mol %) were prepared. Beyond 3 mol % of 3-PDCA content, the polymer was insoluble in water, and therefore, the hydrophobic content was restricted to 3 mol %. The stoichiometry of reagents used in the reactions is reported in **Table 5.1**. The nomenclature of the polymer prepared is described in **Table 5.1**.

Table 5.1. Stoichiometry for the hydrophobic modification of poly(N, N'-dimethyl acrylamide-co- acrylic acid)

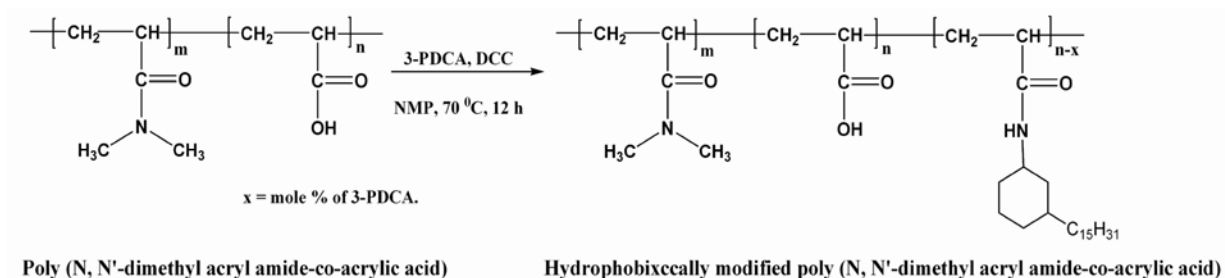
Polymer Nomenclature	Polymer(g)	3-PDCA (Mol %)	3-PDCA (g)	DCC (g)
70DMA/29AA/3-PDCA-1	4	1	0.135	0.45
70DMA/28AA/3-PDCA-2	4	2	0.271	0.90
70DMA/27AA/3-PDCA-3	4	3	0.407	1.36

For example, 70DMA/29AA/3-PDCA-1 corresponds to a copolymer consisting of 70 mol % of DMA, 29 mol % of AA, and 1 mol % of 3-PDCA.

The molar ratio of DMA: AA of 70:30 was chosen in order to have reasonably good solubility of the copolymer in water even after hydrophobic modification of acrylic acid upto 3 mol %. It was observed that if the AA content was chosen to be less than 30 mol %, then the hydrophobically modified polymer became insoluble at 3 mol % of 3-PDCA. The structure of the precursor polymer, poly (DMA-co-AA) (70:30) was confirmed by ^{13}C NMR spectroscopy.

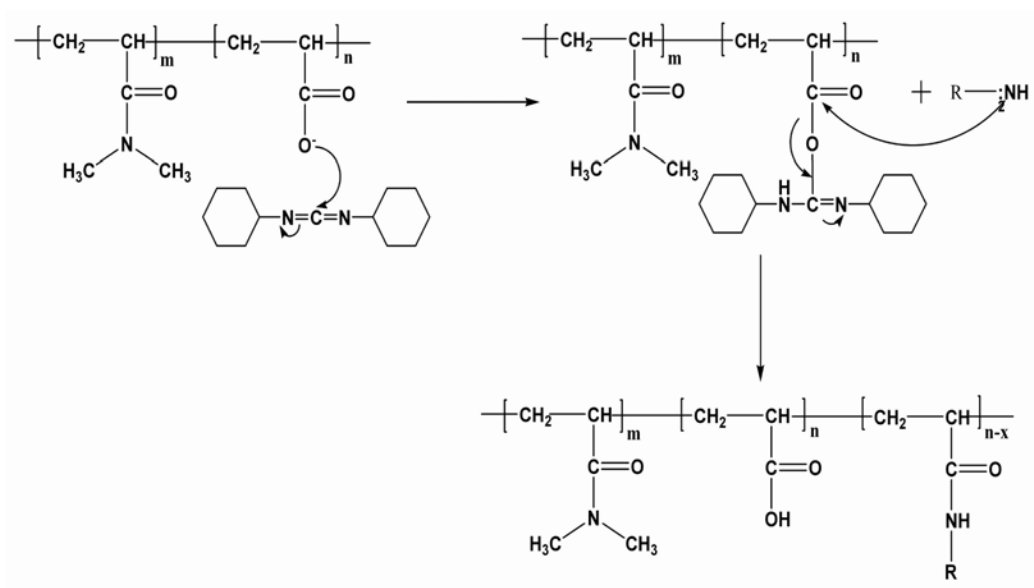
5.7.2 Hydrophobic modification of poly(N, N'-dimethyl acrylamide-co-acrylic acid) using 3-PDCA:

Poly(N, N'-dimethyl acrylamide-co-acrylic acid) was hydrophobically modified with a hydrophobe 3-PDCA using N-methyl-2-pyrrolidone (NMP) as a solvent. The reaction pathway for the hydrophobic modification is shown in **scheme 5.2**.



Scheme 5.2. Reaction pathway for the preparation of hydrophobically modified poly(N, N'-dimethyl acryl amide -co-Acrylic acid)

Coupling between amine group of 3-PDCA and acrylic acid units of poly (N, N'-dimethyl acrylamide-co-acrylic acid) is performed using dicyclohexyl carbodiimide and the reaction mechanism is shown in **Scheme 5.3**.



Scheme 5.3: Coupling reaction for the preparation of hydrophobically modified poly(*N, N'*-dimethyl acrylamide-co-acrylic acid)

5.7.3. NMR spectroscopy:

^{13}C NMR spectrum of poly (DMA-co-AA) recorded in DMSO-d_6 is shown in **Figure 5.1**. The carbonyl ($>\text{C}=\text{O}$) peak coming from the amide group of DMA appeared at 177 ppm and the carbonyl ($>\text{C}=\text{O}$) peak coming from acid group of AA appeared at 174 ppm. This difference in the chemical shifts of the carbonyl carbons was used to determine the composition of the copolymer. Accordingly, the integration of carbonyl signal of amide and acid gave the ratio of DMA:AA as 70:28. This clearly indicates that the reaction goes toward completion with 98 % incorporation of AA units. The other carbon atoms of the main chain and side chain appear in the range 35 - 40 ppm.

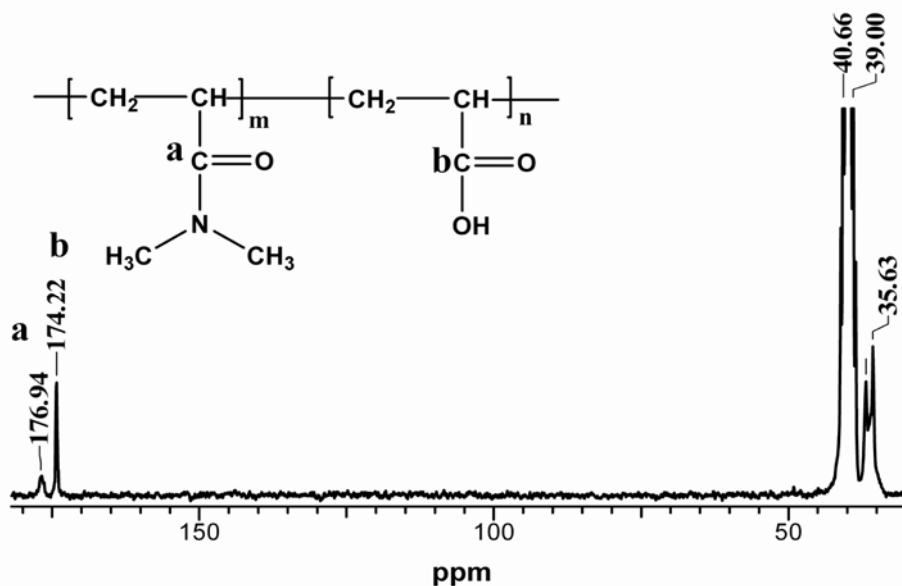


Figure 5.1. ^{13}C NMR spectrum of poly(*N, N'*-dimethyl acryl amide-co-Acrylic acid); 70:30

In the hydrophobic modification the incorporation of 3-PDCA on to the precursor polymer backbone was confirmed from ^1H NMR spectroscopy. In **Figure 5.2**, ^1H NMR spectra of hydrophobically modified poly(DMA-co-AA) with three different contents of 3-PDCA (1, 2, and 3 mol %) are shown and compared with ^1H NMR spectrum of the precursor polymer. The terminal $-\text{CH}_3$ attached to 3-PDCA group appeared at 0.82 ppm. Methylene ($-\text{CH}_2$) and methine ($-\text{CH}$) protons of 3-PDCA and $-\text{CH}$ of polymer backbone appeared at 1.21 ppm. The $-\text{CH}_2$ of the polymer backbone appeared at 1.53 ppm and $-\text{CH}_3$ protons of $-\text{N}-\text{CH}_3$ group appeared at 2.77 ppm (**Figure 5.2**). This gives a clear evidence for the incorporation of 3-PDCA into the copolymer.

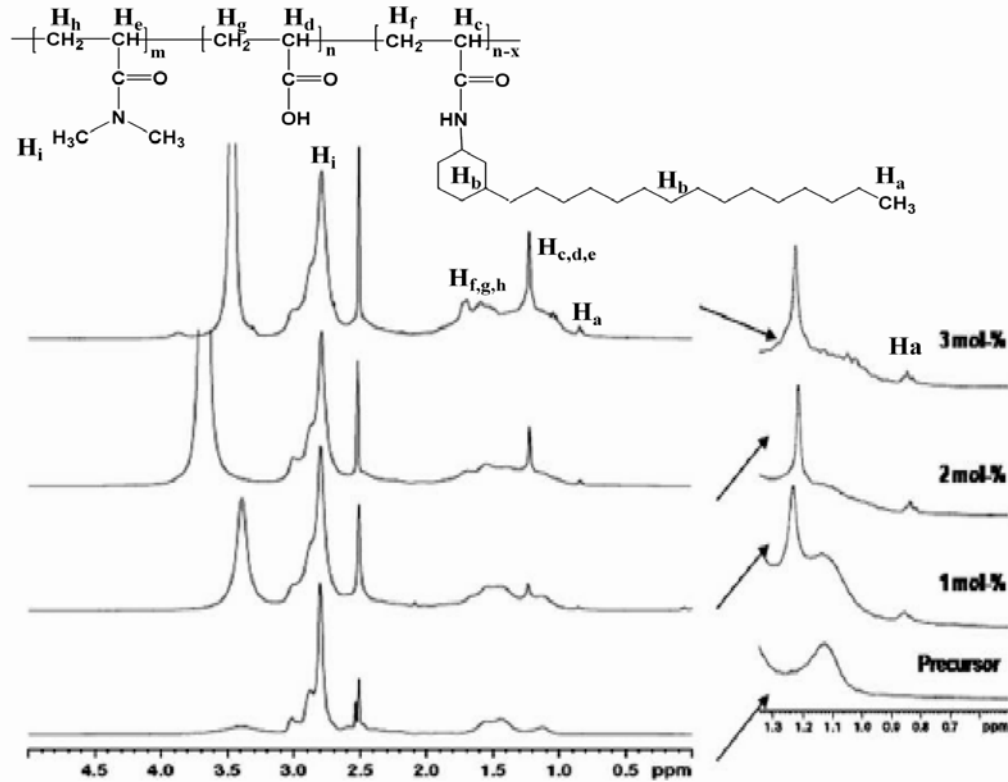


Figure 5.2. ^1H NMR spectra of Hydrophobically modified poly(*N, N'*-dimethyl acrylamide-co-Acrylic acid); 70:30 with different contents of 3-PDCA (1, 2, 3 mol%)

5.7.4 Rheology:

5.7.4.1 Concentration Dependence of Zero Shear Viscosity(η_0):

Concentration dependence of η_0 for the precursor copolymer and for the hydrophobically modified copolymer containing 1, 2, and 3 mol % of 3-PDCA is shown in **Figure 5.3**. For the precursor copolymer, the concentration range investigated in the present study was likely to be above the critical overlap concentration of the polymer, C^* .²⁷ The data in **Figure 5.3** show that the viscosity scaled with concentration as $\eta_0 \sim C_p^{0.7}$. The value of the exponent was in between that predicted by the Fuoss law (0.5) and that of dilute solution (1.0), indicating that the copolymer was a flexible polyelectrolyte which most likely exists in a semi-dilute unentangled state in this concentration range. For the hydrophobically modified polymers, two regimes of $\eta_0 - C_p$ relations were observed. In the low C_p regime, the viscosity scaled with concentration as

$\eta_0 \sim C_p^{0.5}$ following the Fuoss law. In this regime, the viscosity of all hydrophobically modified copolymers was lower than that of the precursor copolymer at identical concentrations. Further, the viscosity decreased with increase in hydrophobic content of the polymer. This lowering of viscosity of the hydrophobically modified copolymer relative to the precursor at low C_p values, can be attributed to the shrinkage of coils due to intra molecular hydrophobic associations. However, upon increase in concentration, the hydrophobically modified polymers showed sharp increase in viscosity above some critical aggregation concentration and surpassed the viscosity of the precursor. The concentration dependence was found to be $\eta_0 \sim C_p^x$, where the exponents were $x = 5.5 - 6.0$. Such a rapid increase in viscosity is due to the transformation of intra-molecular hydrophobic associations (within isolated chains) into intermolecular hydrophobic associations (with overlapping chains) thereby forming aggregates which eventually percolate to form self-supporting gels with further increase in concentration.

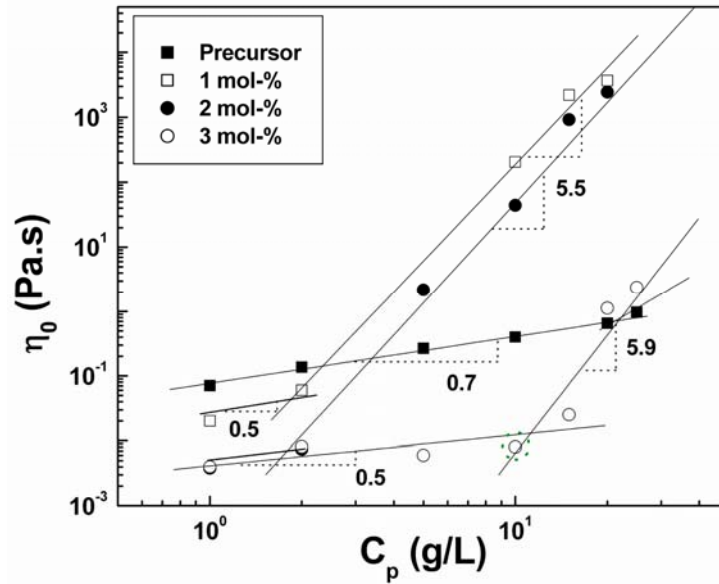


Figure 5.3. Zero shear viscosity (η_0) vs. polymer concentration for precursor and hydrophobically modified poly(*N, N'*-dimethylacrylamide-co-acrylic acid) (3-PDCA = 1, 2, and 3 mol %, $T = 25^\circ\text{C}$)

5.7.4.2 Steady shear experiment:

Viscosity vs. shear rate data for various solutions of hydrophobically modified poly(N, N'-dimethylacrylamide-co-acrylic acid) containing 3 mol % of 3-PDCA at C_p ranging from 5 - 35 g/L is shown in **Figure 5.4**. This data was obtained using a strain-controlled rheometer (ARES). Among the range of concentrations studied, the solution of $C_p = 5$ g/L showed a nearly Newtonian viscosity over the entire shear rate range ($\dot{\gamma} = 10 - 1000 \text{ s}^{-1}$). Samples of higher concentrations, $C_p = 10$ g/L and above, also showed a Newtonian behavior at low shear rates, but this was followed by an abrupt shear thickening behavior of significant magnitude at critical shear rates ($\dot{\gamma}_{crit}$) which decreased with increasing C_p (**Figure 5.4**). The magnitude of shear thickening also decreased with increasing polymer concentration. These results are in qualitative agreement with those reported in the earlier work.^{23, 24}

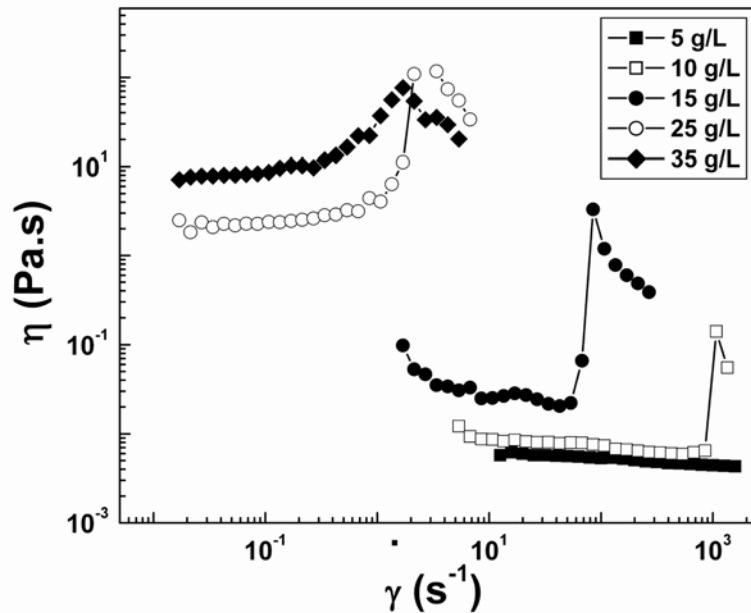


Figure 5.4. Plot of viscosity vs. shear rate for 70DMA/27AA/3-PDCA-3 ($C_p = 5, 10, 15, 25,$ and 35 g/L)

The visual image of shear thickening in sample 70DMA/27AA/3-PDCA-3 upon shaking the glass bottle is shown in **Figure 5.5**.

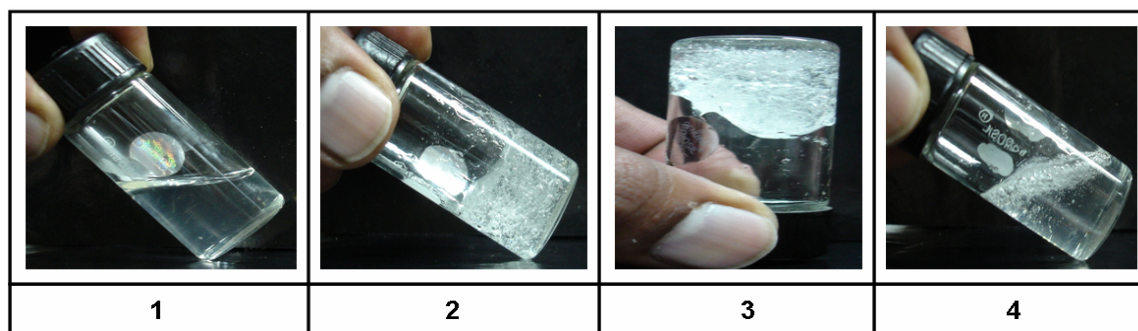


Figure 5.5. Shear thickening behavior (1, 4 sample at rest; 2, 3 sample after shaking)

The phenomenon being reversible the shear thickened gel comes back to liquid state upon cessation of the shear.

These observations can be attributed to the fact that at high polymer concentration there already exist a larger number of intermolecular hydrophobic associations even at near quiescent state so that imposition of shear causes a further small increase in the fraction of bridging chains. Also, since the zero shear viscosity of the samples is high (**Figure 5.3**), the chains have longer relaxation times and therefore, it is easier to stretch them. Hence, the critical shear rate required for further gelation decreases with C_p .

To gain more insights into the abrupt shear thickening phenomenon, the rheological data for 70DMA/27AA/ 3-PDCA-3 polymer is analyzed. In this polymer, the hydrophobic groups are randomly arranged onto the polymer. The number of hydrophobes per chain is estimated to be approximately $R = 124$. In the quiescent state since the viscosity of this sample is much less than that of the precursor polymer, it is reasonable to expect that most of the hydrophobes are micellized within a single chain, i.e., they form intra-chain associations. It has been suggested that hydrophobes containing linear alkyl chains show an aggregate number of 40 hydrophobes per micelle.²⁶ Assuming that this is an approximately correct representation for this polymer with an estimate that there are on an average three micelles per chain. **Figure 5.4** represents the first important result of this work where it provides an unambiguous support for the argument that shear thickening occurs at a critical shear rate which for the sample studied

here was $\dot{\gamma}_{crit} = 800 - 1100 \text{ s}^{-1}$. This suggests that the onset of thickening requires a critical Weissenberg number. Weissenberg number (the dimensionless number) is used to define viscoelasticity of the material which is the product of shear rate and relaxation time of the material $Wi_{crit} = \dot{\gamma}_{crit} \tau$, τ being a characteristic relaxation time of the viscous solution at low shear rates. From small-amplitude oscillatory measurements on this sample it appears that the relaxation time of the solution was less than 0.01 s. It is therefore possible that $Wi_{crit} \geq 1$. As the Weissenberg number reaches a critical value, chains that dissociate from the intra-chain micelles by thermal fluctuations or are pulled out by the imposed shear would stretch out. The free hydrophobes on these chains would then have to quickly find other hydrophobes and since the probability of finding such hydrophobes from other chains is finite in a semi-dilute solution, intra-chain associations might form. These would act as transient cross-links that link bridging chains into a percolating network, resulting in gelation. At this point it is important to look at the physics of coil-to stretch transitions of single flexible polymer chains undergoing shear. In particular, it is worth noting that the results reported by Smith et. al.³⁰ on fluorescent labeled lambda bacteriophage DNA in shear flow do not support the existence of a critical Weissenberg number for the coil to stretch transition. Rather, the time and ensemble average fractional extension of chains increases gradually with Weissenberg number. Observations of several chains at $Wi \gg 1$ showed that only a fraction of the chains are occasionally fully stretched by the flow. However, the frequency of fluctuations in chain extension increases with Weissenberg number. It is reasonable to assume that the high molecular weight hydrophobically modified polymers studied here follow qualitatively the observations made for DNA chains. This implies that the critical Weissenberg number observed for shear-induced gelation is likely to be related to a percolation effect in which a few chains stretch to sufficient extension to cause a percolated network of interconnected inter-chain clusters.

5.7.4.3 Stress ramp experiment:

To study the nature of shear thickened samples, the stress ramp experiments were carried out on a representative sample, 70DMA/27AA/3-PDCA-3; $C_p = 10 \text{ g/L}$. This C_p

of the sample is close to the aggregation concentration and as seen from **Figure 5.6**, an abrupt shear thickening effect was observed at a critical shear rate of $\sim 1000 \text{ s}^{-1}$. At lower shear rate the solution showed a viscosity $\eta = 0.01 \text{ Pa}\cdot\text{s}$ which was nearly independent of shear rate. The small amplitude oscillatory shear data on this solution showed predominantly the viscous behavior.

Results of stress-ramp experiments are shown in **Figure 5.6**. Data is shown from three independent tests in which the shear stress was ramped up from 1 to 60 Pa. At low stresses the sample showed a Newtonian response with a viscosity of $0.01 \text{ Pa}\cdot\text{s}$ (same as that obtained in the steady shear test performed on the strain-controlled rheometer, **Figure 5.4**). Abrupt shear thickening was observed for this sample at a critical shear stress of $\sigma_{crit} \sim 10 \text{ Pa}$ and at a corresponding critical shear rate of $\dot{\gamma}_{crit} \sim 800 \text{ s}^{-1}$. Data obtained from more additional tests on this sample showed that σ_{crit} and $\dot{\gamma}_{crit}$ varied slightly between tests; for this particular sample, σ_{crit} varied between 8 and 10 Pa and $\dot{\gamma}_{crit}$ varied between 800 and 1100 s^{-1} . During all repeated tests the viscosity increased by as much as 5 orders of magnitude at the critical point, indicating the large magnitude of shear thickening effect. As expected, the shear rate dropped considerably upon shear thickening above σ_{crit} since only a small value of shear was required for the thickened sample to maintain the applied stress level. This minimized the rupture or extrusion of the thickened sample from the geometry underlining the utility of performing stress ramp experiments.

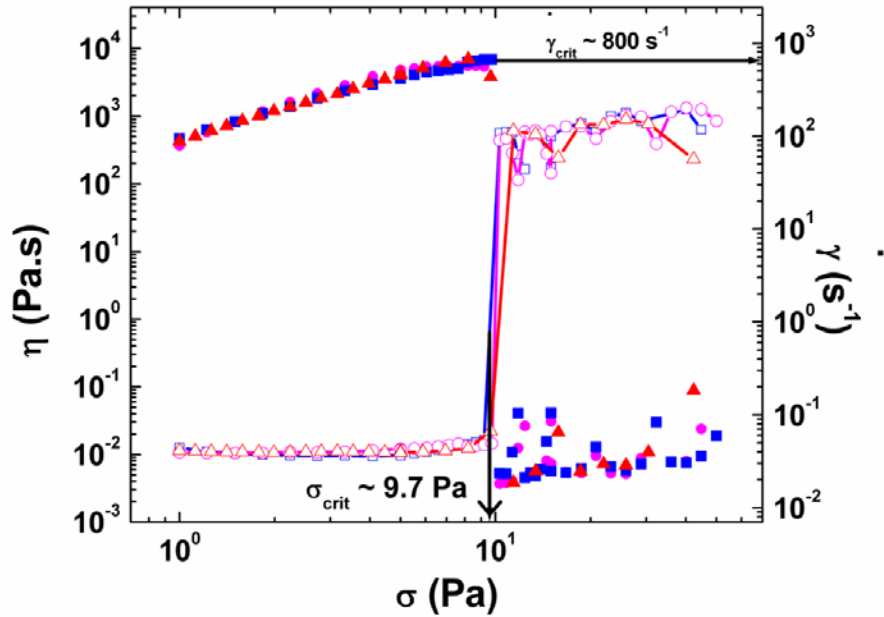


Figure 5.6. Stress-ramp experiment of 70DMA/27AA/ 3-PDCA-3; $C_p = 10 \text{ g/L}$

5.7.4.4 Creep experiments at different stresses:

Figure 5.7 shows the evolution of creep compliance on application of various stresses. At stresses below the critical stress $\sigma < \sigma_{crit}$ such as, $\sigma = 5 \text{ Pa}$ the compliance grew continuously with time following the power law, $J(t) \sim t^2$ at early time followed by a more gradual increase at long time. The early time response indicates inertia controlled regime where the compliance approximately grows as,

$$J(t) = \left(\frac{b}{2I} \right) t^2 \text{ ----- (5.1)}$$

Where,

b = geometrical parameter, I = inertia of the measuring system.³¹

The continuous increase in compliance at long time reflects a typical viscous flow response of the solution. At stresses close to or above the critical stress, ($\sigma \approx \sigma_{crit}, \sigma > \sigma_{crit}, \sigma = 8, 10, 15, \text{ and } 25 \text{ Pa}$), the compliance initially grew as $J(t) \sim t^2$ independent of the applied stress and then abruptly reached plateau values, which decreased with increase in the applied stress. The occurrence of a compliance

plateau is a clear indication of shear-induced gelation. Thus, the observed shear thickening effect is in fact a shear-induced gelation event, as also pointed out recently by Wang et al.²⁶ A decrease in the plateau value of compliance implies an increase in the modulus of the gel.

5.7.4.5 Gelation time & the applied stress:

The time required for gelation (t_{crit}) decreased with increase in applied stress. To understand this, the temporal evolution of shear rate in each of the creep experiments is also plotted in **Figure 5.7**. It can be seen that gelation was observed as soon as the shear rates reached values approximately equal to $\dot{\gamma}_{crit}$. The time to reach the critical shear rate was found to be inversely proportional to the shear stress,

$$t_{crit} \propto 1/\sigma \text{ ----- (5.2)}$$

This happens because in the initial inertia-controlled regime the strain grows as,

$$\gamma = (\sigma b/2I) t^2 \text{ ----- (5.3)}$$

So that,

$$t_{crit} = \left(I \dot{\gamma}_{crit} / b \sigma \right) \text{ ----- (5.4)}$$

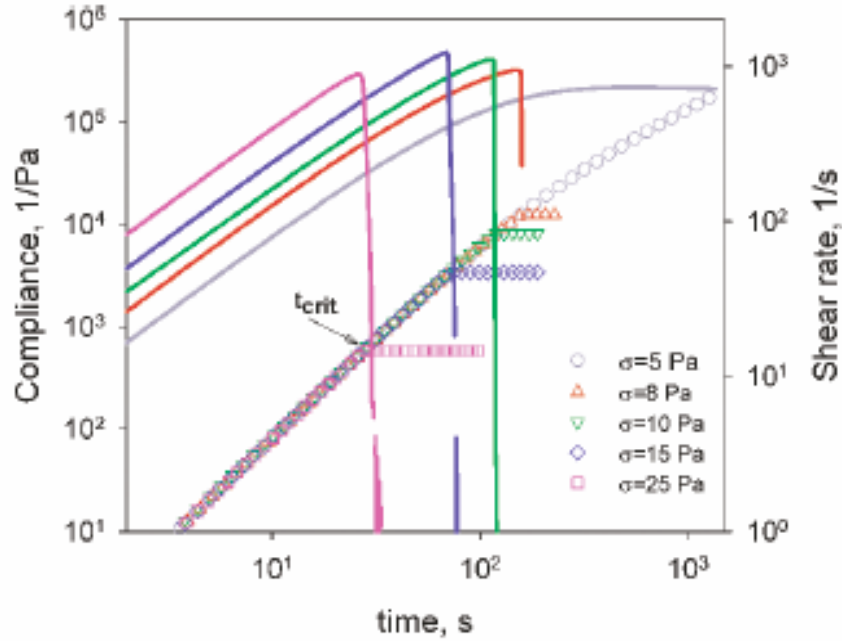


Figure 5.7. Evolution of creep compliance at various stress values for the sample 70DMA/27AA/3-PDCA-3; $C_p = 10 \text{ g/L}$

Data in **Figure 5.7** unambiguously show that the shear induced gelation event always occurs at a critical shear rate. Consequently, the creep experiments enable precise control on the formation of shear-induced gels of different moduli. Such a control is not possible in a step shear experiment since the large imposed strain ruptures the soft gels upon formation.

5.7.4.6 Stability of shear induced gels:

The stability of shear-induced gels was studied by performing sequential creep experiments in which the gels were first formed by applying a stress $\sigma > \sigma_{crit}$ and then subjected to a lower stress $\sigma < \sigma_{crit}$. The compliance data from a typical experiment is shown in **Figure 5.8**. Here the sample was first subjected to a shear stress of 25 Pa until gelation occurred and then to a shear stress of 0.5 Pa for a long time. Upon lowering the stress to 0.5 Pa the compliance showed damped oscillations at short time ($t < t_{ringing}$) followed by a gradual increase at long time ($t < t_{ringing} < \tau_L$). The damped oscillatory

response, also called as creep ringing, occurs because of the coupling between the elasticity of the gel and the inertia of the rheometer.³¹

By fitting the creep ringing data to the Jeffery model, the values of three material parameters: the gel modulus, relaxation time, and retardation time were deduced which described the viscoelasticity of the gel. For the 0.5 Pa creep data shown in **Figure 5.8** these values are reported in **Table 5.2**.

Table 5.2. Values of stress, gel modulus, relaxation time and retardation time calculated from creep recovery data

Stress (σ , Pa)	0.5
Gel modulus (G, Pa)	2.5
Relaxation time (τ_L s)	0.4
Retardation time (τ_g s)	14.5

Two interesting observations were made from **Figure 5.8**, first, the compliance of the gel at $\sigma = 0.5$ Pa was lower than the compliance of the gel at $\sigma = 25$ Pa, implying that the gel formed at the higher stress of 25 Pa had a lower modulus (0.012 Pa) compared to the one that it transformed into (of modulus 2.5 Pa) upon lowering the stress to 0.5 Pa. Consequently, the stability of the gel formed at stresses $\sigma > \sigma_{crit}$ cannot be probed at lower stresses because the shear-induced gel itself transforms into a different state upon lowering the stress.

In previous work the relaxation of shear-thickened solutions was studied by performing small-amplitude oscillatory shear measurements in a time sweep mode and measuring the decrease of dynamic moduli with time.²⁴ The storage modulus was observed to follow a stretched exponential relaxation. In the light of the results shown in **Figure 5.8** it is evident that the relaxation event should not be viewed as the relaxation of a gel formed at the high shear conditions, but rather as the relaxation of a different gel

that is formed when the shear-thickened sample is suddenly subjected to low-shear conditions.

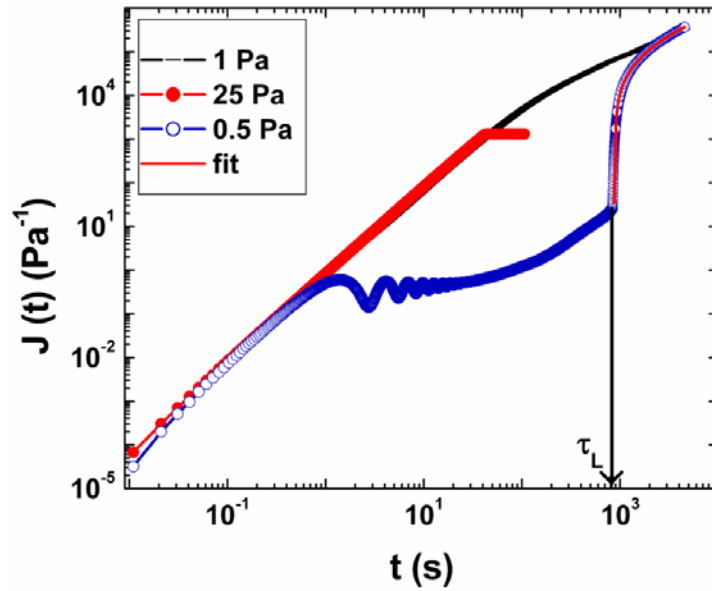


Figure 5.8. Compliance of the gel at 0.5 Pa after shear-induced gelation at 25 Pa. The recovery of compliance to the equilibrium liquids state starts at a critical time τ_L and follows eq 5.1

The second interesting observation from **Figure 5.8** is that there happens to be a critical “liquefaction” time τ_L at which the gel rapidly starts relaxing back to its equilibrium liquid state under quiescent conditions. The increase in compliance during the relaxation process can be described by,

$$J(t) = J_L + J_1 \left[1 - \exp\left(\frac{t - \tau_L}{\tau_g}\right)^\alpha \right] \text{----- (5.5)}$$

J_L is the compliance at τ_L , τ_g is a characteristic retardation time of the gel and J_1 and α are constants. For the data shown in **Figure 5.8** the variables J_L , J_1 , τ_L and τ_g have values of 28.3 Pa^{-1} , $4 \times 10^5 \text{ Pa}^{-1}$, 836 s, and 2000 s, respectively. The value of α was observed to be 1.5, indicating a compressed exponential behavior for the liquefaction

process. At long time the compliance of the sample asymptotically reached that of the equilibrium liquid state at $\sigma < \sigma_{crit}$.

The liquefaction (or gel to sol) transition was further investigated by subjecting the gel formed at a high stress $\sigma > \sigma_{crit}$ to different stress levels below the critical stress. Representative data is shown in **Figure 5.9**. In this experiment the solution was first subjected to a stress of 5 Pa which was below the critical stress. Next, gelation was induced by shearing the solution at a stress of 10 Pa, which is close to the critical stress. In separate experiments the gel was then allowed to recover at different stresses of 1, 2, 3, 5, and 7 Pa, which are all below the critical stress. In each experiment the sample was allowed to recover fully. It was assumed that recovery was complete when the compliance asymptotically reached the 5 Pa data. The next experiment was then performed on the same sample by first shearing it at 10 Pa and then allowing it to recover at the next value of stress.

The data in **Figure 5.9a** show that the short time compliance of the gel (damped oscillatory response) and hence the modulus of the gel formed at 1, 2, 3, 5, or 7 Pa are independent of the applied stress to within an experimental error. However, the critical time (τ_L) at which liquefaction starts and the value of the compliance at that time (J_L) decreased with increase in stress. It was found that J_L varied inversely with the applied stress so that when the same data were plotted as strain versus time (**Figure 5.9b**), the liquefaction of the gel was found to start when a critical strain, independent of the probe stress, was reached. For the particular sample shown in **Figure 5.9**, the critical strain is 1000-%. The liquefaction time τ_L showed a power law decrease with stress, $\tau_L \sim \sigma^{-0.33}$, as shown in **Figure 5.9d**.

This can be explained as follows: The long time Newtonian creep response of the viscoelastic gel is given as,

$$\gamma = t\sigma/\eta \text{ ----- (5.6)}$$

Where, G = modulus and η = viscosity, of the gel.

As mentioned earlier, the modulus G is independent of the applied stress. However, a careful inspection of the data in **Figure 5.9b** shows that the viscosity of the gel increased with the applied stress, $\eta \propto \sigma^{0.67}$ as shown in **Figure 5.9c**. Substitution of this in the equation for strain explains the observed power law for the stress dependence of the critical liquefaction time.

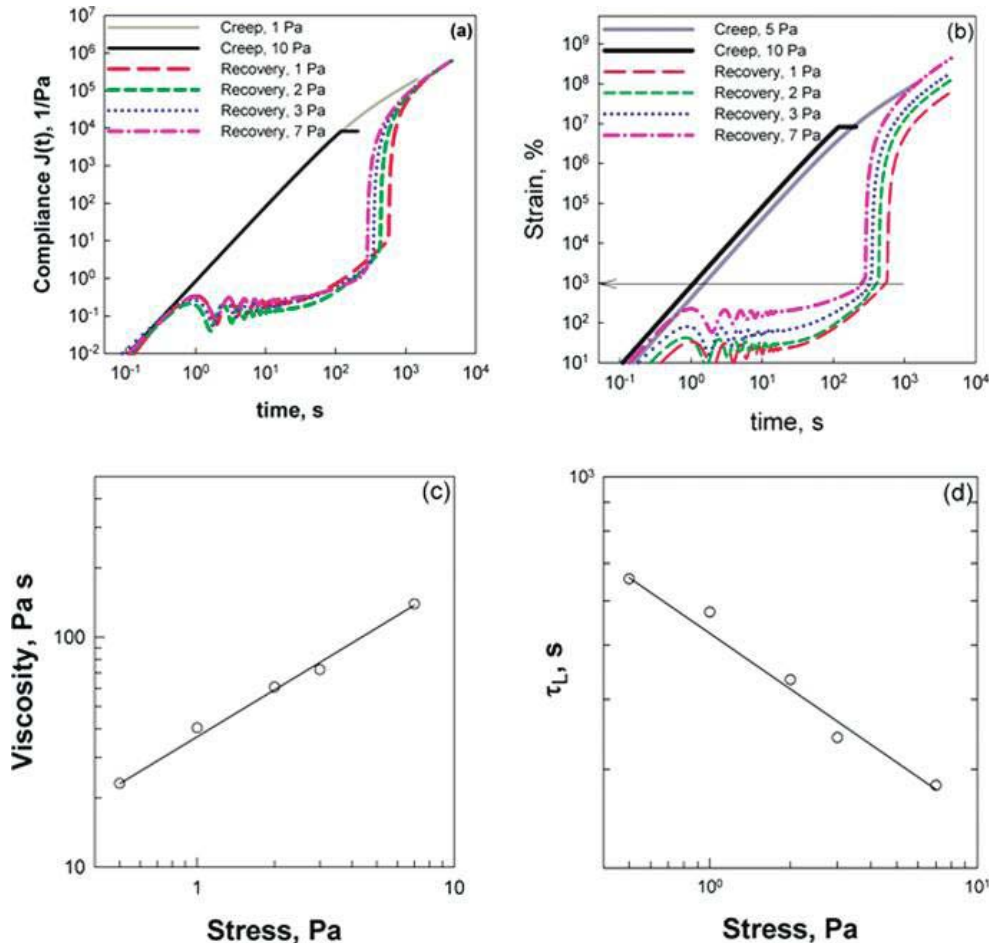


Figure 5.9. Gel to solution transition of a shear-induced gel at various stresses below the critical stress. The modulus of the gel is independent of stress (a), but its viscosity shows a power law dependence on stress (b). The liquefaction happens at a constant critical strain (c), and the critical time for liquefaction decreases with stress (d)

5.7.4.7 Elastically active chains:

The number density of elastically active chains estimated from the plateau compliance values, J_0 , for the different stresses $\sigma > \sigma_{crit}$ shown in **Figure 5.10** are much smaller than the limiting number of elastically active chains suggested by the chemical modification. The number density of elastically active chains at a given imposed stress can be calculated as,

$$\nu = 1/(J_0 kT) \text{ ----- (5.7)}$$

While the theoretical limit of the number density of elastically active chains, assuming that all hydrophobes of a given chain are involved only in inter-chain associations, is given as,

$$\nu_{max} = (\alpha - 1) - C_p N_A / M_w \text{ ----- (5.8)}$$

Where, N_A is the Avogadro's number. **Table 5.3** shows the fraction of elastically active chains created at the different imposed stresses shown in **Figure 5.9**. From these numbers it is clear that shear-induced gelation involves only a small fraction of the maximum available number of elastically active bridging chains. It is interesting to note that ν/ν_{max} increases with stress although gelation happens at nearly the same shear rate $\dot{\gamma} = \dot{\gamma}_{crit}$. This suggests that the fraction of chains that stretch and form elastically active strands seems to increase with the rate of increase of shear rate, which increases with the imposed stress. In other words, at any point of time during the experiment a higher value of imposed stress implies a higher shear rate and consequently a greater fraction of chains that get stretched to form a gel with a higher fraction of elastically active bridging chains.

The above discussion suggests that theoretical models for abrupt shear thickening phenomenon must include the dynamics of shear-induced stretching of chains as well as percolation effects. The second important result of this work is shown in **Figure 5.9**. An intriguing feature of this data is that upon reduction of the imposed shear stress immediately after the shear-induced gelation event the modulus of the gel increases by

several orders of magnitude. None of the existing models for shear thickening can explain this observation. If interpreted in terms of the fraction of elastically active chains, the value of ν/ν_{\max} increases by as much as 3 orders of magnitude upon reduction in stress relative to the modulus of the shear induced gel formed at a high stress (**Table 5.3**).

Table 5.3. Fraction of Elastically Active Chains in Shear-Induced Gels

Stress (Pa)	J_0 (1/Pa)	ν/ν_{\max}
8	12 500	3×10^{-8}
10	8110	5×10^{-8}
15	3410	1×10^{-7}
25	585	7×10^{-7}
a	~ 0.3	1×10^{-3}

However, ν/ν_{\max} is still ≤ 1 . One possible explanation of this phenomenon is shown schematically in **Figure 5.10**.

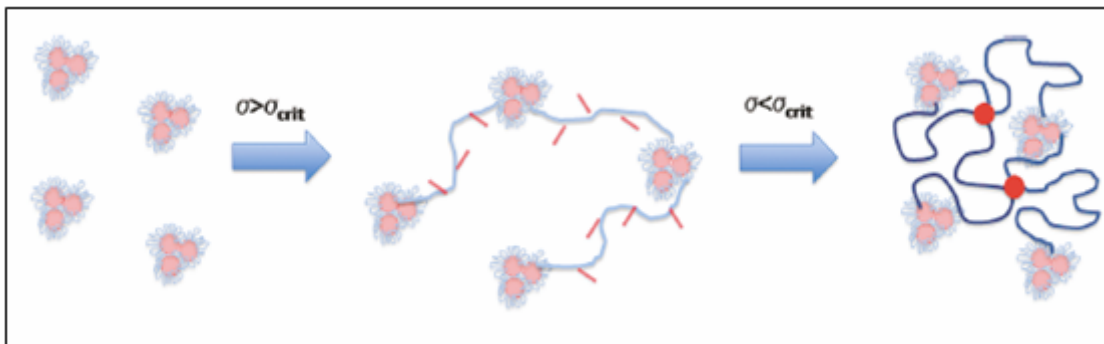


Figure 5.10. Stress induced change from intra-chain hydrophobic interactions to inter-chain hydrophobic interactions for shear thickening polymers

Upon imposition of a high stress $\sigma > \sigma_{\text{crit}}$ a few chains stretch to large enough extension so that a few hydrophobic groups on these chains find hydrophobic groups on other chains to form a gel, whereas a large number of hydrophobic groups on these

stretched chains remain unassociated. Immediately upon reduction of stress to $\sigma < \sigma_{crit}$ the stretched chains undergo affine retraction, and since the hydrophobic groups are as yet unassociated, the chains attain a size that is larger than the equilibrium size of the coil which has intra-chain associations. This causes the dangling groups to form new associations with those of the neighboring chains, thereby increasing the number density of bridging chains. Many repeat experiments were also performed (data not shown) in which shear-induced gels were formed at different values of stresses $\sigma > \sigma_{crit}$ after which the stress was reduced to a fixed value $\sigma < \sigma_{crit}$. It was observed from these experiments that the compliance of the gel formed immediately upon reduction of stress was independent of the value of the high stress at which the gel was formed. This suggests that while the number of bridging chains increases with stress, a much larger number of hydrophobic groups on these stretched chains remain unassociated at the high stresses. A large fraction of these groups associate during retraction of the chains upon reduction of stress, thereby forming gels whose modulus is independent of the initial state of stress. Similarly, the data shown in **Figure 5.8** suggest that the compliance of the gel formed immediately upon reduction of stress is also independent of the value of stress $\sigma < \sigma_{crit}$.

Another interesting observation from **Figure 5.8** is that there appears to be a critical time τ_L at which the gel starts to liquefy rapidly and ultimately reaches the original solution state. The liquefaction of the gel underlines its meta-stable nature. The mechanism suggested in **Figure 5.8** relates the metastability to the existence of coils having size larger than the equilibrium size of the chains. Eventually, the inter-chain associations break by thermal fluctuations and/or the imposed probe stress, causing the coils to reach their equilibrium state. For $t_{ringing} < t < \tau_L$ the average compliance of the gel shows a gradual increase; indeed, the inverse of the slope of this part of the data gives the viscosity of the gel. From a molecular perspective the gel slowly creeps because of breakage of some of the inter-chain associations. Data in **Figure 5.9** show that the viscosity of the gel increases with the applied stress $\sigma < \sigma_{crit}$. The small amount of

thickening is possibly caused by shear-induced reformation of inter-chain associations. Eventually the gel seems to liquefy rapidly when the strain reaches some critical value. Higher imposed stress causes the gel to reach this value earlier so that τ_L decreases with imposed stress. A probable molecular interpretation could be that the tension in strongly held bridging chains reaches a critical point at the critical strain, causing rapid breakage of the inter-chain associations.

5.8 Conclusions:

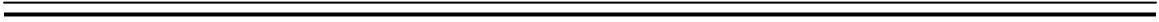
High molecular weight hydrophobically modified poly(DMA-co-AA) copolymers were synthesized using 3-PDCA as a hydrophobe. The solution properties were investigated by rheology. By performing creep experiments on a stress-controlled rheometer, several new attributes of the shear thickening phenomenon and the subsequent relaxation process are reported. In particular, it has been shown that, shear-induced thickening is a gelation process that happens at a critical shear rate and that it is possible to trap the gel in different meta-stable states by imposing different stresses above the critical stress. Furthermore, the linear rheological properties of such shear induced gels cannot be studied by dropping the probe stress values to small levels because the process of doing so itself changes the state of the gel. Remarkably, reducing the stress after gelation in fact results in the formation of stiffer gels. The modulus of the gels so formed is, to a large extent, independent of the stress level at which gelation happened as also the stress level at which recovery was probed after gelation. It is suggested that, the shear-thickened gels are formed when only a few chains are stretched sufficiently at the critical shear rate to enable inter-chain associations of a few hydrophobic groups on these chains. Percolation of these stretched bridging chains causes gelation, but many hydrophobic groups on them remain unassociated. Further stiffening of the shear-thickened gels upon reduction of stress occurs when the bridging chains retract and attain coil size larger than the equilibrium size so that the unassociated hydrophobic groups form further inter-chain associations. Finally, it was demonstrated that, liquefaction of the gels occurs at a critical time, when a critical strain is reached. The present models to explain the shear-thickening phenomenon do not explain any of these observations satisfactorily. Further experimental

investigations in stress-controlled rheometry as well as renewed modeling efforts are necessary to understand the experimental observations presented here.

References:

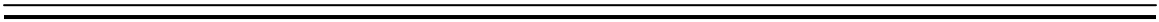
1. Broze, G.; Jerome, R.; Teyssie, P.; Marco, C. *Macromolecules* **1983**, *16*, 996.
2. Ma, S. X.; Cooper, S. L. *Macromolecules* **2001**, *34*, 3294.
3. Egmond von, J. W. *Curr. Opin. Colloid Interface Sci.* **1998**, *3*, 385.
4. Barnes, H. A. *J. Rheol.* **1989**, *33*, 329.
5. Wagner, N. J.; Brady, J. F. *Phys. Today* **2009**, *10*, 27.
6. Tanaka, F.; Edwards, S. F. *J. Non-Newtonian Fluid Mech.* **1992**, *43*, 247.
7. Tanaka, F.; Edwards, S. F. *J. Non-Newtonian Fluid Mech.* **1992**, *43*, 273.
8. Tanaka, F.; Edwards, S. F. *J. Non-Newtonian Fluid Mech.* **1992**, *43*, 289.
9. Tanaka, F.; Edwards, S. F. *Macromolecules* **1992**, *25*, 1516.
10. Green, M. S.; Tobolsky, A. V. *J. Chem. Phys.* **1946**, *14*, 80.
11. Witten, T. A.; Cohen, M. H. *Macromolecules* **1985**, *18*, 1915.
12. Ballard, M. J.; Buscall, R.; Waite, F. A. *Polymer* **1988**, *29*, 1287.
13. Wang, S. Q. *Macromolecules* **1992**, *25*, 7003.
14. Marrucci, G.; Bhargava, S.; Cooper, S. L. *Macromolecules* **1993**, *26*, 6483.
15. Vrahopoulou, E. P.; McHugh, A. J. *J. Rheol.* **1987**, *31*, 371.
16. Vandenbrule, B. H. A. A.; Hoogerbrugge, P. J. *J. Non-Newtonian Fluid Mech.* **1995**, *60*, 303.
17. Vaccaro, A.; Marrucci, G. *J. Non-Newtonian Fluid Mech.* **2000**, *92*, 261.
18. Ahn, K. H.; Osaki, K. *J. Non-Newtonian Fluid Mech.* **1995**, *56*, 267.
19. Lele, A. K.; Mashelkar, R. A. *J. Non-Newtonian Fluid Mech.* **1998**, *75*, 99.
20. Tripathi, A.; Tam, K. C.; McKinley, G. H. *Macromolecules* **2006**, *39*, 1981.
21. Peiffer, D. G.; Lundberg, R. D.; Duvdevani, A. *Polymer* **1986**, *27*, 1453.
22. Dupuis, D.; Lewandowski, F. Y.; Steiert, P.; Wolff, C. *J. Non-Newtonian Fluid Mech.* **1994**, *54*, 11.
23. Bokias, G.; Hourdet, D.; Iliopoulos, I. *Macromolecules* **2000**, *33*, 2929.
24. Cadix, A.; Chasseneux, C.; Lafuma, F.; Lequeux, F. *Macromolecules* **2005**, *38*, 527.
25. Rubinstein, M.; Semenov, A. *Macromolecules* **2001**, *34*, 1058.
26. Wang, J.; Benyahya, L.; Chassenieux, C.; Tassin, J. F.; Nicolai, T. *Polymer* **2010**, *51*, 1964.

27. Shedge, A. S.; Lele, A. K.; Wadgaonkar, P. P.; Hourdet, D.; Perrin, P.; Chassenieux, C.; Badiger, M. V. *Macromol. Chem. Phys.* **2005**, *206*, 464.
28. Tanford, C. *Hydrophobic Effect: Formation of Micelles and Biological Membranes*, 2nd Ed.; John Wiley and Sons Inc.: New York, **1980**.
29. The overlap concentration for aqueous solutions of nonionic polyacrylamide of molecular weight similar to that of the precursor Polymer (≈ 1200 kg/mol) is known to be about 0.8 g/L (Grigorescu, G.; Kulicke, W.-M. *Adv. Polym. Sci.* **2000**, *152*, 1). Therefore, it is likely that the C* for precursor polymer is of the same order or magnitude.
30. Smith, D. E.; Babcock, H. P.; Chu, S. *Science* **1999**, *283*, 1724.
31. Ewoldt, R. H.; McKinley, G. H. *Rheol. Bull.* **2007**, *76*, 4.



Chapter-VI

**Hydrophobically Modified Chitosan: Synthesis, Characterization
and Rheology**



6.1 Introduction:

Amongst the HMPs, hydrophobically modified polysaccharides are attracting increasing attention latterly.¹⁻² They exhibit unique rheological properties. The main micro structural characterization of such polymeric systems is their ability to give use to weak intra and intermolecular interactions in aqueous solutions. The linear and non-linear rheological behavior of such associating systems is expected to be complex and depends on the nature, concentration and distribution of hydrophobic groups in the polymer chain. Studies on some of the hydrophobically modified polysaccharides such as hydrophobically modified ethyl hydroxy ethyl cellulose (HMEHEC) and hydroxy propyl guar gum (HMHPG) have been reported.³⁻⁴

Polysaccharides are available in variety of structures with different properties. Since they contain reactive functional groups, they can be easily modified chemically. Furthermore, their high stability, non-toxicity and biodegradability with gel forming property, lead their applications in food and pharmaceuticals. The commercial production of polysaccharides has expanded steadily over the last 20-30 years. Therefore, there is a great scope for these environmentally friendly renewable resource materials in their practical applications.

The polysaccharide, chitosan is a linear cationic biopolymer obtained from N-deacetylation of chitin, which is the second most abundant natural polymer next to cellulose. Chitosan is a random copolymer containing (1 → 4) linked 2-acetamido-2-deoxy-β-D-glucopyranose and 2-amino-2-deoxy-β-D-glucopyranose. The chemical structure of chitosan is shown in **Figure 6.1**.

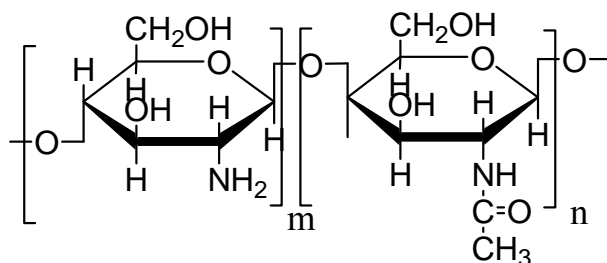


Figure 6.1. Chemical structure of chitosan

Chitosan is water-soluble in acidic pH and exhibit polyelectrolyte behavior due to the presence of protonated amino groups at low pH. The physico-chemical properties of aqueous solutions of chitosan depend on pH, ionic strength, polymer concentration, degree of deacetylation and hydrophobicity of the polymer. Large number of papers concerning the structure⁵⁻⁸ and rheology⁹⁻¹⁰ of unmodified chitosan has been reported in the literature. Attempts have also been made to hydrophobically modify chitosan using long chain alkyl (C₈-C₁₂) aldehydes.¹¹⁻¹² The phase behavior of hydrophobically modified chitosans in aqueous solutions has been investigated using light scattering and rheological experiments.¹³⁻¹⁵

In the present work, the synthesis and characterization of hydrophobically modified chitosans (HMCs) using 3-pentadecyl cyclohexane carbaldehyde (3-PDCAL), an aldehyde derived from a natural resource material (CNSL) is reported. The solution properties of HMCs were investigated using rheological and light scattering experiments. The detailed synthesis of 3-PDCAL has already been given in chapter-III.

6.2 Experimental:

6.2.1 Materials:

Chitosan (degree of deacetylation 85 %), sodium cyanoborohydride were procured from Aldrich chemicals, USA, glacial acetic acid, hydrochloric acid, isopropanol, acetone were of reagent grade and procured from Merck, India. All the chemicals were used as received.

6.2.2 Synthesis of hydrophobically modified chitosans (HMCs) using 3-pentadecyl cyclohexane carbaldehyde (3-PDCAL):

Into a 500 ml round bottom flask, chitosan (4 g, 0.0248 moles) was dissolved in 220 ml of 0.2 M aqueous acetic acid solution. Isopropanol (150 ml) was added to the above solutions in order to have solvating medium for aldehyde. The pH of the solution was adjusted to 5.1. Solution of 3-PDCAL (0.4 g, 0.0012 moles) in isopropanol, was added to the reaction mixture. After 12 h, excess of sodium cyanoborohydride (4.62 g, 0.074 moles) was added to the reaction mixture and reaction was continued for 24 h at

room temperature. pH of the solution was adjusted to 7 and polymer was precipitated in isopropanol, subsequently, washed with IPA/water mixtures with increasing IPA content from 70 % v/v to 100 % and finally with acetone. Final polymer was dried under vacuum at room temperature (3.88 g, Yield = 97 %). HMCs with different contents of 3-PDCAL (2, 3, 5 and 7 mole %) were synthesized using the above procedure. The stoichiometry of reactions is given in **Table 6.1**.

Table 6.1. *Stoichiometry of the reaction between chitosan, sodium cyanoborohydride and 3-pentadecyl cyclohexane carbaldehyde (3-PDCAL)*

Polymer	Chitosan (g)	3-PDCAL (g)	3-PDCAL (mol %)	SCBH (g)
HMC-3-PDCAL-2	4	0.15	2	4.69
HMC-3-PDCAL-3	4	0.24	3	4.69
HMC-3-PDCAL-5	4	0.40	5	4.69

6.3.3 Determination of degree of deacetylation using ¹H NMR spectroscopy:

Degree of deacetylation of chitosan was calculated from the ¹H NMR spectroscopy using the following formula reported earlier. Chitosan was dissolved in the mixture of deuterated solvent CD₃COOD + D₂O and ¹H NMR was recorded at 400 MHz frequency at 70⁰C. The degree of deacetylation was calculated using the following formula,

$$D_{deac}(\%) = \left\{ 1 - \left(\frac{1}{3} I_{CH_3} / \frac{1}{6} I_{H_2-H_6} \right) \right\} \times 100 \text{ ----- (6.1)}$$

From the above formula degree of deacetylation was calculated using the integral intensity of I_{CH₃} of acetamide group and the sum of the integral intensities of I_{H₂-H₆} of H₂, H₃, H₄, H₅, H₆, H_{6'} protons attached to C₂, C₃, C₄, C₅, C₆, C_{6'} carbons of 6 membered heterocyclic ring of chitosan. The degree of deacetylation was 83.3 %.

6.2.4 Sample Preparation:

Polymer solutions of desired concentrations (C_p , g/L) were prepared by dissolving a known amount of polymer in water with gentle stirring. All the solutions were prepared in de-ionized water. (18 Ω) The solutions were homogenized for at least 4 days before using them for measurements. For rheology and light scattering measurements, polymer solutions were prepared in 0.3 M acetic acid and 0.05 M sodium acetate. Solutions were allowed to equilibrate for 5 days before use. All the solutions were filtered through membrane filters (Millipore membrane filters: 0.2, 0.45, 1 μm) and centrifuged before use.

6.2.5 NMR spectroscopy:

^1H NMR spectra of CS and HMCs were recorded on Bruker DRX-400 NMR spectrometers operating at a proton frequency of 400 MHz. The mixture of D_2O and CD_3COOD was used as a solvent. (Concentration of polymer = 30 $\text{mg}\cdot\text{ml}^{-1}$) All the samples were homogenized for at least 5 days before recording the NMR spectra.

6.2.6 Rheology:

Viscosity of very dilute solutions was measured using an Ubbelohde viscometer. For concentrated solutions, viscosity measurements were performed using MCR-301 (Anton Paar) stress controlled rheometer with cup-and-bob geometry. In the case of concentrated gelly samples, MCR-301 with cone-and-plate geometry (cone = 25 $\text{mm}/2^\circ$, plate = 50 mm) was used. All the steady state and oscillatory experiments were performed in MCR-301 rheometer.

6.2.7 Light scattering:

Static and dynamic light scattering experiments were performed on a 3D DLS spectrometer (LS instruments) equipped with a He-Ne laser, operating at a wavelength of $\lambda = 632.8$ nm with a correlator having 256 channels. Experiments were performed at 25 $^\circ\text{C}$ unless otherwise mentioned. In the static light scattering (SLS) experiments, molecular weight (M_w), radius of gyration (R_g) and second virial coefficient (A_2) of the polymer were measured using Zimm equation. In the dynamic light scattering (DLS)

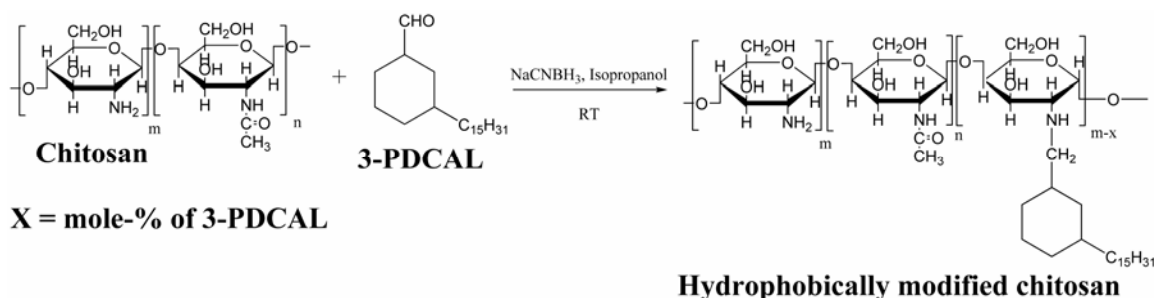
experiments, diffusion coefficient (D), hydrodynamic radius (R_H) and overlap concentration (C^*) were measured.

6.3 Results and Discussion:

6.3.1 Synthesis of Hydrophobically Modified Chitosan:

Chitosan has strong intermolecular forces and highly crystalline structure due to which it is soluble in many organic solvents. It is soluble in only aqueous acidic solutions (at $\text{pH} < 4.0$) such as acetic acid and hydrochloric acid. Chitosan has both reactive amino and hydroxyl groups which can be used for modification. Yalpani and Hall¹² have reported the modification of chitosan with sugars. Shashiwa et. al.¹⁶ have modified chitosan using different acrylic monomers. Long chain aldehyde and ketone derivatives have been used to modify chitosan and solution studies have been reported.¹⁷

In this work, the chitosan was modified with 3-PDCAL via an imine intermediate and subsequent reduction to n-alkyl derivative of chitosan using sodium cyanoborohydride. The reaction pathway is shown in **scheme 6.1**.



Scheme 6.1: Reaction pathway for the hydrophobic modification of chitosan using 3-PDCAL

Hydrophobically modified chitosan with two different contents of 3-PDCAL were prepared and denoted as HMC-3-PDCAL-2 and HMC-3-PDCAL-5 with 2 and 5 mol % of 3-PDCAL respectively. The polymers obtained were in powder form and exhibited enhanced rheological properties as compared to unmodified chitosan. These aspects are discussed in the following sections.

6.3.2 ^1H NMR spectroscopy:

^1H NMR spectra of chitosan, HMC-3-PDCAL-2 and 5 are shown in **Figure 6.2**. For chitosan, acetyl protons ($-\text{NH}-\text{CO}-\text{CH}_3$) appeared at 2 ppm. H_2 proton from the pyranose ring appeared at 3.2 ppm. H_3 , H_4 , H_5 , H_6 , H_6' protons from the pyranose ring appeared in the range of 3.7 - 3.9 ppm. H_1 proton of the pyranose ring appeared at 4.9 ppm. In case of hydrophobically modified chitosan samples, terminal $-\text{CH}_3$ protons from the side chain of the 3-PDCAL appeared at 0.8 ppm. Rest of the side chain protons and the cyclohexyl ring protons as well as the $-\text{CH}_2$ attached to the $-\text{CHO}$ group appeared in the range of 0.9 - 1.3 ppm. This confirmed the incorporation of the 3-PDCAL onto the chitosan.

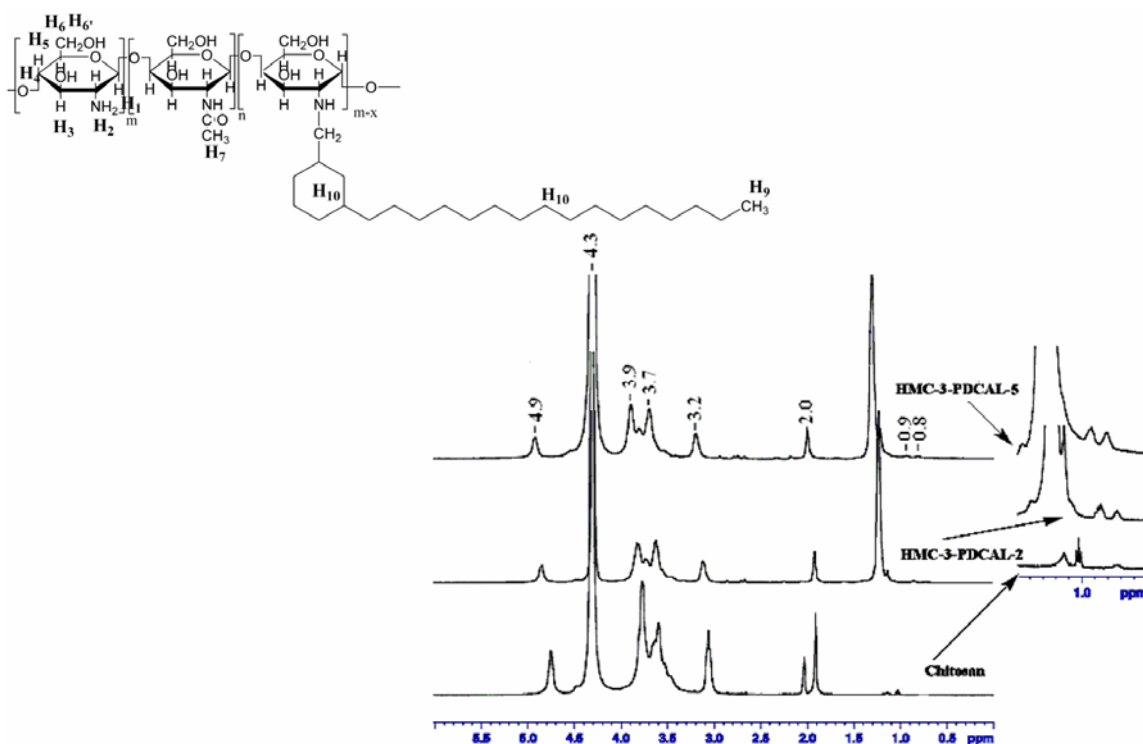


Figure 6.2. Plots of ^1H NMR of Chitosan, HMC-3-PDCAL-2, HMC-3-PDCAL-5 in D_2O + CD_3COOD

6.3.3 Rheology data:

6.3.3.1 η vs C_p :

Figure 6.3 shows the η vs C_p data for CS and HMCs in the concentration range of 0.01 – 2 wt %. It can be seen from the figure that in the semi-dilute regime ($C_p \sim 0.01$ wt), the η_{sp} of CS is higher than the η_{sp} of HMC-3-PDCAL-2 and HMC-3-PDCAL-5. This can be attributed to the fact that, at this, concentration, the polymer chains are isolated with least interactions with each other and the hydrophobically modified polymer undergo chain compaction due to the presence of hydrophobic groups. Thus, these intra-chain compaction leads to lower η_{sp} as compared to CS. However, upon increasing the concentration ($C > C^*$), the intermolecular hydrophobic associations start to play dominating role and lead to the formation of flower-like micelles. The existence of the flower-like micelles has been well established using SANS and fluorescence spectroscopy.¹⁴

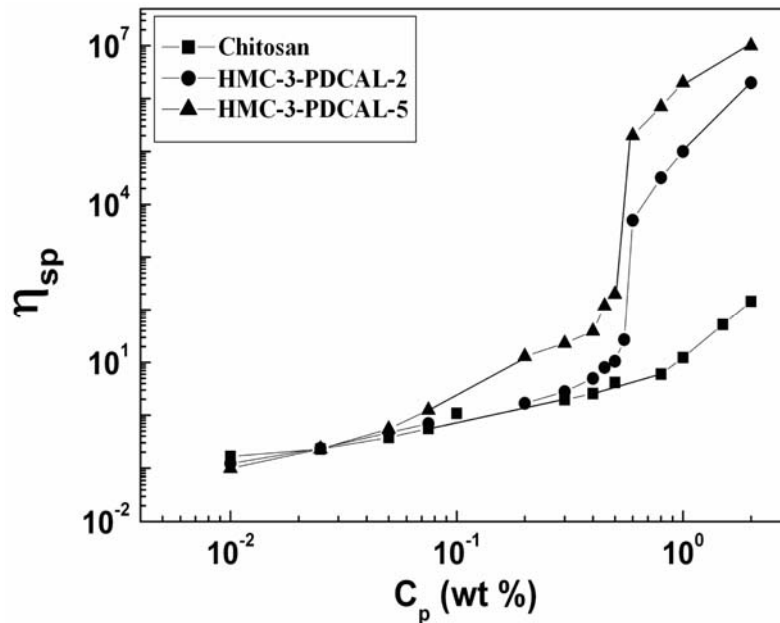


Figure 6.3. Specific viscosity (η_{sp}) as a function of polymer concentration (C_p) for chitosan (■), HMC-3-PDCAL-2 (□), HMC-3-PDCAL-5 (●)

Upon further increase in concentration, the association process leads to the formation of bridges between the neighboring flower-like micelles which eventually percolate to exhibit large increase in viscosity and form gel-like consistencies or soft-solids.

6.3.3.2 Dynamic frequency sweep:

6.3.3.2.1 Oscillatory data as a function of hydrophobic modification:

The viscoelastic properties of CS and HMCs were studied by dynamic frequency sweep experiments. Figure 6.4 show the data of storage modulus (G') and loss modulus (G'') for CS and HMC-3-PDCAL-2 and HMC-3-PDCAL-5 samples at the polymer concentration, $C_p = 2$ wt % which is well above the overlap concentration (C^*). In the chitosan polymer, the storage modulus (G') shows a weak frequency dependence and shows nearly a plateau modulus at about 1 Pa. Whereas the loss modulus (G'') shows a gradual increase with frequency. The sample shows a crossover frequency of G' and G'' at about ~ 20 rad/s which correspond to the relaxation time, $\tau \sim 0.05$ s (**Figure 6.4a**). However, with the hydrophobic modification with 2 mol % of 3-PDCAL and at the same C_p , the G' increased significantly in the entire range of frequency studied and the G'' shows a shallow minimum. The crossover frequency occurred at about $\sim 10^{-2}$ rad/s. This corresponded to the relaxation time, $\tau \sim 100$ s (**Figure 6.4 b**). Upon further increase in the hydrophobic content (**Figure 6.4 c**), the G' reached nearly 70 - 80 Pa and the polymer solutions exhibited soft-solid gelly behavior. The crossover frequency is not observed in the experimental frequency range. This clearly indicates that, the dynamics of CS solution decreases upon hydrophobic modification and the modulus increases to give gel-like consistency to all the polymer solutions.

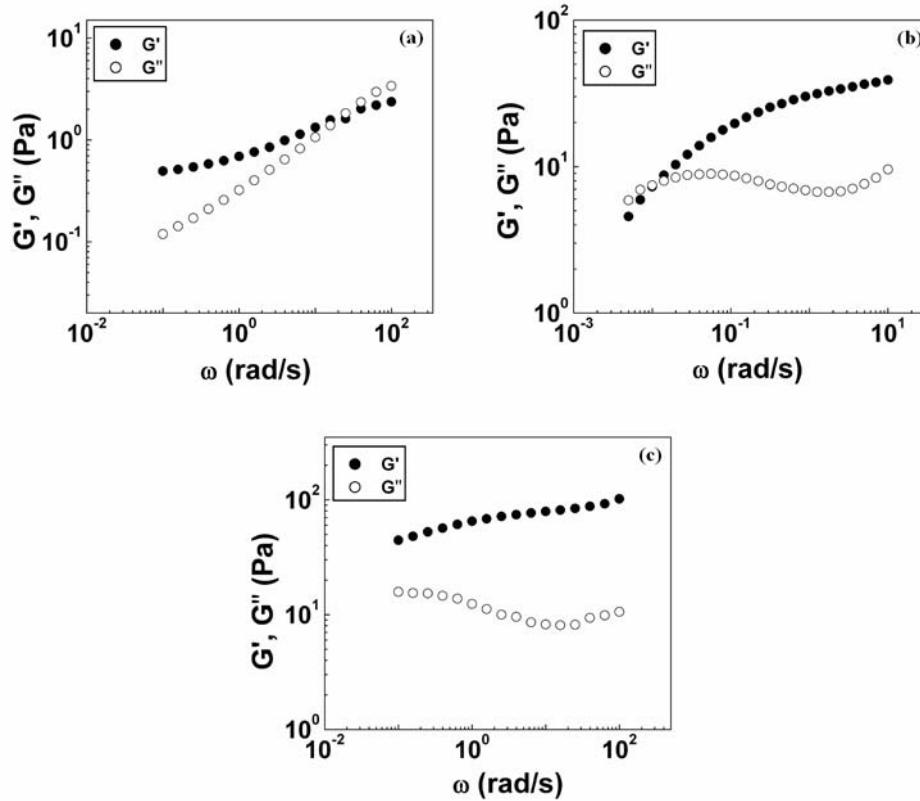


Figure 6.4. Dynamic frequency sweep data as a function of hydrophobic modification ((a) CS, (b) HMC-3-PDCAL-2, (c) HMC-3-PDCAL-5, $C_p = 2$ wt %)

6.3.3.2.2 Oscillatory data as a function of polymer concentration:

The viscoelastic properties of HMCs were also studied as a function of polymer concentration at a constant degree of hydrophobic modification (5 mol %). **Figure 6.5** shows the data on G' and G'' for HMC-3-PDCAL-5 at three different polymer concentrations ($C_p = 0.5, 1$ and 2 wt %). It can be clearly seen that for low polymer concentration ($C_p = 0.5$ wt %) (**Figure 6.5 a**) the loss modulus (G'') is higher than the storage modulus G' and the sample behaves like a liquid. However, with increase in polymer concentration ($C_p = 1$ wt %) (**Figure 6.5 b**) G' becomes larger than G'' and G'' shows a shallow minimum in the intermediate frequency range. Upon further increase in polymer concentration ($C_p = 2$ wt %) (**Figure 6.5c**), G' becomes much larger and the gap between G' and G'' becomes larger. The evolution from liquid-like behavior to a solid like structure clearly depicts a transition to a gel state. In this state the number of

elastically active chains i. e. the bridges between flower-like micelles increase and form extensive network which manifests in high viscosity of samples.

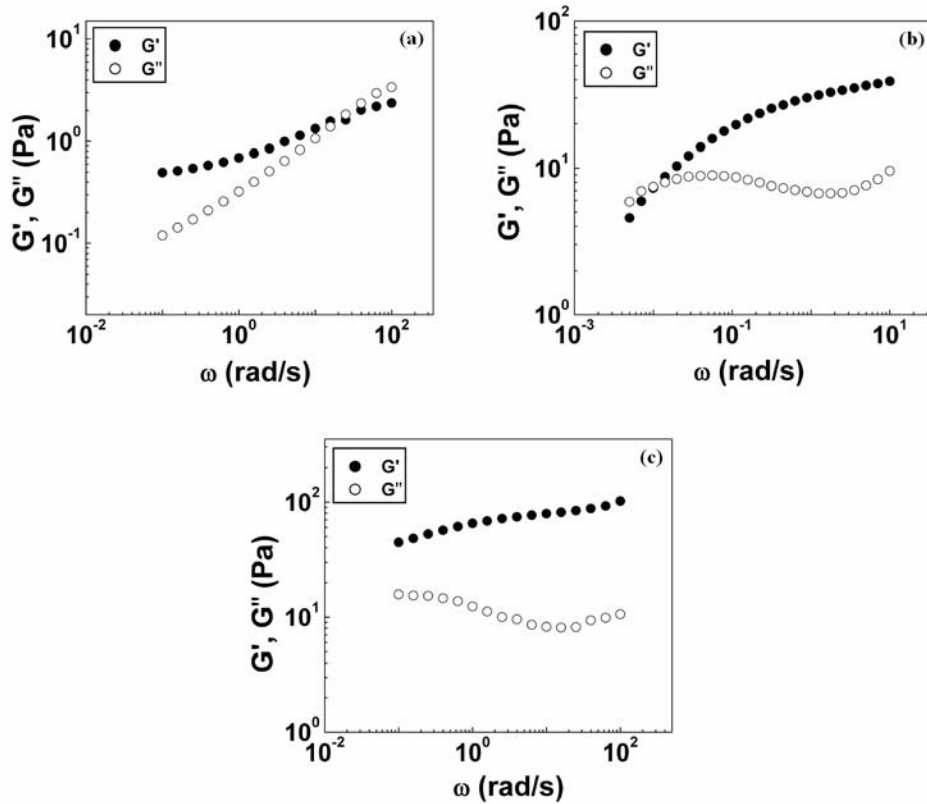


Figure 6.5. Dynamic frequency sweep data for HMC-3-PDCAL-5 as a function of polymer concentration, (a) $C_p = 0.5$, (b) $C_p = 1$, (c) $C_p = 2$ wt %

6.3.4 Light scattering:

6.3.4.1 Static light scattering (SLS):

The static light scattering experiments were performed on unmodified chitosan, HMC-3-PDCAL-2 in the concentration range of 0.01 - 2 g/dL using solvent mixture 0.3 M acetic acid and 0.05 M sodium acetate. From the plot of KC/R_θ vs polymeric concentration and with use of Zimm equation, the absolute molecular weight (M_w), radius of gyration (R_g) and second virial coefficient were determined. The results are shown in **Table 6.2**.

Table 6.2. Data obtained from static and dynamic light scattering analysis

Samples	M_w (g/mol)	R_g (nm)	A_2 (mol g ⁻² cm ³)
CS	2.15×10^5	90	1.52×10^{-3}
HMC-3-PDCAL-2	2.05×10^5	88	1.56×10^{-3}

The concentration range in which the molecular weight of chitosan and hydrophobically modified chitosan was calculated exists in the non-interacting polymer chains. **Table 6.2** shows that, there is no significant change in the values of M_w , R_g and A_2 upon hydrophobic modification to a moderate extent.

6.3.4.2 Dynamic light scattering (DLS):

Figure 6.6 shows the semi-log plot of autocorrelation function vs time for CS and hydrophobically modified chitosan, HMC-3-PDCAL-2 and 5. A comparison of the correlation function reveals that upon hydrophobic modification of chitosan the relaxation process slows down due to the formation of hydrophobic associations in the modified polymers. These associating structures impose dynamical constraints thereby leading to the delayed relaxation.

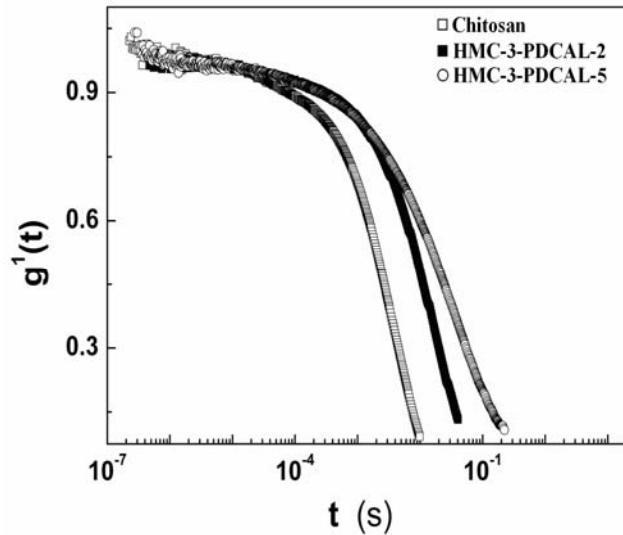


Figure 6.6. Plot of $g^1(t)$ vs t (s) for CS, HMC-3-PDCAL-2 and HMC-3-PDCAL-5

Further in the concentration range, 0.01 - 0.05 g/dL where the non-interacting polymer chains exists, the DLS was analyzed to calculate diffusion coefficient (D) and hydrodynamic radius (R_H) of CS and hydrophobically modified chitosans. The results are shown in **Table 6.3**. The results show that, the values of diffusion coefficient increase upon hydrophobic modification which can be attributed to the restricted motion of chains due to hydrophobic associations.

Table 6.3 Data obtained from dynamic light scattering using autocorrelation function

Polymers	D (m^2/s)	R_H (nm)
CS	4.05×10^{-12}	53
HMC-3-PDCAL-2	5.36×10^{-12}	40
HMC-3-PDCAL-5	8.58×10^{-12}	25

However, the hydrodynamic radius, R_H decreased significantly upon hydrophobic modification of chitosan. This can be explained from the fact that upon hydrophobic modification the polymer coils tend to undergo intra-molecular interactions within the isolated coil leading to the compaction of polymer chains thereby reducing the R_H .

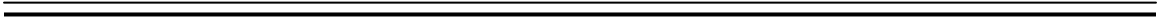
6.4 Conclusions:

In conclusion, hydrophobically modified chitosan polymers (HMCs) were synthesized using hydrophobic compound namely, 3-PDCAL which was prepared from a renewable resource material, CNSL. The structural elucidation of the unmodified chitosan and the modified chitosan polymers was performed by 1H NMR spectroscopy. The MWs and R_g were determined using static light scattering technique. The rheological investigations in the semi-dilute regime indicated sharp increase in viscosity for HMCs as compared to unmodified chitosan. This was explained on the basis of formation of hydrophobic associations above the overlap concentrations. The formation of hydrophobic associations in the modified polymers slowed down the dynamics which

was manifested in autocorrelation function of DLS experiments. Further the diffusion coefficient obtained from DLS increased upon hydrophobic modification.

References:

1. Li, X.; Wu, W.; Liu W. *Carbohydrate Polym.* **2008**, *71*, 394.
2. Shi, Huan-Ying; Zhang, Li-Ming *Carbohydrate Polym.* **2007**, *67*, 337.
3. Germain, Y.; Ernst, B.; Genelot, O.; Dhamani, L. *J. Rheol.* **1994**, *38*, 681.
4. Thuresson, K.; Nilsson, S.; Lindman, B. *Langmuir* **1996**, *12*, 2412.
5. Muzzarelli, R. A. A.; Lough, C.; Emanuelli, M. *Carbohydrate Res.* **1987**, *164*, 433.
6. Matsumoto, T.; Kawai, M.; Masuda, T. *Biopolymer* **1991**, *31*, 1721.
7. Anthonsen, M. W.; Varum, K. M.; Smidsrød, O. *Carbohydrate Polym.* **1993**, *22*, 193.
8. Furuhata, Ken-ichi; Aoki, N.; Suzuki, S.; Sakamoto, M.; Saegusa, Y.; Nakamura, S. *Carbohydrate Polym.* **1995**, *26*, 211.
9. Mucha, M. *Macromol. Chem. Phys.* **1997**, *198*, 471.
10. Wang, W.; Qin, W.; Bo, S. *Makromol. Chem., Rapid Commun.* **1991**, *12*, 559.
11. Moore, G. K.; Roberts, G. A. F. *Int. J. Biol. Macromol.* **1981**, *3*, 337.
12. Yalpani, M.; Hall, L. D. *Macromolecules* **1984**, *17*, 272.
13. Kjoniksen, Anna-Lena; Iversen, C.; Nyström, B.; Nakken, T.; Palmgren, O. *Macromolecules* **1998**, *31*, 8142.
14. Esquenet, C.; Terech, P.; Boue, F.; Buhler, E. *Langmuir* **2004**, *20*, 3583.
15. Esquenet, C.; Buhler, E. *Macromolecules* **2001**, *34*, 5287.
16. Hitoshi, S.; Naoki, Y.; Yoshifumi, I.; Junzo, S.; Sei-ichi, Aiba. *Advances in Chitin Science* **2003**, *7*, 126.
17. Muzzarelli, R. A. A.; Frega, N.; Miliiani, M.; Muzzarelli, C.; Cartolari, M. *Carbohydrate Polymers* **2000**, *43*, 263; Ramos, V. M.; Rodriguez, N. M.; Rodriguez, M. S.; Heras, A.; Agullo, E. *Carbohydrate Polymers* **2003**, *51*, 425; Mourya, V. K.; Inamdar, N. N. *Reactive and Functional Polymers*, **2008**, *68*, 1013; Alves, N. M.; Mano, J. F. *International Journal of Biological Macromolecules* **2008**, *43*, 401.



Chapter VII
Summary and Conclusions



The work reported in the thesis was focused on design and synthesis of new hydrophobically modified water-soluble polymers [HMPs] using hydrophobic compounds derived/synthesized from renewable resource materials such as, cashew nut-shell liquid [CNSL] and gallic acid [GA], which are the byproducts of cashew processing industry and leather industry respectively. Accordingly, four hydrophobic compounds namely, 3-pentadecyl cyclohexyl amine [3-PDCA], 3-pentadecyl cyclohexane carbaldehyde [3-PDCAL] from CNSL and methyl 3, 4, 5-tris octyloxy benzoate [MGC₈], methyl 3, 4, 5-tris octyloxy benzoate [MGC₁₂] from GA were synthesized. The structural elucidation of all the hydrophobic compounds was performed by IR and NMR spectroscopy. The hydrophobic compounds prepared were used for the modification of water-soluble polymers namely, poly(vinyl alcohol) [PVA], poly(N, N'-dimethyl acryl amide-co-acrylic acid) and chitosan [CS]. The new HMPs obtained were studied in terms of their structure-property relationship using spectroscopy, rheology and light scattering techniques. The conclusions from each study are summarized below:

1. Hydrophobically Modified Poly(vinyl alcohol): Synthesis, Characterization and Solution Properties

Poly(vinyl alcohol) [PVA] is one of the largest volume synthetic water-soluble polymers produced and offers advantages for hydrophobic modification. In this work, hydrophobically modified poly(vinyl alcohol) [HMPVA] polymers were prepared using MGC₈ and MGC₁₂. In order to retain aqueous solubility of modified PVA, an ionic moiety namely, 1, 3-propane sultone was incorporated into the polymer backbone. The incorporation of MGC₈/MGC₁₂ and 1, 3-propane sultone into HMPVA was confirmed by NMR spectroscopy. In the semi-dilute regime, the specific viscosity of HMPVAs showed concentration scaling that is typical of polyelectrolytes. However, at higher concentrations, the HMPVA solutions exhibited large increase in specific viscosity. Oscillatory experiments on these solutions showed gel-like behavior at polymer concentrations of 40 - 50 g/L. Confocal microscopy images of concentrated HMPVA samples indicated the existence of microgels. These samples exhibited rheological behavior that is typical of soft-solids and was probed by strain-rate frequency

superposition technique. HMPVAs with improved rheological properties show potential applications as thickeners in cosmetic creams, lotions and as drug carriers in pharmaceutical formulations.

2. Hydrophobically Modified Poly(N, N'-dimethyl acryl amide-co-acrylic acid): Synthesis, Characterization and Rheology

Hydrophobically modified poly(N, N'-dimethyl acryl amide-co-acrylic acid) polymers were synthesized using 3-PDCA as a hydrophobic compound. The choice of the backbone copolymer, poly(N, N'-dimethyl acryl amide-co-acrylic acid) was mainly due to the ease of synthesizing the copolymer with high molecular weight and the possibility of obtaining tunable hydrophilic-hydrophobic property by varying the co-monomer ratios during the copolymerization. Further, 3-PDCA being a cyclic hydrophobe exhibits more hydrophobic character compared to other linear and aromatic compounds with similar number of carbon atoms. Hence, a small amount of hydrophobic compound is sufficient to perform hydrophobic modification. The structural elucidation of the base copolymer was performed by ^1H and ^{13}C NMR spectroscopy. The zero-shear viscosities $[\eta_0]$ of the hydrophobically modified polymers were lower than that of the precursor poly(N, N'-dimethyl acryl amide-co-acrylic acid) until some critical polymer concentration, which increased with hydrophobic modification. Above the critical concentrations, the η_0 of the hydrophobically modified copolymers surpassed that of the precursor copolymer at the same concentration. Interestingly, at moderate shear rates some of these hydrophobically modified copolymers exhibited an abrupt shear-induced thickening in which the viscosity of the samples increased several fold. From the creep experiments, it was shown that the thickening occurs only when the shear rate reaches a critical value, $\dot{\gamma}_{crit}$, and that the thickened sample could be trapped in different metastable states by controlling the applied stress. Surprisingly, the shear thickened samples showed further thickening upon decreasing the applied stress. Eventually, the meta-stable samples reverted back to their equilibrium states at characteristic time which was dependent on (small) probed stress.

3. Hydrophobically Modified Chitosan: Synthesis, Characterization and Rheology

In this work, hydrophobically modified chitosan [HMC] polymers were synthesized using 3-pentadecyl cyclohexane carbaldehyde as a hydrophobic compound. The extent of hydrophobic content was varied from 3 - 7 mol % and the evidence for the incorporation of hydrophobe into chitosan was obtained from ^1H NMR spectroscopy. The solution behavior of unmodified chitosan and HMC was studied using rheology and light scattering techniques. The HMC polymer solutions exhibited enhanced rheological properties as compared to the unmodified chitosan solutions at and above the critical overlap concentrations. This is attributed to the formation of hydrophobic associations in the interacting chains. In the dynamic light scattering studies, comparison of the correlation function of unmodified CS and HMC indicated the slower relaxation/dynamics for HMC due to hydrophobic modifications.

Future Perspectives:

Hydrophobically modified water-soluble polymers [HMPs] are important class of materials and continue to show promising applications as rheology control agents in paint formulations, paper coatings, textile, cosmetics and pharmaceuticals.

Looking into the potential of these polymers in cosmetic and pharmaceutical formulations, there is a great scope for obtaining hydrophobic compounds from renewable resource materials. These hydrophobic compounds can be easily incorporated into commercially available water-soluble polymers which have been already approved by FDA. Hence, the final products obtained will have less stringent requirements from FDA for commercialization.

PVA as a starting material for HMPs has not been fully explored. Because of the reactive $-\text{OH}$ groups in PVA, one can think of several strategies to design HMPs with improved rheological properties. Scientifically, it is of paramount importance to understand the associating behavior of these polymers w. r. t. chemical structure, external environments such as presence of salts, temperature, pH etc.

Some of these HMPs, exhibit interesting shear thickening behavior and show promising applications in Enhanced oil recovery (EOR). There is a lot of scope in designing and synthesizing economically viable shear thickening polymers for specific end applications.

Although several theoretical models have been proposed to explain the phenomenon of shear thickening, the molecular cause for shear thickening in HMPs is yet to be fully understood. In this work, creep experiments have been performed to explain the abrupt shear thickening phenomenon and the shear thickened samples can be trapped in metastable states which upon cessation of shear undergo liquefaction. It can be suggested that further work on stress-controlled rheometer can give greater insight into the shear thickening phenomenon.

Further, functional HMPs can be thought of where the association can be triggered w. r. t. external stimuli such as temperature, light, shear, pH etc. Finally, there exists a continuing interest in developing HMPs based on natural polymers such as chitosan, alginates, guar gum etc which have large potential in pharmaceutical applications.

Synopsis of the thesis entitled:

Novel Hydrophobically Modified Polymers using Hydrophobes derived from Renewable Resource Materials: Synthesis, Characterization and Rheology

Introduction:

Water-soluble polymers (WSPs) are an important class of materials to both society and industry due to their specific properties in thickeners, flocculants, dispersants or emulsifiers in aqueous based media.^{1, 2, 3} In the context of water becoming an absolute requirement in specific fields like food, pharmaceuticals and personal care applications WSPs are gaining more and more importance. Secondly, due to environmental hazardous issues, water-based formulations are replacing organic ones in important areas such as drilling fluids, cosmetics and paints. Despite their importance, conventional WSPs suffer from drawbacks in that their aqueous solution properties are adversely affected by external working conditions such as temperature, pH, shear and the presence of salt.

In order to overcome these problems, associating polymers [APs] or also known as hydrophobically modified polymers [HMPs]^{4, 5, 6} have emerged as frontier materials. Basically, APs are hydrophilic water-soluble polymers that contain a small amount (typically < 2-5 mole-%) of hydrophobic groups. (Such as alkyl, perfluoroalkyl or aromatic) Above a certain polymer concentration, the hydrophobic groups self-associate into micelles-like structures to minimize their exposure to water. The polymer backbone forms bridges between the micelles leading to the formation of a transient network, which results in a several fold increase in viscosity as compared to the unmodified polymer.

These hydrophobic groups called “stickers” in APs can be incorporated into the hydrophilic backbone chain randomly, in a blocky fashion or at the terminal chain ends (telechelic). Therefore, the architectural richness of the associating polymers (i. e. random, block or hydrophobically end-capped) gives diverse physico-chemical properties. In aqueous solutions, these polymers exhibit both intra-molecular and intermolecular interactions depending on the concentrations of the solution. The synthesis of APS/HMPs together with their self-assembling properties in aqueous medium in a semi-dilute regime, have been widely reported during the 90’s and have found industrial

developments. For example, with Hydrophobic Ethoxylated Urethanes (HEUR) and Hydrophobically Modified Alkali-swelling Emulsions (HASE).

Two methodologies could be adopted to synthesize APs/HMPs:

Copolymerization of hydrophilic and hydrophobic monomers using micellar polymerization. Functionalization of hydrophilic polymers using hydrophobic compounds. Different hydrophobic compounds, such as long chain alkyl amines, alkyl halides, alkyl isocyanates and alkyl anhydrides have been used for the hydrophobic modification of both synthetic and natural water-soluble polymers such as poly (acrylic acid) [PAA], polyethylene glycols [PEGs], carboxy methyl cellulose [CMC], and chitosan [CS]. Despite many reports on the study of APs in the scientific literature, their industrial development has not really taken place and only a small number of polymers are commercially available. Therefore, there is a need to design and develop newer APs aiming at specific end-applications.

The main objective of the research was to design and synthesize novel hydrophobically modified associating polymers using hydrophobic compounds derived /synthesized from renewable resource materials. The renewable resource materials used were cashew nut-shell liquid (CNSL) and gallic acid (GA) which are the byproducts of cashew processing industry and leather processing industry and leather industry, respectively.

The thesis has been divided into following chapters:

Chapter-1: Introduction and Literature Review

The introductory chapter gives a comprehensive review of the literature on hydrophobically associating polymers [APs] covering, types of APs, synthetic methodologies for APs, rheological properties etc. The molecular architectures such as random, block and end-capping has been discussed in terms of their structure-property relationships and applications. The techniques like viscometry, rheometry and light scattering which was used for understanding the association behavior are discussed. An

interesting phenomenon of shear thickening in polymeric solutions and molecular origin for shear thickening along with its implication is also described.

Chapter-2: Scope and objective

This chapter highlights the objective and scope of the present work.

Objectives of the present thesis:

- To synthesize hydrophobic compounds from renewable resource materials such as CNSL and Gallic acid.
- To synthesize novel hydrophobically associating polymers using the prepared hydrophobic compounds.
- To characterize novel hydrophobically associating polymers in terms of their structure.
- To study various physico-chemical aspects, which include coordinated studies of self-assembly and viscoelastic properties.
- To understand and correlate the structural attributes which are responsible for exhibiting the shear induced thickening in associating polymers.

Chapter-3: Synthesis and Characterization of hydrophobic compounds

In this chapter, synthesis of new hydrophobic compounds from renewable resource materials such as CNSL (3-PDP) and Gallic acid (3, 4, 5-trihydroxy benzoic acid) is described. The hydrophobic compounds namely, 3-pentadecyl cyclohexyl amine, 3, 4, 5-tris octyloxy benzoate (MGC₈), 3, 4, 5-tris dodecyloxy benzoate (MGC₁₂) and 3-pentadecyl cyclohexane carbaldehyde (3-PDCAI) were synthesized and characterized in terms of their structure by FT-IR and NMR spectroscopy. We synthesized hydrophobic compounds namely, 3-pentadecyl cyclohexyl amine [3-PDCA], C₈, C₁₂ alkoxy substituted methyl gallates and 3-pentadecyl cyclohexane carbaldehyde. The structural characterizations of these hydrophobic compounds were performed using FT-IR and NMR spectroscopy. Subsequently, these hydrophobic compounds were utilized to synthesize novel hydrophobically modified associating polymers taking water soluble polymers, poly (vinyl alcohol), copolymers of N, N-dimethyl acryl amide-co-acrylic acid and chitosan. The novel

hydrophobically associating polymers were characterized in terms of their structure by FT-IR and NMR spectroscopy and their rheological properties in solution were studied using the state-of-the-art rheometers.

Chapter-4: Hydrophobically modified poly (vinyl alcohol): Synthesis, characterization and Rheology

This chapter describes the synthesis of hydrophobically modified poly (vinyl alcohol) [HMPVA] using the hydrophobic compounds namely, 3, 4, 5-tris octyloxy benzoate [MGC₈] and 3, 4, 5-tris dodecyloxy benzoate [MGC₁₂] prepared in our laboratory. The incorporation of hydrophobic compounds in PVA was confirmed by NMR spectroscopy. The formation of transient network structure as a result of the association of hydrophobic groups was largely manifested in macroscopic property of viscosity. The rheological behavior of HMPVA in aqueous solutions was studied in the dilute, semi-dilute and concentrated regime. Oscillatory experiments on concentrated solutions exhibited a gel-like soft-solid behavior and the nature of the soft-solids was probed by the strain-rate frequency superposition. (SRFS)

Chapter-5: Hydrophobically modified poly (NN'-dimethyl acryl amide-co-acrylic acid): Synthesis, characterization and Rheology

This chapter deals with the synthesis and characterization of hydrophobically modified poly (NN'-dimethyl acryl amide-co-acrylic acid) which exhibited both shear induced thickening and thinning in aqueous solutions. This has been explained on the basis of shear-induced structure formation (shear thickening) at low shear rates and shear induced structure breakage (shear thinning) at high shear rates. Steady shear experiments with polymer solutions of different concentrations indicated that the critical shear rate ($\dot{\gamma}_{crit}$) at which the shear thickening occurs depends strongly on the concentration of the polymer. The shear thickening behavior observed in our system has been explained on the basis of shear induced transformation of intra-molecular hydrophobic associations into intermolecular hydrophobic associations. Furthermore, the kinetics of gelation was investigated by performing creep and recovery measurements.

Chapter 6: Hydrophobically Modified Chitosan: Synthesis, Characterization and Rheology

This chapter describes the synthesis of hydrophobically modified chitosan [HMC] using a hydrophobic compound namely, 3-pentadecyl cyclohexane carbaldehyde which was prepared in our laboratory. The extent of hydrophobe content in HMC was varied from 3-7 mole-% and the evidence for the incorporation of hydrophobe into chitosan was obtained from ^1H NMR spectroscopy. The solution behavior of HMC was studied using rheology and light scattering measurements.

Chapter 7: Summary and Conclusions

This chapter summarizes the important conclusions of the work.

References:

1. J. E. Glass, "Water-Soluble Polymers, Beauty with Performance", in: *Advances in Chemistry Series 213*, ACS, Washington, DC 1986.
2. S. W. Shalaby, C. L. McCormick, G. B. Buttler, "Water-Soluble Polymers: Synthesis, Solution Properties and Applications", *ACS Symposium Series 467*, Washington 1991.
3. J. Bock, P. L. Valint, Jr., S. J. Pace, D. B. Siano, D. N. Schultz, S. R. Turner, in: *Water-Soluble Polymers for Petroleum Recovery*, G. A. Stahl, D. N. Schultz, Eds., Plenum Press, New York 1988, chapter 9, 147.
4. [2a] USP 4 228 277 (1980), Hercules Incorporated (Wilmington, DE), inv.: L. M. Landoll; [2b] USP 4 352 916A (1982), Hercules Incorporated (Wilmington, DE), inv.: L.M. Landoll.
5. J. E. Glass, "Polymers in Aqueous Media: Performance Through Associations", *ACS 223*, 1989.
6. P. Dubin, J. Bock, R. M. Davies, D. N. Schultz, C. Thies, "Macromolecular Complexes in Chemistry and Biology", Springer-Verlag, Berlin 1994.

Publications:

1. Hydrophobically modified poly (vinyl alcohol) using alkoxy-substituted methyl gallate: Synthesis and rheology; Aarti S. Shedge, Prakash P. Wadgaonkar, Ashish K. Lele, Manohar V. Badiger *Journal of Polymer Science Part B: Polymer Physics*, *48* (10), 1054, 2010.
2. Abrupt shear thickening of aqueous solutions of hydrophobically modified poly (*N,N'*-dimethyl acrylamide-*co*-acrylic acid); Ashish K. Lele, Aarti S. Shedge, Manohar V. Badiger, Prakash P. Wadgaonkar, Christophe Chassenieux *Macromolecules*, *43* (23), 10055, 2010.

Conference papers:

1. Synthesis and rheology of Hydrophobically Modified Poly (vinyl alcohol) [HMPAA] using gallic acid derivatives; Aarti S. Shedge, Ashish K. Lele, Prakash P. Wadgaonkar, Manohar V. Badiger The Society of Rheology, 78th Annual Meeting, Portland (Maine) October 2006.
2. Unusual Shear Induced Thickening in Aqueous Solutions of Hydrophobically Modified Polymer; Manohar V. Badiger, Aarti S. Shedge, Ashish K. Lele, Prakash P. Wadgaonkar Abstract for ICPPC-2010, 2010 Kottayam, Kerala.